

Cranfield Institute of Technology  
Silsoe College

Thesis submitted for the degree of  
Doctor of Philosophy

1991

Jeffrey A. Lines

BSc(Dunelm) MSc(Cranfield)

# The Suspension Characteristics of Agricultural Tractor Tyres

Supervised by Dr P.A. Cowell

Presented June 1991

for Ruth, Jennifer and Kirstine

### Acknowledgements

I wish to thank the Ministry of Agriculture, Fisheries and Food for supporting this study and Professor John Matthews, formerly director of the Silsoe Research Institute for enabling me to undertake this study as a part of the research programme of this institute.

I am grateful to Richard Stayner, formerly head of Terramechanics Division, who provided much advice and support, both while was at the institute and after he left it.

Thanks are also due to Stan Collins and Axle Kising with whom I have had many fruitful discussions while I have been working on this problem. Stan Collins kindly provided the simulation software and the assistance with its use which enabled me to model the vibration of a four wheel tractor. Axle Kising and his colleagues at the University of Berlin allowed me the use of a four ram hydraulic test stand with which I measured the transfer functions between ground input and vehicle vibration.

I acknowledge gratefully the willing assistance and loyal support given by Neil Young, Kimberly Murphy and Rosemary Peachey, without whom much of the work described here would not have been achieved.

I also wish to thank Allan Boldero, Dennis Pack and my many other colleagues within the institute who have provided much valued assistance.

### ABSTRACT

A method used to measure the radial suspension properties of agricultural tractor tyres is described. The stiffness and damping of a range of tyres have been measured. The effects on tyre stiffness and damping coefficient of rolling speed, inflation pressure, load, amplitude, frequency of vibration, driving torque, surface type, tyre size, ply rating, construction, wear and age are reported.

A relationship is developed which enables the stiffness of a rolling tyre to be estimated from the tyre size, age and inflation pressure. It is shown that this is a more accurate estimate of rolling tyre stiffness than measurement of the stiffness of a stationary tyre.

The measured tyre characteristics are used to predict the vibration of a single degree of freedom system and of a four wheel tractor. Significant improvements in accuracy are found when the results are compared with those obtained using stationary tyre characteristics. The frequencies of the natural pitch and vertical modes of vibration are usually predicted to within  $\pm 10\%$ . Predictions of rms acceleration levels are less accurate. Further improvements in modelling accuracy should be achieved by more accurate measurement and modelling of the suspension characteristics of the drive wheels in the longitudinal direction.

<u>List of Figures</u> .....	iii
<u>List of Tables</u> .....	vi
<u>Introduction</u> .....	1
1 <u>The vibration problem</u> .....	2
1.1 Welfare considerations .....	2
1.2 Economic considerations .....	3
1.3 Methods of reducing vibration levels .....	4
1.4 Modelling the vibration behaviour of tractors .....	6
1.5 Modelling the tyre behaviour .....	8
1.6 Measurements of tyre suspension characteristics .....	11
1.7 Factors affecting radial stiffness of tyres .....	12
1.8 Factors affecting the radial damping coefficients of tyres .....	14
1.9 Factors affecting horizontal tyre stiffness .....	15
1.10 Conclusions .....	16
1.11 Research Objectives .....	17
2 <u>Ride vibration transfer functions between ground and tractor</u> .....	19
2.1 Introduction .....	19
2.2 Laboratory method .....	19
2.3 Test track method .....	21
2.4 Results .....	22
2.5 Discussion .....	26
2.6 Conclusions .....	27
3 <u>Method used to measure the stiffness and damping of tyres</u> .....	29
3.1 Introduction .....	29
3.2 Description of the dynamic tyre testing vehicle .....	30
3.3 Data analysis .....	38
3.4 Comparison with alternative measurement methods .....	41
3.5 Tyre measurement procedure .....	43
3.6 Reliability of measurements .....	45
3.7 Conclusions .....	46

4	<u>Variations in the stiffness of tractor tyres</u> . . . . .	47
	4.1 Introduction . . . . .	47
	4.2 Description of tyres measured . . . . .	47
	4.3 Environmental Factors which affect the stiffness of a tyre . . . . .	48
	4.4 Factors dependent on the choice of tyre . . . . .	54
	4.5 Discussion of results . . . . .	56
	4.6 Conclusions . . . . .	65
5	<u>Variations in the damping characteristics of agricultural tyres</u> . . . . .	66
	5.1 Introduction . . . . .	66
	5.2 Identity of the tyres tested . . . . .	66
	5.3 Environmental factors which affect tyre damping . . . . .	66
	5.4 Factors dependent on the choice of tyre . . . . .	72
	5.5 Discussion . . . . .	74
	5.6 Conclusions . . . . .	82
6	<u>Application of improved tyre description to a simple dynamic system</u> . . . . .	83
	6.1 Introduction . . . . .	83
	6.2 Measurement of vibration . . . . .	83
	6.3 Model of dynamic system . . . . .	84
	6.4 Analysis of results . . . . .	88
	6.5 Discussion of results . . . . .	95
	6.6 Conclusions . . . . .	100
7	<u>Application of improved tyre description to an agricultural tractor</u> . . . . .	102
	7.1 Introduction . . . . .	102
	7.2 Measurement of vibration . . . . .	102
	7.3 Model of dynamic system . . . . .	103
	7.4 Analysis of results . . . . .	106
	7.5 Discussion of results . . . . .	109
	7.6 Conclusions . . . . .	111
8	<u>Prediction of the natural frequencies for a range of tractors</u> . . . . .	112
	8.1 Introduction . . . . .	112
	8.2 Analysis using existing data . . . . .	112
	8.3 Discussion . . . . .	116
	8.4 Conclusions . . . . .	116
9	<u>General Conclusions</u> . . . . .	118
10	<u>References</u> . . . . .	122

Figure 1	Range of vibration levels recorded on tractors for different agricultural operations .....	2
Figure 2	Average incidence of spine deformation in some occupational groups .....	4
Figure 3	Physical representation of the tractor model frequently used in computer simulation .....	7
Figure 4	Physical representation of some simple tyres models .....	9
Figure 5	Four ram hydraulic test stand .....	20
Figure 6	Track method used to excite tractor with a rear wheel input and a front wheel input .....	22
Figure 7	Transfer functions showing vertical response to high and low amplitudes of rear wheel excitation for stationary and rolling wheels .....	23
Figure 8	Laboratory experiment. Ride vibration transfer functions at 0 km/h, 6 km/h and 11 km/h .....	24
Figure 9	Test track experiment. Ride vibration transfer functions at 0, 6, 11 and 15 km/h .....	25
Figure 10	Coherence between rear wheel input and vertical response in test track and laboratory experiment at 0, 6, 11 and 15 km/h .....	26
Figure 11	Sketch of the rotating belt machine (from Kising 1988) .....	30
Figure 12	AFRC Engineering dynamic tyre testing vehicle .....	31
Figure 13	Schematic diagram of tyre test vehicle .....	31
Figure 14	Actuator and inertial mass positioned on dynamic tyre test vehicle to produce lateral vibration .....	35
Figure 15	Free body diagram of forces on axle .....	36
Figure 16	Diagrammatic representation of the measurement system .....	37
Figure 17	Example of calibration transfer function between calculated and measured tyre force .....	38
Figure 18	Load deflection curve for stationary tyre T1 .....	42
Figure 19	Example of transfer function between axle acceleration and tyre force .....	44
Figure 20	Variation in stiffness of tyre T2 with inflation pressure .....	49
Figure 21	Variation of stiffness with rolling speed: Tyres T1 to T5 measured at 1.38 bar .....	50
Figure 22	Variation in stiffness of tyre T3 with load at 1.38 bar inflation pressure .....	51
Figure 23	Variation of stiffness of tyre F1 with amplitude of vibration .....	52

Figure 24	The stiffness variation of tyre T1 with changing vibration frequency at various driving speeds .....	53
Figure 25	The relationship between stiffness and inflation pressure for all the tractor tyres .....	55
Figure 26	Variation of tyre carcass stiffness with tyre age for rolling and stationary tyres .....	56
Figure 27	Variation in tyre stiffness under normal operating conditions .....	57
Figure 28	Change in axle height with time of a loaded 13.6R38 tyre and wheel after stopping .....	58
Figure 29	Relationship between tyre creep and stiffness of tyre T1 measured at driving speeds from 0 to 15 km/h .....	59
Figure 30	Relationship between the product of tyre section width and rim diameter and observed rate of increase of stiffness with inflation pressure .....	62
Figure 31	Relationship between tyre carcass stiffness and rim diameter .....	63
Figure 32	Relationship between predicted and measured tyre stiffnesses .....	64
Figure 33	Variation of damping of tyre T2 with inflation pressure .....	67
Figure 34	Variation in damping coefficient with rolling speed at 1.38 bar .....	68
Figure 35	Variation in damping of tyre T3 with load at 1.38 bar inflation pressure .....	69
Figure 36	Variation of damping with amplitude for ribbed front wheel tyre F1 .....	70
Figure 37	Variation of damping coefficient of tyre T1 with vibration frequency at various rolling speeds .....	71
Figure 38	Change in damping coefficient with driving torque for tyre T2 .....	71
Figure 39	Variation of carcass damping and inflation pressure dependence with tyre age .....	73
Figure 40	The effect of tyre lugs on damping at 15 and 20 km/h .....	73
Figure 41	Variations in tyre damping under normal variations in operating conditions .....	74
Figure 42	Rotating spoke tyre model .....	76
Figure 43	Relationship between damping force and rate of change of axle height for various forward rolling speeds .....	78
Figure 44	Apparent values of viscous damping for the tyre modeled in Figure 43 .....	78
Figure 45	Variation of apparent viscous damping coefficient with rolling speed using combination of viscous and coulomb damping in model .....	79
Figure 46	Modeled variation of tyre damping with forcing frequency .....	79
Figure 47	Variation of modeled damping coefficient with amplitude of vibration .....	80
Figure 48	Variation of modeled tyre damping coefficient with tyre deformation .....	80
Figure 49	Variation in damping with rolling speed of tyre F1 and tyre T5 .....	82



Figure 50	Schematic model of the vibrating wheel carriage .....	85
Figure 51	Power spectral estimates of the profile of the rough surface used to excite the wheel carriage .....	86
Figure 52	Measured and modelled acceleration time histories. Heavy load condition at 12.5 km/h. An example of one of the best predictions. ....	88
Figure 53	Measured and modelled acceleration time histories. Light load condition at 5 km/h. An example of one of the worst matches .....	89
Figure 54	Measured rms acceleration levels compared with those predicted .....	90
Figure 55	Ratio errors in the prediction of rms acceleration levels. ....	90
Figure 56	The measured and predicted vibration power spectra at 12.5 km/h .....	92
Figure 57	Ratio errors in the prediction of natural mode frequency using rolling and stationary tyre characteristics .....	93
Figure 58	Ratio error in the prediction of half power width of spectra peaks characteristics .....	93
Figure 59	Similarity of envelope shapes evaluated as the maximum value of the normalised cross-correlation between measured and predicted envelopes .....	94
Figure 60	Calculation of the root mean square of the envelope error .....	95
Figure 61	Normalised root mean square acceleration envelope error .....	95
Figure 62	Ratio errors in the prediction of acceleration rms .....	98
Figure 63	Measured and predicted vertical rms acceleration for different conditions of load and tyre inflation pressure .....	108
Figure 64	Vertical acceleration spectra for tractor on the artificial rough track at 10 km/h with load condition 1 .....	109
Figure 65	Vertical acceleration spectra for tractor on the artificial rough track at 17.5 km/h with load condition 1 .....	109
Figure 66	Comparison of the ratio errors of the prediction of mode frequencies made using rolling and stationary tyre characteristics .....	110
Figure 67	Measured and predicted pitch vibration rms acceleration .....	111
Figure 68	Representation of tractor model with vertical and pitch freedom .....	113
Figure 69	Predicted and measured natural frequencies of vibration in pitch and vertical directions .....	115
Figure 70	Natural frequency predictions obtained by variation of the rear and front tyre stiffness by factors of 1.2, 0.8 and 0.6 .....	117

Table I	Comparison of results for different methods of measuring tyre stiffness and damping. . . . .	41
Table II	Tyres used in the experiments . . . . .	48
Table III	Carcass stiffness, inflation pressure dependence and coefficient of determination for rolling and stationary tyres . . . . .	50
Table IV	Measured variation in stiffness with increasing amplitude of vibration . . . . .	52
Table V	Effect of different ground surfaces on apparent tyre stiffness . . . . .	54
Table VI	Summary of results, showing the rate of change of tyre stiffness with the variation of various conditions . . . . .	57
Table VII	Variation of tyre carcass damping and the inflation pressure component with rolling speed . . . . .	68
Table VIII	Measured variation in damping with increasing vibration amplitude . . . . .	70
Table IX	Changes in tyre damping on various surfaces. . . . .	72
Table X	Summary of damping results, showing the rate of change of damping with various factors. . . . .	74
Table XI	Summary of experimental conditions . . . . .	84
Table XII	Tyre characteristics used for simulation. . . . .	87
Table XIII	Comparison between the accuracy of the vibration predictions made using rolling and stationary tyre characteristics. Predictions made using the surveyed estimate of the surface profile . . . . .	91
Table XIV	Comparison between the accuracy of the vibration predictions made using rolling and stationary tyre characteristics. Predictions made using the recorded estimate of the surface profile . . . . .	97
Table XV	The Massey Ferguson MF698T . . . . .	103
Table XVI	Tyre characteristics used for simulation . . . . .	105
Table XVII	Comparison between the measured and predicted vibration of the tractor . . . . .	107
Table XVIII	Effect of longitudinal stiffness and damping on predicted vibration at 10 km/h on the artificial rough track with load condition 1 . . . . .	107
Table XIX	Tractor data . . . . .	113
Table XX	Tyre stiffnesses and the predicted and measured natural frequencies of vertical and pitch vibration . . . . .	115

## Introduction

The environment in which a tractor driver works has improved substantially and in many ways over the last thirty years. Climatic protection, roll over protection, noise reduction and improved controls have all made the tractor driver's job easier and safer. However the vibration to which the driver is subjected has been reduced very little. This vibration limits the speed at which tractors are operated, it causes long term injury to the driver and it generates high levels of stress in parts of the machine. Tractor based operations take up a large part of the time of farm workers. By reducing the vibration of these machines the health and comfort of tractor drivers could be improved. Working time lost through illness or wasted due to low driving speeds could also be reduced.

A complete wheel suspension system would reduce vibration very effectively, but this solution is unlikely to be universally applied. The complexity of a suspension system necessary to be effective on general purpose farm tractors would make it too expensive to be commercially attractive on many of the smaller vehicles. Partial suspensions, secondary suspensions and other less fundamental changes to the vehicle design are able to reduce vibration levels significantly without the cost and complexity of a full suspension.

A means of predicting the vehicle vibration is required in order to develop effectively such vibration reducing measures. Computer models to predict the vibration of agricultural tractors have been produced by a number of authors, however they are unable to predict the vibration with an acceptable degree of accuracy. The main reason for this inaccuracy appears to be a lack of information about the behaviour of the tyres.

## 1 The vibration problem

The level of vibration which occurs on tractors depends on the tractor design, the driving speed, the terrain and the work the tractor is performing. A survey of tractor vibration by Stayner and Bean (1975) showed that most agricultural tractor operations caused vibration in excess of the levels considered to be safe by International Standards Organisation for an eight hour working day (ISO 1974), Figure 1. For many of the tractor operations the vibration also exceeded the maximum level recommended for 2½ hours exposure per day. Developments in tractor design since this survey give no reason to expect the situation to be any better now. The only significant changes are the increase in size and power of the tractors and the improvements in seat suspension design. Travel speed has a very significant effect on vibration so the trend towards higher power tractor units has resulted in higher levels of vibration for which modern suspension seats are not suited (Lines, Whyte and Stayner 1989). The performance of seat suspensions cannot be improved much more since the available suspension stroke on seats must be limited to enable the driver to maintain control of the vehicle. The trend towards heavier tractors has exacerbated this problem because the dominant frequency of vibration is lower and so closer to the natural frequency of the seat suspension. Type approval tests according to EEC directive 78/764/EEC (EEC 1978) show that while a seat suspension can be expected to reduce the vertical vibration of a tractor weighing say three tons by up to sixty percent, on a larger tractor the reduction may be less than twenty percent. Recent work by Whyte and Lines (1987) has indicated that tractor drivers are accustomed driving at vibration levels far greater than those measured by Stayner and Bean.

### 1.1 Welfare considerations

A comprehensive survey of the health problems associated with tractor driving by Rosegger and Rosegger (1960) showed that spinal and stomach disorders occurred in significantly higher numbers with tractor drivers than in the population as a whole. This damage was related to exposure over long periods to excessive levels of vibration. The severity of this problem is illustrated in Figure 2.

In another study made during the period 1963 to 1972, Dupuis and Christ (1966,1972) followed the progress of over one hundred young tractor drivers and examined them

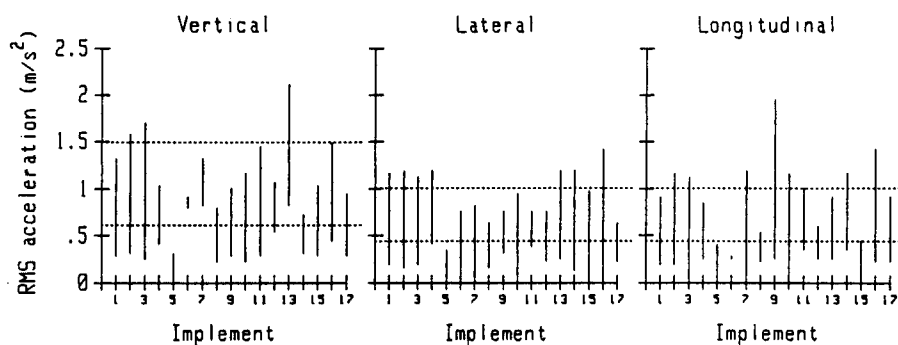


**Figure 1** Range of vibration levels recorded on tractors for different agricultural operations showing the 8 hour (lower dotted line) and 2½ hour (upper dotted line) recommended exposure limits. Mouldboard ploughing (1); heavy cultivating (2); light cultivating (3); disc harrowing (4); drag harrowing (5); rotary cultivating (6); drilling (7); rolling (8); manure spreading (9); fertiliser spreading (10); spraying (11); mowing (12); hay making (13); bailing (14); potato harvesting (15); trailer work (16); loader work (17) from Stayner and Bean 1975

for back and stomach disorders. They concluded that there was a well founded suspicion that whole body vibration may cause injury to the spinal column. The effects of whole body vibration on health have recently been extensively reviewed by Dupuis and Zerlett (1986). They conclude that chronic changes arising from whole body vibration occur in the spinal column and in the stomach. Since these changes are not specific to vibration stress, a causal relationship is difficult to prove. However examination of the many epidemiological studies leads inevitably to the conclusion that long term vibration stress in excess of the levels specified by International Standard IS2631 (ISO 1974) leads to an increased risk of danger to health, particularly of the spinal column.

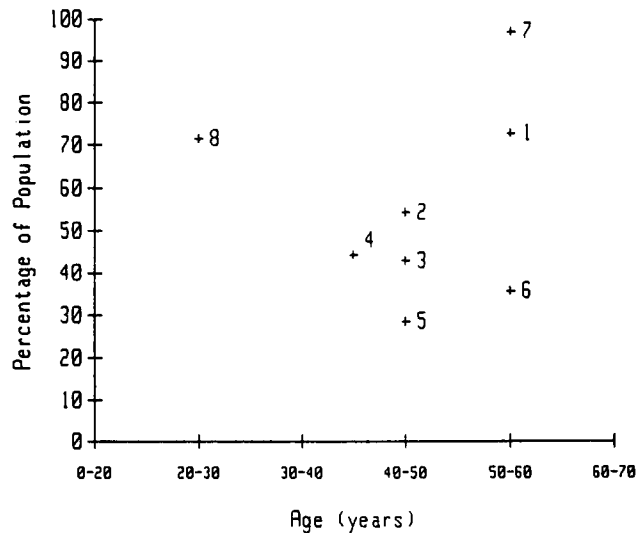
Research into discomfort and injury caused by vibration has lead to the development of weighting curves, with which vibration of different frequency and in different directions can be compared. International Standard IS2631 incorporates such a weighting curve. Assessment of vibration levels occurring on tractors should be done using the frequency weighted levels when operator health or welfare is being considered.

## 1.2 Economic considerations

The economic benefits associated with reduced ride vibration include reduced costs due to worker injury and time off work, reductions in machinery failure caused by

vibration and increased productivity of tractors and tractor drivers through higher driving speeds.

**Figure 2** Average incidence of spine deformation in some occupational groups: miners (1); farmers (2); factory workers (3); bus drivers (4); craftsmen (5); building labourers (6); labourers carrying heavy loads (7); tractor drivers (8). from Rosegger and Rosegger 1960



Evidence of increases in tractor operating speeds as a result of decreased vibration levels is given by Lines and Stayner (1989). They used an experimental tractor with a switchable suspension to show that a reduction in vibration of as little as ten or twenty percent were clearly perceived by tractor drivers as improvements in comfort, and that for many tractor operations this resulted in an increase in operating speed of a similar amount. An overall increase in tractor operating speeds of as little as five percent would produce savings of around £400 per tractor per year (Nix 1987).

Lower vibration levels will reduce mechanical stress in the tractor and implements. This will enable such machines to be designed to lower specifications, resulting in less weight, lower cost, and greater versatility.

### 1.3 Methods of reducing vibration levels

Most farm tractors have no form of suspension (other than tyres) to reduce the vibration of the vehicle despite the fact that they are designed to travel over very rough ground surfaces. In contrast, specialised agricultural vehicles designed for low draught, high speed operations are frequently suspended. The reasons for this are discussed by Stayner (1988). In brief, they are the high levels of torque which a suspension system and a flexible drive line would have to react; the very wide range in load which the axle may have to support; the common misconception that a suspension would make it

impossible for the tractor to maintain an even working depth for soil engaging implements; and the large suspension stroke which would be necessary to achieve good vibration reduction.

Although the greatest vibration reduction is to be gained from full suspension, its cost and complexity suggest that it will not become the universal means of reducing ride vibration within the foreseeable future. Partial suspensions offering more limited benefits at lower cost may be useful in several applications.

Suspending the front axle of a tractor only is very much easier than suspending the whole tractor. This has been done successfully on several research machines (Peachey, Lines and Stayner 1989). Front axle suspension has also appeared on some commercially available tractors, however usually these suspensions are too stiff to make a really significant reduction to the vibration levels (Harrison 1984).

Specialised solutions such as suspending the hitch point of a tractor and trailer combination (Crolla, Horton and Alstead 1987) or using the mass of a carried implement as a dynamic absorber (Ulrich 1983) have been shown to have potential for reducing vibration significantly when they are applicable.

Secondary suspensions which protect only the driver also have potential. Seat suspensions have been fitted as standard to tractors for many years and good designs of these on small tractors can reduce the vibration significantly (Stayner, Hilton and Moran 1975). The main limitation with suspended seats is the amount of suspension stroke which can be provided without making it difficult for the driver to maintain contact with the tractor controls. The low frequency, large amplitude, vibration characteristic of large tractors cannot therefore be as effectively controlled as the higher frequency vibration of smaller tractors.

A logical progression from the suspended seat is to suspend the entire cabin of the tractor. This relaxes the limit on suspension stroke and so enables effective protection to be provided for the drivers of all sizes of tractors. Such cab suspensions have been constructed and tested at various research establishments (Hilton and Moran 1975; t'Hart 1977; Kauss and Weigelt 1980; Lines, Whyte and Stayner 1989). Although cabin suspension protects the driver from vibration, it does little to reduce the vibration of the vehicle. The higher driving speeds made possible by such a suspension can result in significantly greater loads on the vehicle structure and loss of road contact for the tyres.

It was noted by Matthews (1973) that ride vibration levels on unsuspended tractors are influenced by relatively small changes in design. Some general relationships between levels and tractor parameters have been indicated by Collins (1982) but the results were not conclusive or specific enough to be used as guide lines for designing tractors with inherently lower vibration levels.

An accurate and reliable means of predicting the vibration of agricultural tractors would enable designers to make use of these variations to produce tractors with inherently better ride vibration characteristics. It would also enable suspension systems to be designed more efficiently.

#### 1.4 Modelling the vibration behaviour of tractors

Many efforts have been made to simulate the vibration characteristics of tractors with and without suspension systems. Unfortunately there are very few cases in the published literature where these ride vibration predictions have been tested against measured results. Experience has shown that when this comparison is made over a representative range of tractors, the results are rather poor (Crolla 1981; Stayner, Collins and Lines 1984). Crolla, Horton and Stayner (1990) show that errors in the prediction of vertical root mean square (rms) acceleration in excess of 40% are not unusual, and that for some tractors trends in the predicted rms levels with changing vehicle speed are quite different from those which occur in practice.

Despite this poor agreement, computer simulation has been used to assess the effect on vibration of large changes to the tractor system. Examples of this are the effect of tractor wheel suspension (Claar II *et al* 1980), trailer suspension (Crolla, Horton and Alstead 1987), and a mounted implement suspension (Ulrich 1983). Provided they are used cautiously, it is possible to extract useful information from such results.

For most purposes it is sufficient to describe the tractor body as a rigid mass which may have connected to it other suspended masses, representing the cab or suspended seat. This body is connected to the ground profile by elements representing the characteristics of the tyres (Figure 3). Linear equations representing this are straightforward to develop and are widely published in the literature (Claar II 1982; Stayner, Collins and Lines 1984). It is now widely accepted that poor tyre description within the simulation is the main source of error (Matthews 1977; Crolla 1981; Stayner, Collins and Lines 1984; Crolla and Maclaurin 1985).



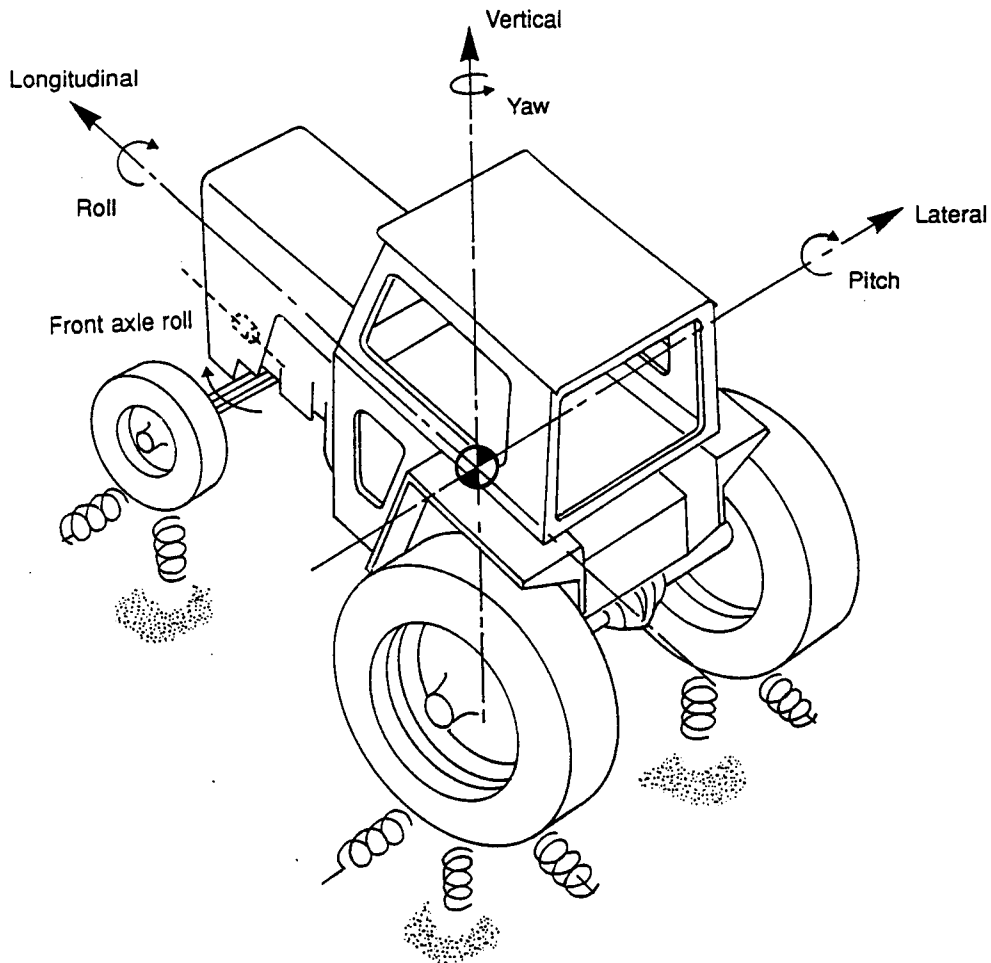


**Figure 3** Physical representation of the tractor model frequently used in computer simulation

Examination of the equations of motion shows that the vibration of a tractor can be split into two separate systems. Vertical, pitch and longitudinal vibration are linked together in one system. Lateral, roll, yaw and front axle freedom are linked together in another, separate system. Within each system the vibration is great enough to cause discomfort and potentially injury to the driver. Within each system the natural modes of vibration cannot be modeled in isolation, but must be considered together. Consideration of the vertical vibration of a tractor therefore involves a consideration of the longitudinal characteristics of the tractor tyres as well as the vertical characteristics. Similarly consideration of the lateral and yaw vibration of the tractor involves the characteristics of the tyres in both the vertical and lateral directions.

Since the greatest use for a means of predicting the vibration of a tractor is to enable comparisons to be made between possible designs, absolute accuracy in the prediction of vibration levels is not of primary importance. It is more important that the difference

between the designs is predicted reliably. However without an accurate means of prediction, this reliability must always be in question.

Correct prediction of the frequencies of vibration is necessary in so far as it affects the identification of the different modes, their interaction and the resulting vibration levels. For the purpose of secondary suspension design it is necessary to know the dominant frequencies of vibration of the vehicle to ensure that those of the suspension are sufficiently below them to avoid amplification of the vibration and to maximize its attenuation. Since the roughness of most random profiles changes with the spatial frequency, correct frequency prediction is also important in order to obtain the correct levels of excitation at the natural frequencies.

In order to avoid an endless and increasingly trivial pursuit of accuracy it is necessary to have some realistic levels of accuracy which will be sufficient for most purposes. Reductions in vibration of much less than 10% are unlikely to be very useful, therefore the ability to predict vibration levels, specifically the acceleration root mean square level (rms), to within 10% would be adequate. For many purposes, prediction of the frequency of vibration to within a third of an octave or about  $\pm 30\%$  would be sufficient. However a 30% error in frequency prediction is likely to result in a 30% error in the level of excitation at the natural frequencies and so errors in the rms level prediction of less than this would be entirely fortuitous. Frequencies of the natural modes of vibration should therefore also be predicted to within  $\pm 10\%$

### 1.5 Modelling the tyre behaviour

There are two aspects to the behaviour of a tyre which have to be included in the tyre description. The first is the way in which the tyre develops a reaction force when it is deformed by pressing it against a flat surface. The second is the way this force changes when the ground is not flat. The difference between these situations arises because the tyre contacts the ground surface over a finite area rather than at a point. In reality these two processes are not separable because the size of the contact patch is determined by the instantaneous compression of the tyre. However separating the two processes is attractive because it makes both gathering of tyre data and simulating vehicle vibration quicker and simpler.

The simplest physical model likely to be acceptable for use in simulating the ride vibration of an unsprung vehicle such as a tractor is a single spring and viscous damper in parallel. This is sometimes referred to as the Voigt-Kelvin model (Figure 4). It gives

results which are acceptable for some purposes, however it contacts the ground at a single point, so if the ground profile has wave length components comparable with, or smaller than, the tyre contact patch length, then a better description is needed. For instance, it is clear that a point contact model cannot give an adequate description of the forces involved in traversing a vertical step. Because of the finite length of the contact patch, the development of force is gradual rather than instantaneous. These characteristics can be approximated by redefining the ground input.

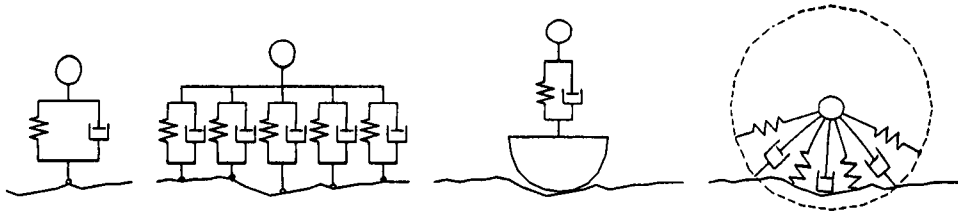


**Figure 4** Physical representation of some simple tyres models, from left to right: simple Voigt-Kelvin model; fixed footprint model; rigid tread band model; radial spring or adaptive footprint model

One such redefinition is the rigid tread band model (Captain, Boghani and Wormley 1979). The ground profile is replaced by the locus of the centre of a rigid wheel rolling over the ground. In this way short wave length components of the ground profile are filtered out. This process results in a non-linear transform of the ground profile. It behaves like a rolling tyre in that it moves the contact patch forwards for positive gradients and back for negative gradients. Unlike a real tyre, the enveloped ground profile always reaches the height of the highest obstacle. Captain *et al* have compared it with other models and found that within the frequency range of interest for ride vibration studies it has no particular advantage over other descriptions.

Another redefinition of the surface profile is the fixed footprint model. Each point on the profile is replaced by a local average of the profile elevation calculated over the assumed length of the tyre contact patch. This is equivalent to replacing the single Voigt-Kelvin element by a number of elements contacting the profile over the contact patch length.

An empirical method for redefining the profile is to measure the effective filtering of the tyre. Such measurements have been made by Dale (1978). A tractor was driven over a rough surface very slowly and the locus of the wheel centre was measured. The transfer function calculated between the track profile and the wheel locus was used to redefine the track profile. Nguyen and Lines (1988) followed a similar method but used

a single wheel rather than a four wheeled vehicle to avoid any effects from the other wheels. Rather than using a random profile, they used ramps and steps of various heights and angles. Measurements were made with a single tyre but the inflation pressure and tyre load was varied. A simple non-recursive digital filter was constructed which had characteristics similar to the measured transfer function. This filter calculated the local average of the profile over the tyre contact patch length but was tapered at each end to reduce the magnitude of the side bands which result from the simple rectangular filter shape of the fixed footprint model.

Some authors have suggested more sophisticated descriptions to replace the spring and viscous damper used in the models just described. However such variations are frequently made in order to more closely match the non-linear behaviour of stationary tyres. Gehman (1957) and Hooker (1980) have attempted to model the variation in stiffness with vibration frequency. Wolken (1972) and Painter (1981) attempted to model the variation in stiffness with deflection. Recent work by Kising (1988) has shown that both of these non-linearities are very small for rolling tractor tyres.

Other authors have considered the ground enveloping and the suspension aspects of the tyre behaviour together. One result of this is the adaptive footprint or radial spring tyre model. In this model the wheel is represented by a number of Voigt-Kelvin units, arranged radially. Combining the vertical and longitudinal components of the forces produced by these elements gives the forces on the axle. This model allows the contact patch to vary with vehicle motion and ground profile, enabling more realistic tyre envelopment of obstacles to take place. This model clearly has much more conceptual similarity to the real situation than the simpler models and it is amenable to many additional refinements adding to both its realism and its complexity. However the only author to show a significant improvement in the accuracy of simulation using this model is Kising (1988). This is because in his model the springs have different lengths representing the non-roundness of the tyres which he measured. At high rolling speeds it appears that this varying radius of the tyre contributes significantly to the vehicle vibration.

Apetaur (1968) approached the problem of uneven ground in a slightly different way. Assuming that on a flat surface the tyre acts as an ideal spring and damper system and that the spring and damping forces are produced by the change, and the rate of change of tyre volume respectively, he calculated the horizontal and vertical spring and damping forces as a tyre passed over obstacles. However the assumption on which this

method was based was not demonstrated and no comparison with experimental results was made.

In a quite different approach to this problem Lippmann *et al* (1966,1967) measured the forces occurring as tyres rolled on a large drum with cleats on it. The wheel centre was maintained at a fixed height above the drum surface and the transient vertical and longitudinal forces were measured. The information gained from measuring the force as the tyre passed over a step was used to predict the forces occurring when the wheel rolled over arbitrary shaped objects. All the measurements refer to forces developed with the wheel centre at a fixed height.

If the force developed by a tyre as it passes over a unit step at  $x = X$  is given by  $f(x)$ , then by assuming that the principle of linear super-position holds for tyre enveloping forces, the force  $F(x)$  produced as the tyre passes over an irregularity of elevation  $G(x)$  can be given by

$$F(x) = \int_0^x \frac{dG(X)}{dX} f(x-X) dX.$$

This relationship can also be translated into a frequency domain analysis. If  $D(\omega)$  represents the spectral content of the road irregularities at spatial frequency  $\omega$ , and  $E(\omega)$  represents the spectral content of the force response to a square cross section cleat of unit height and length, then the force developed can be represented as

$$F(\omega) = \int_{-\infty}^{\infty} D(\omega) E(\omega) e^{i\omega x} d\omega.$$

Using this method time histories of the force are calculated for a tyre rolling over small obstacles. The examples given in the publication indicate that the predicted force time histories correspond well with the measured ones. This method has not been used or demonstrated for situations where the profile is long or where the wheel axle height changes. Both situations would make it more complicated to apply. Further investigation into this method could be worthwhile.

### 1.6 Measurements of tyre suspension characteristics

Most of the published literature makes use of a Voigt-Kelvin element to describe tyre suspension characteristics. In the following paragraphs experimental data from various authors is presented which describes the characteristics of tyres in terms of the stiffness and damping of this unit. Deviations from the linearity which this description imposes are considered as variations of the main characteristics. Many of the measurements

have been made on car and lorry tyres which differ from tractor tyres in that they have no lugs, are constructed from different rubber compounds, and operate at higher pressures. Therefore the conclusions and trends which are drawn from these experiments may not be directly applicable to tractor tyres.

Some data from a significant set of experimental results (Kising 1988, Kising and Göhlich 1988 a,b,c) are not included in this discussion. This experimental work was done in parallel with the work reported in this thesis. The experiments were similar to those made by the author and the results are complimentary. It has been analysed further and the results are presented together with analysis of tyre characteristic measurements made by the author in Chapters 4 and 5. Instead of describing the damping coefficient of the tyres, they have reported the damping ratio of the system. Where the stiffness and damping ratio for the same conditions have been presented it has been possible to derive from these results the damping coefficient of the tyres. However this only happens in only a few cases.

Stiffness and damping of tyres can be determined by several different methods.

- a) From the load deflection relationship curve (stiffness only).
- b) From the natural frequency and rate of decay of free vibration.
- c) From the frequency and spectral width of the natural frequency peak in the transfer function measured between force and displacement.
- d) From the magnitude and phase lag of the transfer function measured between force and displacement at any frequency.

These measurements can be made with either a rolling tyre or a non-rolling tyre. The results are not generally the same. The rolling tyre usually has lower values of stiffness and damping and the values change less with variations in other parameters such as frequency or pressure. Göhlich and Sharon (1975) have concluded that the characteristics of a tyre, as they affect vehicle ride, can be derived only from experiments on rolling tyres.

## 1.7 Factors affecting radial stiffness of tyres

### 1.7.1 Inflation pressure

The stiffness of rolling radial ply tyres increases almost linearly with pressure. A far less linear relationship is observed with non rolling tyres (Hooker 1980). Rasmussen and

Cortese (1968) claim that this increase is greater in cross ply tyres than in radial tyres and decreases with increasing cord angle.

#### 1.7.2 Rolling speed

The stiffness of a tyre in the radial direction is widely reported to decrease at the onset of rolling, reaching a minimum value which can be as much as 30% lower than the stationary tyre stiffness. Several authors report a subsequent increase in stiffness with further increases in speed (Hooker 1980, Hahn 1973). There are large differences between reports of the rolling speed at which the minimum stiffness is reached. It varies from 1 km/h with a very small decrease in stiffness (Laib 1979) to 20 km/h (Chiesa and Tangorra 1959). Göhlich, Schütz and Jungerberg (1984) and Kutzbach and Schrogl (1987) found a decrease in stiffness at the onset of rolling, but no subsequent increase. The differences are likely the originate in the different tyre types and sizes being tested. Göhlich and Kutzbach both reported measurements on agricultural tractor tyres. Radial tyres appear to show less velocity dependence than cross ply tyres (Hahn 1973, Chiesa 1965).

#### 1.7.3 Load

Overton, Mills and Ashley (1970) report a complex relationship between load and stiffness which at various points show the stiffness to increase, to remain constant, and to decrease with load. However these measurements were made with a stationary tyre so this gives little indication of the behaviour which might be expected from a rolling tyre. Göhlich, Schütz and Jungerberg (1984) report an increase in tyre stiffness with load. The vertical stiffness has been reported by Chiesa and Rinonapoli (1967) to decrease with lateral loading.

#### 1.7.4 Amplitude

For small oscillations, the stiffness of a rolling tyre is almost independent of amplitude. Chiesa and Tangorra (1959) find that at high pressures the stiffness of road vehicle tyres decreases slightly with amplitude.

#### 1.7.5 Frequency

The stiffness of non-rolling tyres increases with forcing frequency. Rolling tyres have a much smaller dependence, with radial tyres showing a smaller a increase than cross-ply tyres (Hooker 1980, Hahn 1973).

#### 1.7.6 Torque

Matthews and Talamo (1965) have made measurements which indicate a small decrease in stiffness with applied torque.

#### 1.7.7 Rim size

Rasmussen and Cortese (1968) found that for a given tyre the stiffness increases with the width of the rim that it is mounted on.

#### 1.7.8 Tread type

Yong et al (1980) have made measurements on a tyre with a dense road tread, they then removed this tread, and subsequently replaced it with a more open agricultural tyre tread. They found that a dense tread increases the stiffness considerably, while an agricultural tyre tread, although possessing more stiffness than a buffed tyre, has less effect.

#### 1.7.9 Tyre wear

Non-rolling tyre experiments by Stayner and Boldero (1973) indicate that a severely worn tractor tyre has considerably lower stiffness than a new one. The results however showed that the stiffness of a partially worn tyre did not necessarily lie between those of the new and severely worn tyres.

#### 1.7.10 Ballast

Siefkes (1989) found that substantial increases in tyre stiffness can be caused by changes in the filling material. His results suggest increases in the order of 25% for water filled tyres.

#### 1.7.11 Surface

Siefkes has also published results indicating that the apparent stiffness of tyres decreases by up to 30% when the tyre is on a grass or earth surface. Hlawitschka (1971) has observed tyre stiffness to increase with the increasing radius of convex ground curvature.

### 1.8 Factors affecting the radial damping coefficients of tyres

Although the damping coefficient of tyres is small, attention needs to be paid to it because it is by increasing the damping coefficient that the ride of an unsprung vehicle can be most noticeably improved. Since much of the tyre research reported here is



concerned with vehicles which have separate suspension systems with high damping coefficients, many researchers have disregarded this tyre property.

It has been shown by Göhlich and Sharon (1975) and by Hahn (1973) that the damping of tyres is dependant on the rolling speed. Work on road vehicle tyres has shown a dependence on vibration frequency which decreases with increasing rolling speed and a dependence on vibration amplitude. Göhlich, Schütz and Jungerberg (1984) made observations of the behaviour of four agricultural tractor tyres. They found that the damping coefficient of a cross-ply tyre decreased slightly with inflation pressure and that the damping of a radial tyre of similar size was almost independent of pressure. This is in apparent contradiction to earlier work by Göhlich and Sharon (1975) where the damping coefficient of a tyre was observed to increase with pressure. Since 1988 further information has been published by Kising (1988); Kising and Göhlich (1988 a,b,c) and by Siefkes (1989). In these papers the influence of rolling speed, inflation pressure, tyre load, tyre size, lug length, ground surface, tyre ballast, etc are observed for a wider range of tyres. Unfortunately all the results given refer to the damping ratio of the tyres rather than the damping coefficient. This enables the overall effect on vibration of changing tyre stiffness and damping to be visualized. However for understanding the energy dissipating mechanism of the tyres and for simulating the motion of tractors, the damping coefficient is the more important quantity. The damping ratio is a function of both the tyre damping coefficient and the tyre stiffness. For only a few cases are both the damping ratio and the stiffness under the same conditions shown. Therefore much of the available information cannot be used for vibration simulation or to investigate the way that tyre damping coefficients change.

Siefkes has shown increases in apparent tyre damping of up to 150% when the tyre is on earth and grass surfaces. He also indicated that tyre damping does not vary much when the tyre is filled with water ballast.

### 1.9 Factors affecting horizontal tyre stiffness

The horizontal compliance of road vehicle tyres is usually considered to be of interest only for vehicle handling studies. Off road vehicles roll and pitch much more than road vehicles, so, on such vehicles without suspensions these factors also have an important effect on the vibration. It has been shown (Stayner Collins and Lines 1984) that the vertical, pitch and longitudinal motion of a tractor are closely coupled together, and that these motions are almost independent of the Roll, lateral and yaw motion. Since the

vertical vibration is closely coupled to longitudinal and pitch motion, a model to predict vertical, pitch or longitudinal tractor vibration must include both vertical and longitudinal tyre characteristics. Likewise a model to predict the lateral or roll motion must include both the lateral and vertical tyre characteristics.

The only dynamic measurements of agricultural tyre characteristics in the horizontal directions which appear to be available are those by Stayner and Boldero (1973). These measurements were made with a stationary tyre. The damping in the longitudinal and lateral directions was found to increase with vertical tyre load. The longitudinal tyre stiffness was also found to increase but the lateral stiffness appeared to be independent of load. Inflation pressure had little effect on the longitudinal tyre stiffness but possibly increased the lateral stiffness. Both longitudinal and lateral stiffness increased with tyre wear. Stayner and Boldero suggest that the tyre longitudinal characteristics are dominated by bending in the tyre lugs.

Measurement of the dynamic responses of vehicles with rolling and stationary tyres has indicated that tyre damping in the longitudinal and lateral directions is very dependant on rolling speed. Consideration of the slip between tyre and ground surface suggests that the tyre should be modelled not as a Voigt-Kelvin unit but as a Voigt-Kelvin unit in series with a viscous damper. The damping coefficient of this additional unit is likely to be inversely proportional rolling speed (Lines 1987). Crolla, Horton and Stayner (1990), using a simplification of this form of tyre model to describe the lateral and longitudinal tyre characteristics, have shown that significant improvements in the prediction of vehicle vibration are possible. This is a very important aspect of tyre modelling since it affects the determination of vibration in all directions. It appears to be a significant source of vibration energy dissipation which varies with the driving speed.

#### 1.10 Conclusions

Ground induced ride vibration on agricultural tractors is a significant problem. It causes discomfort and may, in the long term, cause injury to tractor drivers. It causes high stress levels in the machines, and limits the efficiency with which they can be used. There are several possible methods of reducing this vibration but the development of any of these would be simpler and quicker with a reliable means of predicting ground induced vibration.

At present the accuracy of such vibration predictions is poor due to inadequate knowledge of tyre behaviour. Some studies of tyre behaviour have been made which reveal that rolling tyres behave very differently from stationary tyres. There is very little information available concerning the dynamic behaviour of rolling agricultural tyres. Further research into the way agricultural tyres behave would enable more accurate prediction of vibration and of the effectiveness of vibration reducing measures.

The radial, the tangential and the lateral tyre characteristics are all areas which require study. It is possible to test the effect on vibration simulation of improved radial tyre characteristics in isolation from the horizontal characteristics by measuring and predicting the vibration of a vehicle excited only in the vertical direction. This could be achieved with a carriage with only one wheel or with a symmetric two or four wheel carriage where each wheel receives the same excitation.

Following measurements of the radial characteristics of tyres, detailed studies of the longitudinal characteristics of tyres will be required in order that the vertical, pitch and longitudinal vibration of tractors can be predicted with confidence.

### 1.11 Research Objectives

The objective of the research described in this thesis was to show that the accuracy of tractor ride vibration simulation could be significantly improved by making use of the radial suspension characteristics of rolling tyres instead of stationary tyres, as was the practise at the time. The accuracy limitations of such a simulation needed to be established since this could indicate the extent to which accurate modelling of the horizontal plane characteristics of rolling tyres were also required.

In order to achieve this it was necessary to

establish clearly that rotation the tyres affected the vibration characteristics of the vehicle,

design and build an experimental machine which would enable the radial characteristics of a range of agricultural tyres to be measured as they rolled over both hard and yielding surfaces,

to measure the radial suspension characteristics of tractor tyres and identify the variables which significantly affected these characteristics and to

test the tyre data collected in vibration simulation models to show how far it improved to simulation accuracy.

Following this work it was envisaged that further work would be required by other researchers to establish a similar basis of understanding of the lateral and longitudinal tyre characteristics and so further improve vibration simulation accuracy.

## 2 Ride vibration transfer functions between ground and tractor

### 2.1 Introduction

The available literature at the start of this research clearly indicated differences between rolling and stationary tyres. However all tractor vibration simulation made up to this time had relied on the measured characteristics of stationary tyres. Research had suggested that the differences between rolling and stationary tyre characteristics could be a source of inaccuracy in the simulation results, yet no observations had been made of the effect that this change in tyre behaviour had on tractor vibration. It was considered that direct observation of the difference in tractor behaviour with stationary and rolling tyres was necessary. This would confirm the importance of the effect and so provide evidence which would enable a program for measuring the characteristics of rolling tyres to be initiated confident that the differences between rolling and stationary tyres were large enough to justify the considerable investment of time and money required.

The vibration characteristics of the tractor can be described by the transfer function between the elevation of the profile under the tyre contact patch and the vibration of the tractor. In order to measure the transfer functions of the tractor between the ground contact patch at one of its wheels and the vehicle body response, it was necessary to excite one wheel with a signal which was independent of the signals at the other wheels. This situation does not occur during normal tractor driving because on each side of the tractor the front and rear wheels pass over virtually the same ground profile. These inputs are therefore correlated. There is also likely to be a correlation also between the left and right wheel tracks of track. Two different methods which were used to create a situation where wheel inputs were un-correlated and so such transfer functions could be measured.

### 2.2 Laboratory method

An agricultural tractor was placed on an hydraulic test stand which enabled each of its wheels to be independently vibrated in the vertical direction by an hydraulic actuator. This test stand has been described by Jungerberg (1984) and is shown in use in Figure 5. The surface on which each of the tractor wheels rested was covered by small diameter (50 mm) rollers so that the wheels could be rotated. On this stand the tractor

wheels were driven under tractor power at various speeds. The tractor was excited by vibration under one or more wheels. The vertical acceleration of the pads on which the wheels rested was measured, as was the acceleration of the tractor body, measured on the cab floor under the operator's seat in the vertical, longitudinal, lateral, roll, pitch and yaw directions. From this information the transfer functions of the tractor through each wheel could be calculated at various tyre rolling speeds and vibration amplitudes with and without the presence of un-correlated vibration input at the other wheels. The wheel for which the transfer function was being calculated was excited with random excitation which had a reasonably flat acceleration power spectrum from 0.5 to 12 Hz. The other three wheels were either not excited or excited with vibration, approximately equal in acceleration rms to the first wheel. This excitation was similar to that which would be received travelling along a rough track and was correlated accordingly.



**Figure 5** Four ram hydraulic test stand

Advantages of this method of exciting the tractor were that vibration amplitude and driving speed could be independently controlled, the filtering effect of the tyre enveloping the track did not confuse comparisons made between different driving speeds and that long statistically reliable signal lengths could be used and easily repeated. The method produced repeatable and well correlated measurements.

The disadvantage of this method was that the excitation used was somewhat removed from reality. Because the rollers under the tyres were free to rotate in response to the tyres rather than being constrained to rotate at a given velocity by the momentum of the tractor, any longitudinal deflection of the tyre is likely to have resulted in

acceleration of the rollers rather than the tractor. The longitudinal vibration of the tractor was also affected by the horizontal steel hawser which restrained it from driving off the front of the test stand. Since the longitudinal vibration of the vehicle is linked by the inertia of the tractor to the pitch and vertical vibration measurement in these other two directions too may not be fully representative of the real situation. A further drawback to this test method is that in real life a change of ground level under a wheel is always accompanied by a change of gradient whereas on the test stand the surfaces remained level. The response of a tractor wheel to such a change of gradient is not yet fully understood, but one would expect it to affect the longitudinal, and hence also the pitch and vertical response.

### 2.3 Test track method

The transfer function characteristics of a different tractor were obtained by driving it over a standard rough track (Lines 1983) with one wheel on the rough profile and the other three on relatively smooth concrete. This was achieved by changing the wheel track width asymmetrically (Figure 6). In this way the main vibration input was through only one wheel, and this input was not correlated with any input from the other three wheels. The transfer function was again measured between the second differential of the ground elevation under the tyre and the acceleration in six directions measured on the cab floor under the driver's seat. The ground elevation was measured simultaneously with the tractor acceleration, using an optical non-contacting displacement transducer described by Harral and Cove (1982). A similar tractor had been excited by a vertical input at one wheel only using a hydraulic actuator, from which comparable non-rolling transfer functions could be calculated. In this way comparison could be made between the response of the tractor when the tyres were rolling, and when not rolling. Further details of this experiment are given by Lines (1985).

The advantages of this method are that it very closely represents the actual situation of a tractor driving on a rough surface. The disadvantages are that only one rather short (100 m) track could be used which resulted in noisy and somewhat unreliable transfer function measurements. It was not possible to alter the profile or amplitude of either the rough profile for the measured wheel or the smooth profile for the other three wheels. In order to interpret the measurements made at different speeds it was necessary to model the spatial filtering effect of the tyre as it enveloped the ground profile. The filtering model used, smoothly decreased the levels of the ground excitation as its frequency increased, so that a 50% decrease in input level was reached as the



**Figure 6** Track method used to excite tractor with a rear wheel input (left) and a front wheel input (right)

ground input wavelength approached a length twice that of the tyre contact patch. Details of the filter are given by Lines (1985). To assess the effect which the wheel track asymmetry had on the tractor performance, it was driven with both standard and asymmetric track widths over a track and the measured ride accelerations were compared. These indicated that no significant difference in the vehicle behaviour resulted from the asymmetric track widths.

## 2.4 Results

### 2.4.1 General description

Transfer functions of the stationary tractor showed a highly resonant system which is similar for the two tractors used. Pitch and longitudinal transfer functions showed a common resonance frequency with the vertical and in addition one other resonance. Roll and lateral transfer functions had both of their resonance frequencies in common. The yaw transfer function was less distinct but appeared to share resonance frequencies with roll and lateral. In this way the transfer functions were consistent with linear analysis which shows that the system can be split into two independent sub-systems, one involving vertical, longitudinal and pitch motion, the other involving roll, lateral and yaw motion (Stayner, Collins and Lines 1984).

### 2.4.2 Changes with amplitude

When the wheels were not rolling, changes in the amplitude of the input to the wheels caused significant changes in the transfer functions (Figure 7). In general the natural



frequencies of the system decreased - typically by 10% for a 1:5 increase in r.m.s level, and the transfer function magnitudes decreased. The changes varied in size considerably from one transfer function to another. In most cases transfer functions for the front wheel inputs were more sensitive to amplitude than those for the rear. Since the change in input amplitude represented a proportionally greater deflection of the smaller front tyres than the rear tyres, this is perhaps understandable.

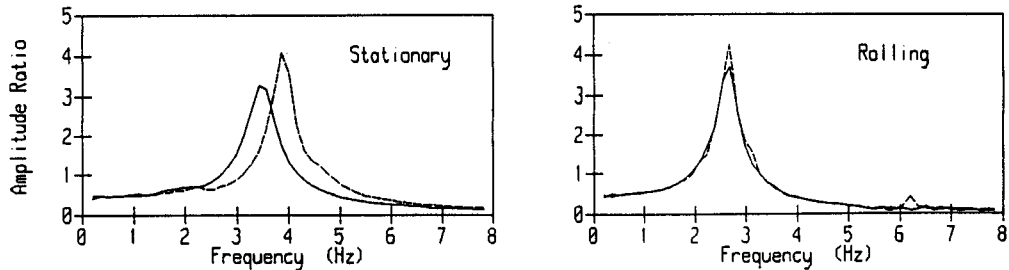


**Figure 7** Transfer functions showing vertical response to high (—) and low (---) amplitudes of rear wheel excitation for stationary wheels (left) and rolling wheels (right)

The effect of changes in excitation level on rolling wheels was much less than on stationary wheels. An increase in the excitation level did not have an observable effect on the natural frequencies but in some cases it increased the level of damping slightly. This effect seemed to be greatest for the front wheels and for low driving speeds.

In the laboratory tests all the transfer functions were measured both with the other three tractor wheels receiving no input, and with them receiving approximately equal amounts of excitation to that of the measured wheel. This excitation was similar to that which might be received travelling along a rough track, and the three inputs were correlated accordingly. There was no evidence that the addition of this extra "noise" in the system changed the transfer functions in any way.

#### 2.4.3 Changes with rolling speed in the laboratory experiment

There were large differences between transfer functions measured with wheels rolling and not rolling (Figure 8). At a tyre rolling speed of 6 km/h the natural frequencies were found to be up to 30% lower than for non-rolling tyres. No significant change could be observed between the natural frequencies at 6 km/h and 11 km/h. This observation is consistent with those of previous authors that tyre stiffness drops sharply at the onset of rolling and thereafter changes only gradually.

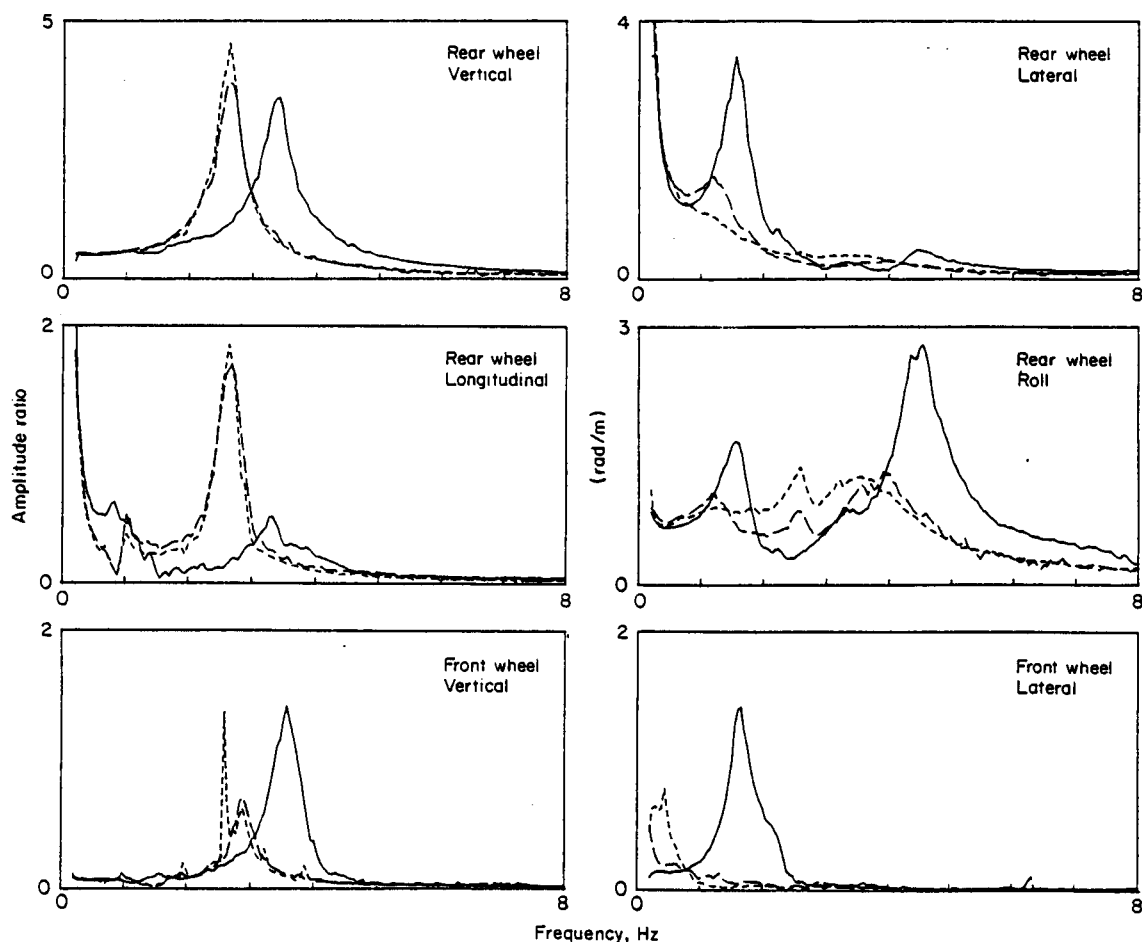


**Figure 8** Laboratory experiment. Ride vibration transfer functions at 0 km/h (—), 6 km/h (---) and 11 km/h (-.-)

The measurements showed large changes in damping as speed varied between 0 km/h and 11 km/h. Damping of the lateral mode increased from about 20% to around 100% of the critical level. Roll and yaw transfer functions showed similar effects. The vertical transfer function showed only a small change in damping. Longitudinal and pitch transfer functions developed very much stronger resonances perhaps indicating a decrease in the damping level.

The transfer functions measured at 6 km/h showed that the damping in the lateral, roll and yaw modes increased gradually with rolling speed. However the apparent decrease in damping in vertical, longitudinal and pitch modes appears to be closely linked to the change in tyre stiffness, varying as it does only slowly with rolling speed after a large the initial change at the onset of rolling. It would seem then, that these two effects originate from two different sources.

#### 2.4.4 Changes with rolling speed on the test track

Measurements of the transfer functions made on the test track produced results that were consistent with reduction of tyre stiffness at the onset of rolling and only slow change thereafter (Figure 9). The decrease in the apparent damping observed in the laboratory experiment for longitudinal and pitch motion was not shown in these measurements. The results showed a progressive decrease in damping with increasing rolling speed. The transfer function measured on the stationary tractor showed a much stronger second resonance than any of the rolling measurements. The increase in damping observed for roll, lateral and yaw movements in the laboratory experiment was only apparent in the test track experiment results for the front wheel of the tractor. The rear wheel transfer function damping did not appear to change substantially.

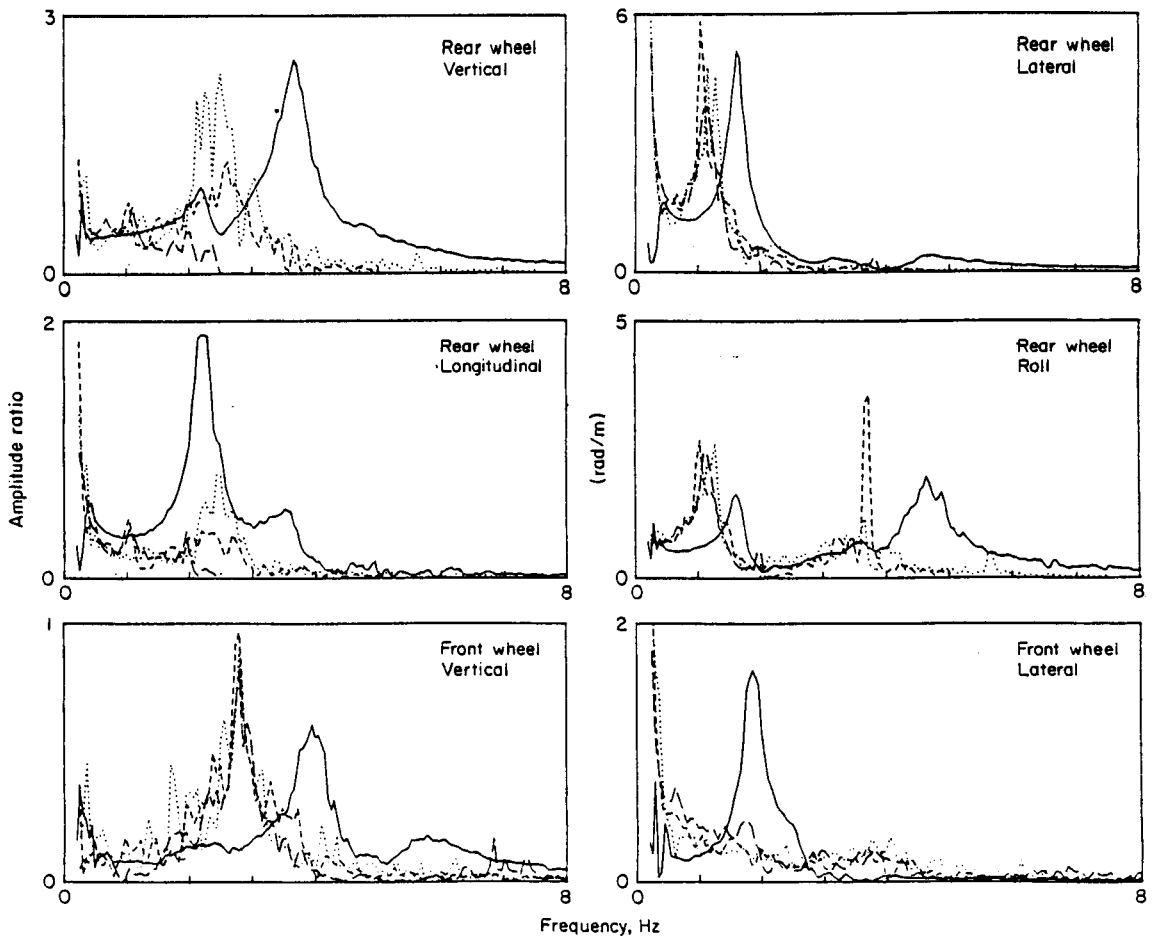


**Figure 9** Test track experiment. Ride vibration transfer functions at 0 km/h (—), 6 km/h (---), 11 km/h (-·-·-) and 15 km/h (.....)

### 2.4.5 Additional excitation

The coherence associated with the measurements made in the laboratory was generally good (Figure 10). However at the wheel rotation frequencies (both front and rear), and at harmonics of these, the coherence dropped, indicating that the tractor was being excited by wheel rotation at these frequencies. At half the tyre lug passing frequency and at the tyre lug passing frequency of each wheel the coherence again dropped. Because of the power of excitation at these frequencies and small variations in the driving speed, these bands of low coherence were wide. Above half of the lug passing frequency the coherence remained much poorer than it was at lower frequencies.

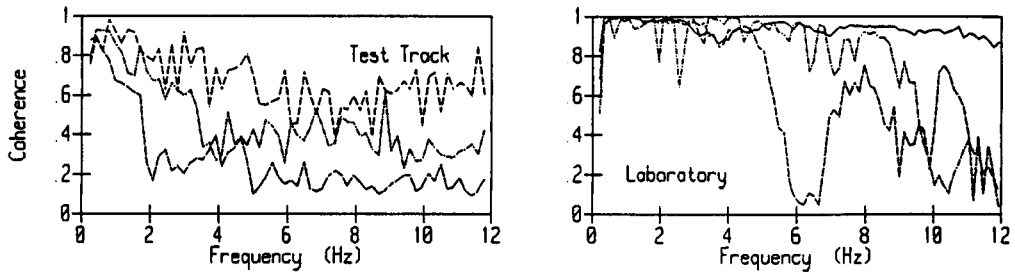


**Figure 10** Coherence between rear wheel input and vertical response in test track (left) and laboratory experiment (right) at 0 km/h (—), 6 km/h (---), 11 km/h (-·-·-) and 15 km/h (····)

The coherence between excitation and response signals measured in the track experiment was much poorer than for the laboratory experiment. In this case it decreased to a very low value at a frequency which appeared to be proportional to driving speed. This frequency however was not obviously related to the tyre lug passing frequency as it was in the laboratory experiment and was lower than the track slat passing frequency. The most likely cause of this low value of coherence was the precision with which the profile of the track was measured. Since the power in the ground surface displacement profile decreases rapidly with increasing spatial frequency, the upper frequency limit of accurate frequency response functions depends on the precision with which the track profiles have been surveyed.

## 2.5 Discussion

These results clearly showed that in order to produce accurate results, ride vibration simulation of an unsprung vehicle must use the characteristics of rolling tyres. The way in which the apparent damping of some modes changes with rolling speed must also be understood and incorporated into the model.

It was noted by Stayner Collins and Lines (1984) that the predicted longitudinal ride vibration for a tractor is closer to the measured vibration if the longitudinal damping of the tyres is increased to a near critical level. It was therefore encouraging to see that the longitudinal damping in the field experiment appeared to be much higher for rolling than non-rolling cases. There is good reason to suppose that the Voigt-Kelvin model which was used by Stayner *et al* to model the longitudinal characteristics of tyres was inappropriate. A spring and damper connected in series is theoretically plausible (Lines 1987). It would provide the additional velocity dependant damping which the results of this experiment indicated exist. Such a model has subsequently been shown to give more satisfactory simulation results by Crolla, Horton and Stayner (1990).

Neither of the experiments described produce reliable well defined transfer function for the tractors in all modes. There were limitations to the results of both experiments originating in the artificial nature of the conditions of the laboratory experiment and in the limitations of the input data for the test track experiment. However the purpose of this experiment was to observe the differences in tractor vibration behaviour between conditions of stationary and rolling wheels. It is very clear from these results that such difference do exist and that they are likely to be large.

The amplitude non-linearity of the rolling tyre transfer functions appear to be small. An important consequence of this is that the principle of superposition is valid, so that the vibration due to the input at each wheel can be computed separately and summed to give the motion of the tractor subjected to all four inputs simultaneously. Because of this it may well be possible to make use of frequency domain methods for simulating ride vibrations, rather than the comparatively slow and complex time domain methods.

## 2.6 Conclusions

The characteristics of rolling tyres are significantly different from those of non-rolling tyres. The tyre stiffness characteristics appear to decrease at the onset of rolling and thereafter to remain relatively constant with further increases in rolling speed. The vibrational energy dissipated by the tyres in some modes of tractor vibration may however increase proportionally with rolling speed. Measurement of the characteristics of rolling tyres is therefore necessary and justified.

Amplitude non-linearities appear to be negligible for rolling tyres and the principle of superposition therefore is applicable.

Wheel eccentricity and tyre lugs excite the tractor at specific frequencies. It appears that at frequencies above half the tyre lug passing frequency, tractor vibration is only poorly correlated with ground excitation.

### 3 Method used to measure the stiffness and damping of tyres

#### 3.1 Introduction

It has been established in the previous chapter that the relevant suspension properties of tyres can be measured only when the tyres are rolling. These measurements could be made in the laboratory by rolling the tyre on a rotating drum or a belt, or by rolling the tyre over real ground surfaces.

Rotating drums are the most common way of measuring tyre characteristics. However the drum must be several times larger than the tyre under test to avoid the curvature of the drum affecting the results. Such a drum size is impractical for agricultural tyres.

A test stand where the tyre rolls on a belt is more complex than a drum device but it can be much smaller. It can be operated at high speeds for long periods of time and since it is a stationary machine in a laboratory, it is easy to instrument and the environmental conditions can be controlled. Such a machine has been successfully used by Kising and Göhllich (1988) and by Kutzbach and Schrogl (1987). A sketch of the machine used by Kising is given in Figure 10. In this machine the entire belt assembly was vibrated by electro-hydraulic actuators. The response of the wheel assembly, which was free to vibrate vertically was measured and used to identify characteristics of the tyre. The wheel assembly was pivoted about a horizontal pivot some distance away from the tyre and additional mass was added to provide realistic tyre loading.

A machine which rolls the tyre over real ground surfaces is more expensive to develop, and may be less convenient to operate and more difficult to control precisely. However it can be used to investigate the interaction between tyres and various types of ground surface which may be both rough and yielding. It can also be used to investigate the lateral and longitudinal characteristics of tyres. The advantages of a field machine were considered to be great enough to justify its development. Such a machine was designed by the author. It is able to measure the suspension characteristics of tyres fitted to a range of driven and undriven tractor wheels in the radial, longitudinal and lateral directions over a wide range of surfaces.

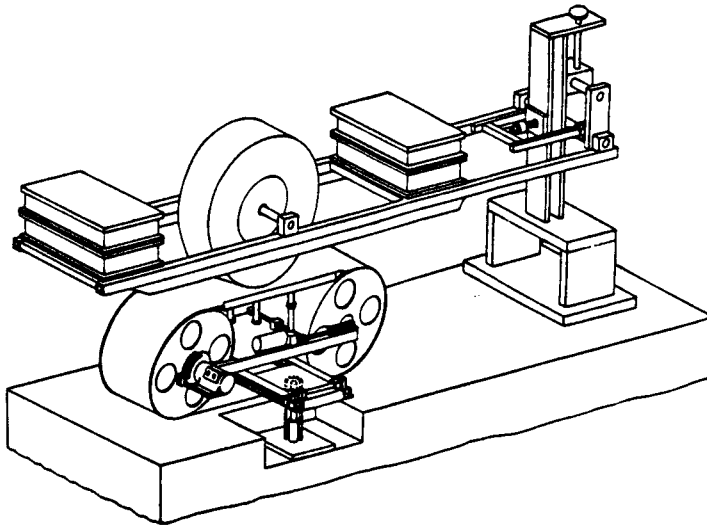


**Figure 11** Sketch of the rotating belt machine (from Kising 1988)

### 3.2 Description of the dynamic tyre testing vehicle

The dynamic tyre test vehicle (Lines and Young 1989) comprises a driven test wheel mounted on an instrumented carriage behind an agricultural tractor. The tyre carriage is vibrated by reacting it against a large inertial mass. The force on the test wheel axle and the axle acceleration are measured and used to calculate the suspension characteristics of the test tyre. A photograph of the machine is given in Figure 12 and a schematic diagram showing the components is given in Figure 13. These components are identified in the text with numbered superscripts.

#### 3.2.1 Power Source

The vehicle is based on a standard 53 kW forward control Deutz Intrac 2004A tractor<sup>(1)</sup>. Because of the forward position of the cab a load carrying platform exists over the rear wheels of the tractor. On this platform was mounted a second cab<sup>(2)</sup> providing a working place for the experimenter and room for the hydraulic and electronic instrumentation and controls. Some of the simpler instrumentation controls were also duplicated in the front cab so that for some experiments the vehicle could be operated by a single person from the tractor driving seat. Another reason for selecting this tractor on which to base the dynamic tyre test vehicle was that it has two independently controllable power take off shafts. The tractor carries hydraulic power-packs<sup>(3)</sup> on both front and rear power take-off shafts to power the various hydraulic components of the machine. It also carries a small generator to provide mains power for the instrumentation. The driving speed of the vehicle and test wheel is determined by the



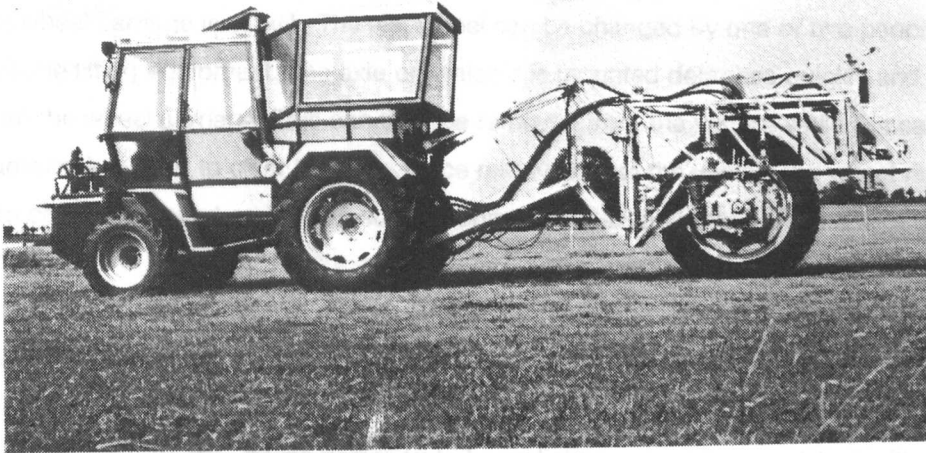


**Figure 12** AFRC Engineering dynamic tyre testing vehicle

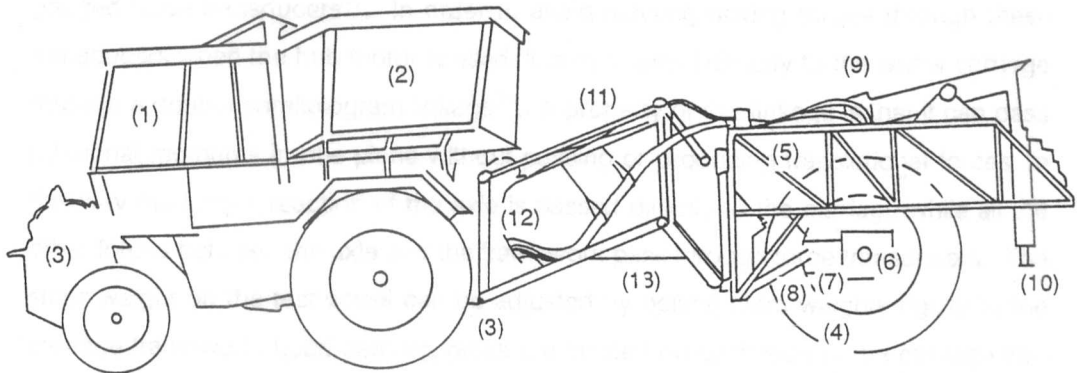


**Figure 13** Schematic diagram of tyre test vehicle

tractor engine speed and gear selection. When the test wheel is being driven the tractor acts as a braking unit, absorbing energy through its wheels and transmission system and recycling it to the hydraulic power-packs.

### 3.2.2 Test wheel

The test wheel<sup>(4)</sup> can vary in size from a diameter of 1.8 m and width of 0.5 m, down to the smallest size which can support a load of 11 kN. A tyre larger or wider than these sizes would not fit within framework of the wheel carriage<sup>(5)</sup>. The diameter of the

hydraulic hub motor<sup>(6)</sup> which is used to drive the wheel demands that the internal diameter of the wheel rim be at least 0.5 m. Smaller wheels than this can be used by discarding the hydraulic motor in favour of an undriven axle. The restriction on wheel size then arises from the load carrying capacity of the wheel. The minimum weight of the wheel carriage is 11 kN. The test wheel can be changed by one or two people with suitable lifting equipment. The axle on which it is mounted detaches quickly and easily from the wheel carriage. This can then be removed from the vehicle while the carriage framework is lifted to clear the tyre. Once removed from the vehicle the wheel rim and tyre can be removed and, using suitable adaptor plates, any other rim and tyre can be attached.

### 3.2.3 Wheel carriage

The wheel carriage<sup>(5)</sup> is constructed as a space frame structure from steel rectangular hollow section (RHS). It was designed to be as light as possible, consistent with being able to transfer the forces placed upon it. It was necessary to cross brace the framework to ensure that the frequencies of resonances between the axle and the framework were substantially above the frequencies at which tyre measurements were to be made. The carriage is connected to the test wheel axle at each side by strain gauged force transducers<sup>(7)</sup>. In order to avoid reacting driving torque through these transducers when the hub motor is used, it is transferred directly to the wheel carriage through a double parallelogram linkage<sup>(8)</sup>. A property of this linkage is that it can pass rotational moments in one plane without passing or producing translational forces. In this way the torque reaction of the axle is passed directly to the carriage while all the other forces between the axle and the framework pass through force transducers. The static weight on the test wheel can be adjusted by bolting extra weights rigidly to the carriage framework. Load carrying racks are located on each side of the carriage into which steel rods can be inserted up to a total addition load of 500 kg. Also mounted on the carriage is an electro-hydraulic ram<sup>(10)</sup>, and a lever arm carrying the inertial mass<sup>(9)</sup> used to drive the vibration of the test wheel.

### 3.2.4 Main linkage

The carriage is connected to the tractor by the main linkage<sup>(11)</sup> mounted on a vertical pivot<sup>(12)</sup>. This linkage also has a double parallelogram configuration so as to allow the test wheel freedom to move independently of the tractor in the vertical, longitudinal and lateral directions. Because of the linkage design, there is no weight transfer between tractor and test wheel when traction is applied either to the test wheel or to the tractor rear wheels. For vertical and lateral excitation of the tyre, longitudinal freedom between

the tractor and test wheel is not required so the central angle of the double parallelogram linkage is locked<sup>(13)</sup>. This in effect turns it into a single parallelogram linkage. Since this linkage is almost 2 metres long, vibration in the vertical direction does not cause a significant amount of longitudinal motion. With the central angle of the linkage locked and the two ends of the parallelogram linkage level with each other, driving thrust from the test wheel can be transferred through to the tractor. In order to enable the linkage to be level regardless of the size of tyre being used, a sliding adjustment is provided between the carriage and the main linkage which can be altered by a hand operated lead screw.

When the tyre is being vibrated in the longitudinal direction the lock on the central angle is replaced by a spring. This decouples the test wheel from the tractor for the test vibration frequencies, yet still enables the driving thrust of the test wheel to be passed through to the tractor. This spring is set in series with a small hydraulic ram which is used to maintain a constant linkage angle regardless of the thrust being generated by the test wheel.

### 3.2.5 Vibrator

The carriage is vibrated against an inertial mass<sup>(9)</sup> using an electro-hydraulic actuator<sup>(10)</sup>. The inertial mass is adjustable in six increments from 250 kg to 400 kg by adding extra weights. The adjustment is necessary to reduce the load on the test wheel when this is required, and yet, under other circumstances to enable large amplitudes of vibration at low frequencies to be created.

The actuator is capable of producing 20 kN force and absorbing 20 kW of tractor engine power. It has 200 mm of stroke available which, because of the leverage arrangement, results in over 250 mm of motion at the mass. Motion of the actuator is controlled by conventional electro-hydraulic control system with input from an electrical signal provided by the experimenter, and position feed-back directly from the position of the actuator ram measured by an internal displacement transducer (LVDT). Electro-hydraulic valves require very clean oil in order to work reliably. To meet this requirement the oil passes through three filters between leaving the oil tank and entering the actuator. Long hoses are provided so that the ram can be removed from the vehicle during servicing or re-positioned on the carriage without breaking into the system and so risking introducing contamination.

Using this system the wheel can be excited with sinusoidal vibration or narrow band random vibration over a range frequency from 1.5 to about 6 Hz. The actuator and inertial mass assembly can be positioned so as to produce vibration in the vertical, longitudinal or lateral directions (Figure 14).

When used to vibrate the carriage in the vertical direction, the inertial mass is positioned directly over the centre of the axle. The position of application of the vibration force to the carriage is close to the centre of the inertial mass. By having the point of application of the force, the centre of mass of the carriage and the tyre contact patch in a line, pitching and rolling motion of the carriage is reduced to a minimum.

When used to produce longitudinal or lateral vibration of the test wheel this ideal geometry cannot be achieved since the centre of mass of the carriage cannot be lowered to the height of the tyre contact patch. It can be shown that the actual height at which the force should be applied to minimise rolling motion of the carriage in this configuration varies with the characteristics of the tyre and the frequency of the vibration. However for most circumstances a position close to the ground is sufficient. Therefore when used to produce lateral and longitudinal vibration it is necessary to use an extension to the lever arm hold the inertial mass close to the ground.

The moment of inertial of the arm can be increased by adding weights to the other end of the lever arm. The combined reaction of the carriage to the torque provide by accelerating this moment of inertia and force provide by accelerating the inertial mass has the effect of moving the point of application of the net force beyond the position of the inertial mass. This can be used to position the force being applied very close to, or even below the ground level if this is required.

### 3.2.6 Measurement transducers

Measurements of the tyre characteristics is based on a knowledge of the acceleration of the axle and the force required to accelerate it.

The acceleration of the axle is sensed by strain-gauge type accelerometers positioned at each end of the axle. Since the axle is rigid at the frequencies of interest, the mean of the acceleration values detected by these two transducers is the acceleration at the centre of the axle.

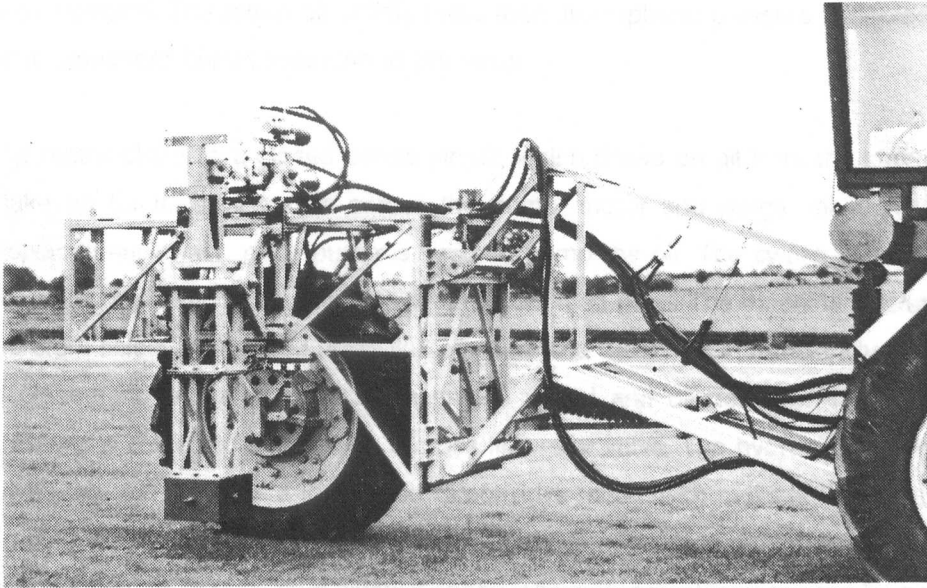


**Figure 14** Actuator and inertial mass positioned on dynamic tyre test vehicle to produce lateral vibration

In the early stages of development of this machine, triaxial force transducers were used to sense axle force. These were 'L' shaped strain gauged beams similar to those used to sense lower link forces in three-point linkage dynamometer described by Schöltz (1966). It was found however that these transducers were not stiff enough as they allowed the axle mass to vibrate against the carriage mass with a natural frequency of about 5 Hz. This resonance made accurate measurements impossible. Subsequently commercially available strain gauged load beams were used<sup>(7)</sup>. These transducers are stiffer than the previous transducers by a factor of ten and so this moved this natural frequency of vibration away from the frequencies of interest. The load beams measure force in one direction only so they have to be oriented in the direction required. Two load beams are used in parallel at each end of the axle in order to provide good axle location.

### 3.2.7 Hydraulic circuits

Two independent hydraulic circuits are used on this machine, one driving the wheel motor and one driving the electro-hydraulic actuator.

The actuator circuit derives its power from a power pack mounted around the front power take off shaft of the tractor. The oil is filtered before being drawn through a fixed displacement gear pump. Oil pressure is maintained at about 140 bar by a pressure control valve which passes excess oil back to the tank via a heat exchanger. Oil flow is similarly controlled by a three port flow control valve. Large accumulators close to

the pressure and exhaust ports of the ram ensure adequate oil flow during periods of peak demand. The return oil at little more than atmospheric pressure is cooled in the heat exchanger before returning to the tanks.

The motor circuit is a closed centre circuit, which draws on oil from the tank only to make up for leakage losses across the pump, motor and purge valve. A variable displacement swash plate pump is used to pump the oil. The swash plate angle is controlled by a servo mechanism with pressure feed back. The machine operator can therefore select the desired cross line pressure and the pump automatically adjusts its displacement to match changes in engine speed and oil demand. The cross line pressure is limited to 310 bar by a cross line relief valve. The hydraulic motor which drives the test wheel is a low speed direct drive motor with multiple internal pistons working on an external cam. This motor is capable of working at high torque levels at all speeds up to its maximum allowed speed. The motor displacement can be changed from 1.979 l/rev 0.990 l/rev by disengaging some of the pistons in the motor. This change can be made using a hydraulic control line from the operators position. It enables high rotational speeds to be achieved using a smaller flow of oil.

### 3.2.8 Instrumentation

The four force transducers and two accelerometers are connected to suitable amplifiers in the cab. Analog voltage signals representing these quantities are then manipulated by a addition, subtraction and amplification to provide signals representing the wheel rim acceleration and the force at the tyre contact patch. Signals representing these quantities are recorded by an FM data tape recorder for analysis later. An rms meter is used to monitor the axle acceleration to in order to achieve constant levels of acceleration on the axle regardless of changes in the tyre characteristics.

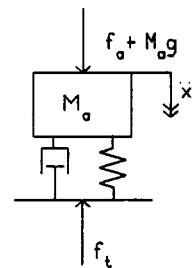


**Figure 15** Free body diagram of forces on axle

The force at the contact patch is derived in the following way. In the vertical plane the only external forces acting on the axle and tyre are the measured force applied by the force transducers to the axle ( $f_a$ ), the ground reaction force on the tyre ( $f_t$ ) and the gravitational force ( $M_a g$ ). The imbalance of these forces results in acceleration of the axle and tyre assembly  $\ddot{x}$ . The ground reaction force can therefore be calculated as

$$f_t = M_a \ddot{x} - M_a g - f_a$$

where  $M_a$  is the mass of the axle and tyre, typically about 600 kg. The mass of the part of the tyre which does not move with the axle is very small compared with this mass and is neglected. In the above equation the gravitational force can also be neglected since it is a steady state force with no component at the frequencies of interest. A voltage signal representing the axle acceleration  $\ddot{x}$  is amplified by a factor representing the axle mass. The signal representing the axle force  $f_a$  is then subtracted from this signal, resulting in a signal representing the force at the tyre contact patch  $f_t$ .

The instrumentation system used to obtain the tyre force  $f_t$  and the axle acceleration  $\ddot{x}$  is shown schematically in Figure 16.

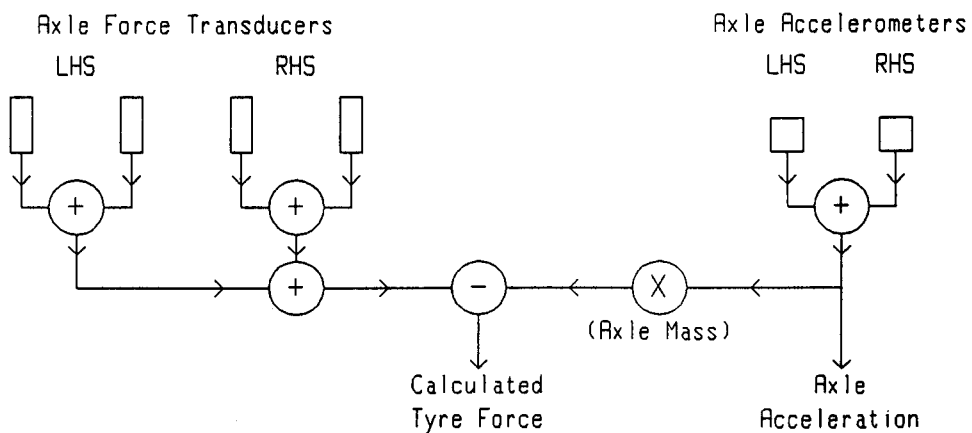


**Figure 16** Diagrammatic representation of the measurement system

### 3.2.9 Calibration

The calibration of the accelerometers and their amplifiers was checked regularly by inverting them to create a 2 g acceleration. The calibration of the force transducer amplifiers was checked using a precision dummy transducer. The adjustment of the other amplifiers was also regularly checked using known voltages. The most critical part of the system calibration is to ensure that the ground reaction force is obtained correctly, since this involves the subtraction of two similar quantities and is therefore ill conditioned. This part of the system was therefore checked on a daily basis in the following way. The test wheel was placed on a calibrated force plate. The actuator was then driven with random noise, band pass filtered between the frequencies of 1 and 8 Hz. A transfer function was then calculated between the force signal from the force plate and that derived by the instrumentation of the experimental machine. The magnitude of the transfer function was required to be  $\pm 3\%$  and the phase  $0 \pm 1$  degree between the frequencies of 2 and 6 Hz. For a tyre with a stiffness of 230 kN/m and damping of

2.4 kNs/m (as in the example given on page 44) this is equivalent to an error in stiffness of  $\pm 3\%$  and in the damping of  $\pm 10\%$ . This checking procedure ensured that ground reaction force when the test wheel was rolling was calculated accurately and that the whole instrumentation system was working correctly. An example of the calibration transfer function calculated between the force measured on the force plate and that calculated by the test vehicle instrumentation is given in Figure 17.

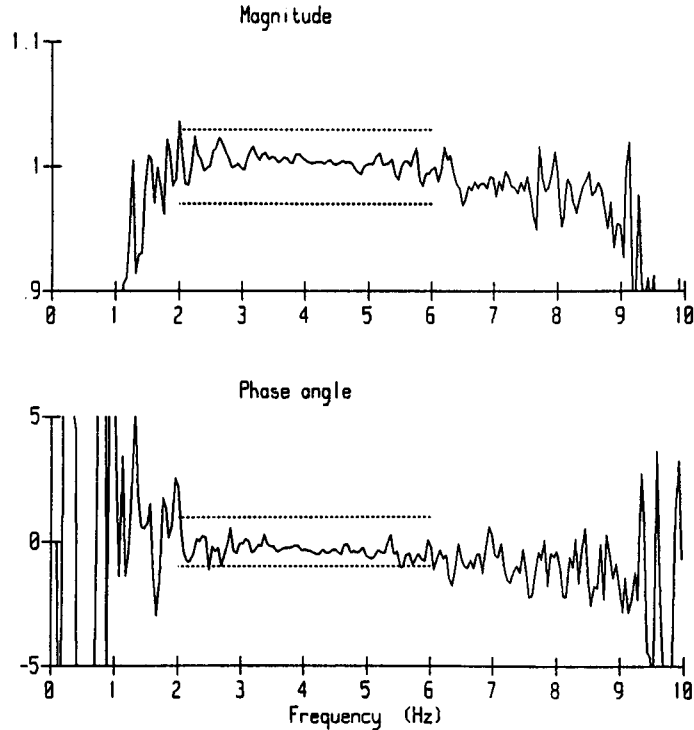


**Figure 17** Example of calibration transfer function between calculated and measured tyre force. Limits of  $\pm 3\%$  and  $\pm 1^\circ$  are shown in dotted lines

### 3.3 Data analysis

#### 3.3.1 Flat ground

When the test wheel is run on flat ground the vibration of the tyre is almost entirely due to the reaction force against the vibrating inertial mass. Under these circumstances the transfer function between the axle acceleration and the tyre force is calculated. This is the apparent mass (force/acceleration). From this can be derived the mechanical impedance (force/velocity) and the dynamic stiffness (force/displacement). The real parts of the mechanical impedance and dynamic stiffness represent apparent damping and stiffness of the tyre respectively. This can be demonstrated as follows.



If we assume that the tyre force signal,  $f_t(t)$  is made up from the force generated by a spring stiffness ( $K$ ) and the damping coefficient ( $C$ ) as the axle moves with displacement  $x(t)$  and velocity  $\dot{x}(t)$ , plus some un-correlated force  $n(t)$  due to measurement noise and non-linearities, then the relationship can be written as

$$f(t) = Kx(t) + C\dot{x}(t) + n(t), \dots\dots\dots 1$$

where both the stiffness ( $K$ ) and the damping ( $C$ ) may be slowly varying with frequency. Taking the fourier transform of both sides of the equation gives

$$F(\omega) = KX(\omega) + C\dot{X}(\omega) + N(\omega), \dots\dots\dots 2$$

and since  $\dot{X}(\omega) = j\omega X(\omega)$ , equation 2 can be written as

$$F(\omega) = (K + j\omega C) X(\omega) + N(\omega), \dots\dots\dots 3$$

where  $F(\omega)$ ,  $X(\omega)$  and  $N(\omega)$  are the transforms of  $f(t)$  and  $x(t)$  and  $n(t)$  respectively and  $j$  is the square root of -1.

Multiplying both sides of this equation by the complex conjugate of  $F(\omega)$  produces

$$G_{FF} = (K + j\omega C)G_{FX} + G_{FN}, \dots\dots\dots 4$$

where  $G_{FX} = F(\omega)^* X(\omega)$ , similarly for  $G_{FF}$  and  $G_{FN}$  and where  $F(\omega)^*$  is the complex conjugate of  $F(\omega)$ .

Dividing each side by  $G_{FX}$  gives a representation of the transfer function between  $x(t)$  and  $f_t(t)$ ,  $H_{FX}$

$$H_{FX} = \frac{G_{FF}}{G_{FX}} = K + j\omega C + \frac{G_{FN}}{G_{FX}} \dots\dots\dots 5$$

Since  $F$  and  $N$  are un-correlated, averaging over several estimates reduces  $G_{FN}$  to zero

$$H_{FX} = \frac{\overline{G_{FF}}}{\overline{G_{FX}}} = K + j\omega C \dots\dots\dots 6$$

$H_{FX}$  is the dynamic stiffness of the system. This is related to the mechanical impedance  $H_{F\dot{X}}$  and the apparent mass  $H_{F\ddot{X}}$  by the relationship

$$\omega^2 H_{F\ddot{x}} = j\omega H_{F\dot{x}} = H_{F_x} \dots\dots\dots 7$$

So the real part of  $H_{F_x}$  represents the tyre stiffness,  $K$

$$\Re [H_{F_x}] = \Re [\omega^2 H_{F\ddot{x}}] = K \dots\dots\dots 8$$

and the real part of  $H_{F_x}/j\omega$  represents the tyre damping,  $C$

$$\Re [H_{F_x}/j\omega] = \Re [j\omega H_{F\dot{x}}] = C \dots\dots\dots 9$$

Values for the stiffness and damping coefficient of the tyre under test were therefore obtained from the transfer function between the axle acceleration and the tyre force. The real and imaginary parts of the transfer function were evaluated at the frequency at which the axle was being excited. The tyre stiffness was given obtained by multiplying the value of the real part of the transfer function at this frequency by the square of the frequency (in radians/sec) and the damping coefficient was obtained by multiplying the value of the corresponding imaginary by the frequency. The amplitude of vibration at this frequency was obtained from the power spectrum of the axle acceleration.

### 3.3.2 Uneven ground surfaces

When a tyre is rolling over uneven ground surfaces, the motion of the axle is no longer a measure of the tyre deflection because the height of the tyre contact patch is also changing. However if the tyre is excited with a sinusoidal signal of a certain frequency then at that frequency the vibration of the axle is many times greater than the variation in the ground surface level. As most of the axle vibration at that frequency originates from the inertial mass vibration rather than the ground profile, the correlation between the axle vibration and the ground surface variation is low. Since the correlation is low and the axle motion is so much greater than the ground variation, the axle motion can be used as a measure of tyre deflection. Because of this, when sinusoidal excitation is used tyre characteristics can be measured in the same way as they are on flat ground surfaces. Although the ground roughness does not affect the measurement method, any effect which the ground roughness may have on the tyre characteristics could be detected. Such changes might occur because on rough ground the tyre is in contact with a smaller surface area than on flat ground or because at some points the tyre is deformed more than it would be on flat ground. Any compliance of the ground

surface or energy dissipation of the ground would also be measured and included in the apparent tyre characteristics.

### 3.4 Comparison with alternative measurement methods

Measurement of the apparent mass is only one of several ways which can be used to determine the stiffness and damping of the tyre. Other methods which can be used are

- a) the load-deflection method -measuring the load deflection relationship
- b) the free vibration method -by exciting the system and measuring the natural frequency and rate of decay of the resulting free vibration or
- c) the forced vibration method -by exciting the system with a swept sine or a randomly varying force and measuring the frequency and spectral width of the resulting transfer function peak

The characteristics of a stationary tyre have been measured by the author using the apparent mass method which has been described and the three alternative methods given above. For these measurements the tyre used was a 13.6R38 tyre, inflated to a pressure of 1.38 bar (20 psi) and supporting a load of 1860 kg. The results of this comparison are given in Table I.

**Table I** Comparison of results for different methods of measuring tyre stiffness and damping.

	Stiffness (kN/m)	Damping (kNs/m)
Apparent mass method	450	3.0
Load deflection	330	-
Free vibration	485	3.8
Forced vibration	480	3.6

The measured load-deflection relationship is given in Figure 18. In order to avoid dynamic effects the application of the load must be done slowly. However this allows time for the tyre rubber to creep and so reduces its apparent stiffness substantially. The viscous damping coefficient cannot be measured by this means. The hysteresis of the tyre displayed by this measurement method is dependant on the rate of loading and unloading.

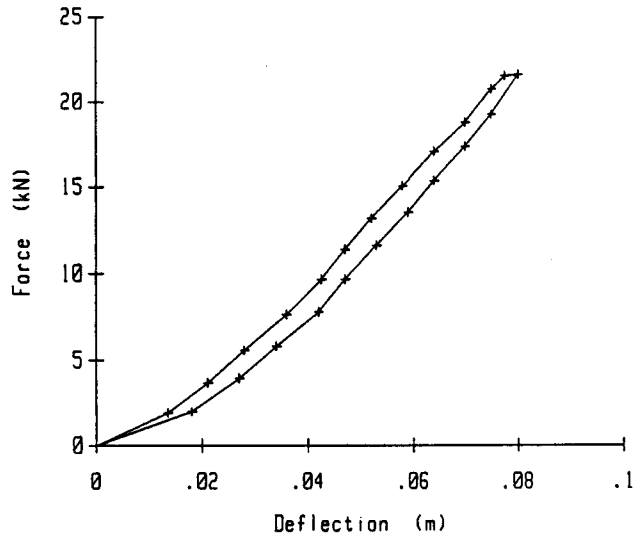


**Figure 18** Load deflection curve for stationary tyre T1

A disadvantage to using the rate of decay of free vibration to measure the damping of a rolling tyre is that there is no way to distinguish between the decaying vibration and additional vibration exciting the system due to ground or tyre irregularities. This method could therefore be expected to provide inaccurate information about rolling tyres.

It is apparent from the results in Table I that the tyre stiffness values obtained from the three dynamic measurement methods are reasonably consistent. The damping value measured by the apparent mass method however is lower than those values produced by the other methods. One reason for this is that in the apparent mass method the phase difference between the force and acceleration is measured. This measures the tyre damping regardless of any other constraints on the motion of the tyre imposed by the linkage etc, so the damping measured is only that which occurs on the tyre side of the transducers. This is in contrast to the other methods which all measure the resulting motion response to the imposed force. These therefore take into account the damping imposed by the linkage between the tractor and the test tyre.

The damping due to the linkages has been estimated by suspending the tyre carriage from steel springs rather than allowing it to rest on the tyre. This experiment gave an upper bound on the linkage damping of 1.2 kNs/m. Some of this damping occurred in the steel springs and the remainder in the linkage. This amount of damping is consistent with the differences indicated between the apparent mass method of measurement and the other methods. The friction force in the linkage is expected to

become even greater when the tyre is being driven and the reaction torque from the wheel motor and the wheel thrust are being transferred through these links.

### 3.5 Tyre measurement procedure

The variables which influence tyre behaviour have been divided into two categories. In one category are those factors which effect the environment in which the tyre works - such as load, inflation pressure, rolling speed or surface type. In the other are those which over a short period are specific to the tyre - such as tyre age or size.

The effect of most of the environmental variables were tested in separate sets of measurements. This increased the number of measurements which were made because in each set of measurements some combinations of conditions occurred which had been measured previously. However this approach was adopted to minimise unknown or uncontrollable variations in conditions. One such factor was the ambient temperature, another the condition of the track surface. Each tyre was subjected to a similar series of tests. The exact procedure followed for each set of measurements was varied slightly depending on the environmental variable being examined, however the general pattern is given below.

Measurements were made of the force and acceleration as the vehicle was driven around a flat concrete track with the inertial mass causing the axle to vibrate at a frequency of 4 Hz and an rms amplitude of 5 mm. About 50 seconds of data was recorded for each measurement of tyre stiffness and damping. Since each value represents an average over several hundred oscillation cycles repeat measurements were not usually made. Exceptions to this were measurements at rolling speeds of 15 km/h or greater where there was insufficient track available to collect 50 seconds of data in one straight run and measurements made at the beginning and end of an experiment to check that there had been no change in the system during the course of the measurements.

During a series of measurements checks would be frequently made to ensure that the conditions remained as constant as reasonably possible. The tyre pressure was maintained constant to within 0.015 bar, the amplitude was measured and variation limited to about 20% and the frequency of vibration of the tyre maintained within 0.1 Hz.

A typical procedure for assessing the effect of, for example, vibration frequency, would be as follows. A range of frequencies was chosen for which a common amplitude of oscillation could be achieved. Recordings of force and acceleration were made at several rolling speeds at the first chosen frequency; the frequency of oscillation was then altered, the amplitude adjusted and the measurements repeated. This continued until measurements had been made at all the frequencies of interest.

The recordings would then be analysed to extract the tyre stiffness, the tyre damping and the rms vibration amplitude. A typical transfer function between the axle acceleration and the tyre force might be as given in Figure 19. The power spectrum of the axle acceleration shows the excitation to be sinusoidal at a frequency of 3.8 Hz. Both the real and the imaginary part of the transfer function are valid at this point, whereas at other frequencies they are completely unreliable due to lack of data. The value of the transfer function at 3.8 Hz can be obtained from the transfer function. In this case it is  $-400-100j$ . It has been shown that the tyre stiffness is given by the real part of the transfer function multiplied by  $-\omega^2$  and that the damping is given by the imaginary part of the transfer function multiplied by  $j\omega$ .

$$\text{Stiffness} = \Re \{ -(2\pi \times 3.8)^2 \times (-400 - 100j) \} = 228027 \text{ N/m}$$

$$\text{Damping} = \Re \{ (2\pi \times 3.8)j \times (-400 - 100j) \} = 2388 \text{ Nm/s}$$

Direct output of the tyre characteristics in engineering units is achieved by ensuring that the input force and acceleration signals are appropriately calibrated.

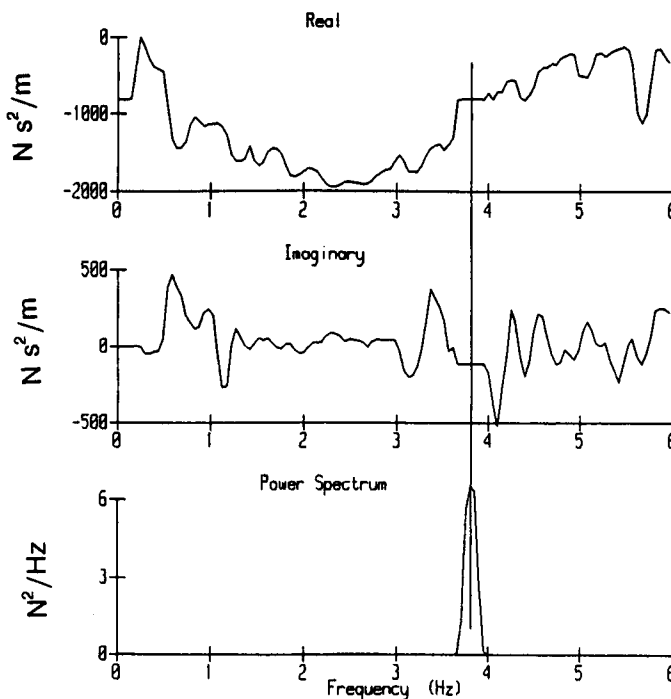


Figure 19 Example of transfer function between axle acceleration and tyre force

In this way the effect on the tyre of inflation pressure, load and deflection, rolling speed, driving torque, amplitude and frequency of vibration have been investigated. Measurements have also been made of the effect of the surface over which the tyre is rolling on the tyre characteristics. Almost all of the information used to investigate these environmental effects was gathered by the author. Data published by Kising (1988) was analysed to provide information about the effect of inflation pressure on tyres of different sizes. Measurements by Kising at rolling speeds above 20 km/h were also used extend the information available concerning the effect of rolling speed on tyre characteristics.

The information necessary to examine the effect of the tyre specific variables was drawn from the data gathered during the measurements described and from data published by Kising. The factors investigated in this way were tyre size, construction, ply rating, age and wear.

Two factors not investigated which could effect tyre characteristics are the effect of tyre ballast and tyre temperature. The effect of ballast has been investigated by Siefkes (1989) and further investigation of this was not attempted. Temperature could also affect the tyre characteristics, however it is under the control of neither the manufacture nor user. It was considered that investigations into this variable would be most effectively made using a laboratory test machine where the environmental temperature could be controlled, rather than a field machine such as that available at to the author.

### 3.6 Reliability of measurements

Reliability of measurements was ensured by regular calibration checks of the measurement system. At the frequencies of interest the tyre force was maintained correct to within  $\pm 3\%$  in magnitude and  $\pm 1$  degree in phase. When it was considered that this level of accuracy might be insufficient, such as when comparing the tyre behaviour at different frequencies, the transfer function obtained from this calibration check was used to correct results.

It has been found that individual measurements of stiffness and damping made under the same conditions and within a few minutes of each other are generally repeatable to less than 10 kN/m in stiffness ( $\sim 4\%$ ) and to 0.2 kNs/m in damping ( $\sim 8\%$ ). When measurements of the tyre characteristics under the same nominal conditions were made in different series of experiments at different times the variations in results can be a little greater. These variations are probably due to variations in the ambient conditions.

### 3.7 Conclusions

A dynamic tyre test vehicle has been built to provide measurements of the suspension characteristics of agricultural tyres. It is a field test machine which is capable of driving over a wide range of agricultural surfaces. Tyre characteristics can be measured in all three axial directions. The driving speed, driving torque, tyre load, excitation frequency and amplitude of vibration can be varied independently. The measurement system used produces measurements of the radial suspension characteristics of tyres which are similar to those produced by other valid measurement methods. However it allows more control over the experimental conditions than other methods.



## 4 Variations in the stiffness of tractor tyres

### 4.1 Introduction

Examination of the literature has indicated that there is no reliable information regarding the suspension characteristics of typical agricultural tyres. Poor information about tyre behaviour is considered to be one of the sources of error in simulations. In order to improve vibration simulation accuracy measurements have been made by the author at AFRC Engineering, Silsoe and by Kising (1988) at the Technical University of Berlin. Measurements by the author have concentrated on the variations occurring between tyres of similar size and construction, while those made by Kising have examined the influence of size and construction.

The objective of these measurements was to establish values of tyre stiffness which could be used for vehicle simulation, to observe the way these values change under different conditions, and try to develop a method for predicting tyre stiffness.

The stiffness of some tyres has been measured and the way that the stiffness is influenced by various factors investigated. These factors have been divided up into two groups. In the first group, are those factors which make up the environment in which the tyres work such as the tyre inflation pressure, rolling speed and tyre load. In the second group are the factors which are specific to a tyre, such as tyre size, tyre age and ply rating.

### 4.2 Description of tyres measured

Details of the tyres used in this investigation are given in Table II. Five rear traction tyres and a ribbed tyre for an undriven front wheel of a tractor were measured in the investigation in Silsoe. They were all made by the same manufacturer. Some of these tyres had been previously used on general purpose tractors for several years and so showed various degrees of wear, however none of the tyres had any major damage to the carcass or sidewalls. In an attempt to quantify the amount of wear each tyre had received the height of the tyre lugs on the centre line of the tyre was measured relative to the tyre carcass between adjacent lugs. There were changes in the tyre rubber composition between the years in which these tyres were manufactured. These rubber

compounds have been numbered, but are not specifically identified. The tyres were measured stationary and at rolling speeds between 0.1 and 25 km/h. The frequency of excitation, the load, torque, inflation pressure and amplitude of vibration were varied.

The tyres measured by Kising in Berlin were all new and came from a variety of manufacturers. Their characteristics were measured stationary and at speeds between 5 and 50 km/h at various inflation pressures.

**Table II** Tyres used in the experiments

Silsoe Experiments						
	Size	Ply	Wear	Age	Lug ht.	Rubber
Rear traction tyres						
T2	13.6R38	6	Much	16 years	20 mm	Type 1
T1	13.6R38	8	Some	11 years	42 mm	Type 2
T4	13.6R38	6	Some	9 years	38 mm	Type 2
T3	13.6R38	8	None	4 years	45 mm	Type 3
T5	13.6R38	8 (146/A8)	None	1 year	45 mm	Type 3
Front Ribbed Tyre						
F1	7.50-18	8	None			
Berlin Experiments						
Rear Traction Tyres (all new tyres)						
AS10	18.4R38	8 (146/A8)	None			
AS2	16.9R34	6	None			
AS12	16.9R34	6	None	(30% lower tread than AS2)		
AS3	16.9R34	6	Buffed	(as AS2 with tread removed)		
AS11	13.6-38	6	None			
AS9	9.5R44	8	None	(Row crop tyre)		
Front Traction Tyres (all new tyres)						
AS6	14.9R24	6 (125/A8)	None	(70% low aspect ratio)		
AS4	13.6R24	6 (6/A8)	None			
AS8	13.6R24	6 (6/A8)	None			
AS7	13.6-24	6	None			
AS1	12.4-28	6	None			

### 4.3 Environmental Factors which affect the stiffness of a tyre

#### 4.3.1 Tyre inflation pressure

At all measured driving speeds and over all recommended operating pressures there is a simple linear relationship between the inflation pressure and tyre stiffness (Figure 20). This linear relationship suggests that the tyre stiffness is the sum of a stiffness which originates in the tyre carcass and a stiffness which is proportional to the inflation pressure.

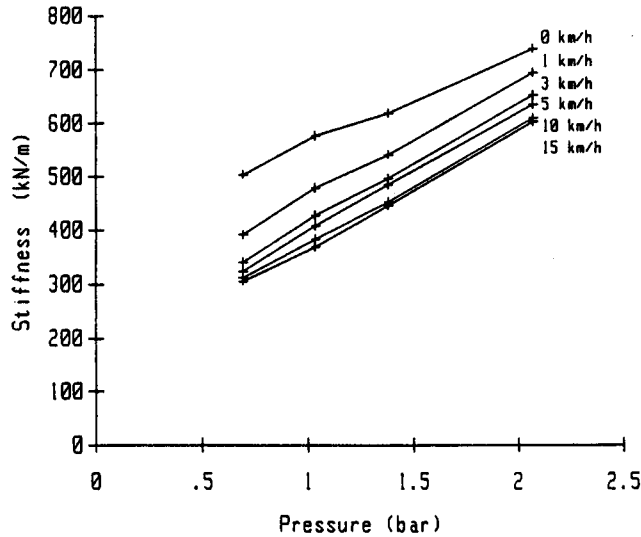


**Figure 20** Variation in stiffness of tyre T2 with inflation pressure

A linear regression has been calculated between the stiffness and inflation pressure from the data measured on the tyres T1 - T5, F1 and from data published by Kising. The zero intercept provides an estimate of the carcass stiffness and the gradient an estimate of the inflation pressure dependence. The coefficient of determination has also been calculated. This gives an indication of how well the straight line fits the data. The coefficient of determination is the ratio of the variation in the data which is explained by this regression, to the total variation in the data. It is the square of the correlation coefficient and so is denoted  $r^2$ . It is calculated as

$$r^2 = \frac{\sum (\hat{y}_i - \bar{y})^2}{\sum (y_i - \bar{y})^2}$$

where  $\hat{y}_i$  represents the expected value of  $y_i$  and  $\bar{y}$  the mean value of  $y$ .

Values for the carcass stiffness, the inflation pressure dependence and the coefficient of determination are given in Table III.

#### 4.3.2 Rolling speed

The stiffness of a rolling tyre depends on the speed at which it is rolling (Figure 21). At very low rolling speeds the tyre stiffness decreases rapidly with speed but at higher speeds this dependence becomes much less. Between rolling speeds of about 10 km/h and 50 km/h the tyre stiffness remains almost constant. The change in stiffness with speed originates in changes in the tyre carcass stiffness rather than changes in the inflation pressure dependence.

**Table III** Carcass stiffness,  $K_c$  (kN/m), inflation pressure dependence,  $\Delta K_p$  (kN/m.bar) and coefficient of determination  $r^2$  for rolling and stationary tyres

tyre	size	stationary			rolling		
		$K_c$	$\Delta K_p$	$r^2$	$K_c$	$\Delta K_p$	$r^2$
T2	13.6R38	393	166	0.99	150	217	>0.99
T1	13.6R38	396	172	0.99	141	175	>0.99
T4	13.6R38				145	179	>0.99
T3	13.6R38	184	200	>0.99	112	177	>0.99
T5	13.6R38	176	174	0.96	80	181	>0.99
F1	7.5-18	96	158	0.96	-3	134	0.99
AS2	16.9R34	145	139	>0.99	112	191	>0.99
AS12	16.9R34	159	129	0.99	112	194	0.98
AS3	16.9R34	125	116	>0.99	55	182	>0.99
AS10	18.4R38	190	116	>0.99	114	197	>0.99
AS11	13.6R38	121	181	0.96	108	201	>0.99
AS9	9.5R44	86	134	>0.99	99	141	>0.99
AS1	12.4R28				134	112	0.96
AS6	14.9R24	125	139	>0.99	131	109	>0.99
AS4	13.6R24				120	98	>0.99
AS8	13.6R24	59	166	>0.99	132	98	>0.99
AS7	13.6R24	94	189	>0.99	131	107	>0.99

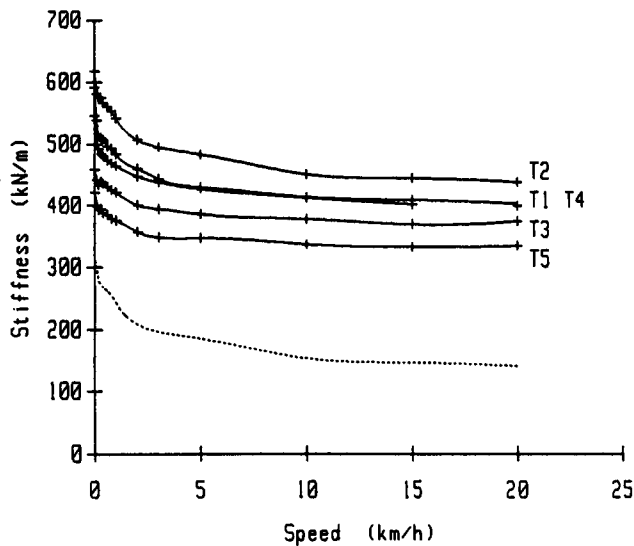


**Figure 21** Variation of stiffness with rolling speed: Tyres T1 to T5 measured at 1.38 bar. The dotted line shows the carcass stiffness of T2

The stiffness of a tyre when it is stationary is usually greater than when it is rolling. However it can be predicted from the results given in Table III that for some tyres at high inflation pressures the stiffness of a stationary tyre might be expected to be lower than that of a rolling one. This has not been observed, however it was not specifically sought.

#### 4.3.3 Tyre load and deflection

Loads of 15.9, 18.3 and 22.6 kN were imposed on the tyres. For the stationary tyre and at low rolling speeds an increase in tyre load gave rise to a small increase in tyre stiffness. At speeds of 10 and 15 km/h no consistent change in stiffness with load was detectable. Figure 22 shows the measured stiffness of tyre T3 at different loads.

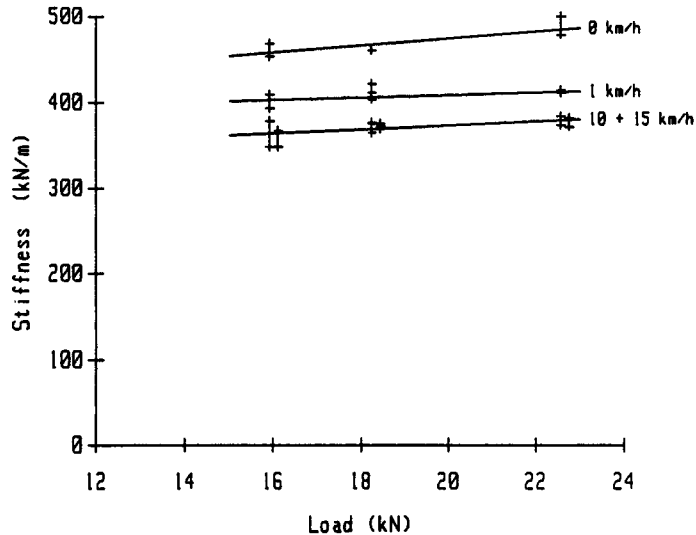


Figure 22 Variation in stiffness of tyre T3 with load at 1.38 bar inflation pressure

#### 4.3.4 Amplitude of vibration

Tyres T1, T2, T3 and F1 were excited with sinusoidal vibration with a range of peak to peak amplitudes between 4 and 30 mm. The variation of stiffness with amplitude for tyre F1 is shown in Figure 23. Linear regressions calculated between the amplitude and stiffness showed changes in stiffness of between +1 and -1 kN/m per mm amplitude (Table IV). The changes measured were only a little larger than the random variation in stiffness measurements so the coefficients of determination are correspondingly low. The stiffness of stationary tyres was found to decrease with increasing vibration amplitude very much more than the rolling tyres. The stiffness of the ribbed front tyre F1 varies more with changes in amplitude than the larger tyres. This is probably because it is a much smaller tyre and so the changes in amplitude represent greater changes in tyre deformation.

#### 4.3.5 Frequency of vibration

The measurements were made between frequencies of 2 and 5 Hz. This frequency range encompasses most of the ground induced ride vibration encountered on agricultural tractors. The stiffness of stationary tyres was found to increase slightly with increasing vibration frequency. Rolling tyres were found to be less dependent on

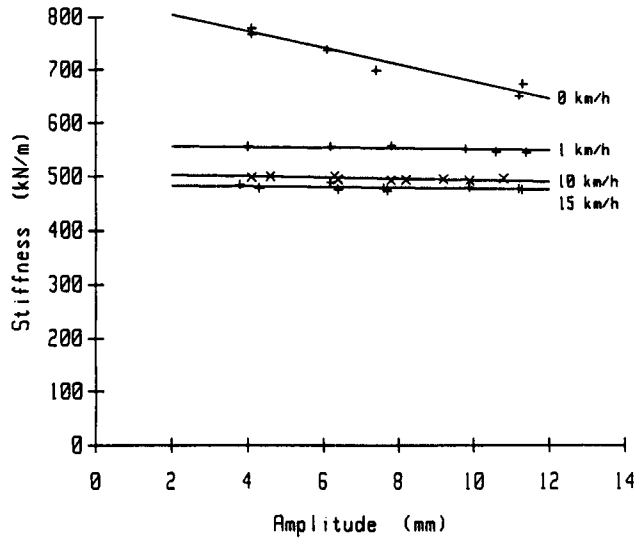


**Figure 23** Variation of stiffness of tyre F1 with amplitude of vibration

**Table IV** Measured variation in stiffness with increasing amplitude of vibration (kN/m per mm). Coefficients of determination given in parentheses

	0 km/h	1 km/h	10 km/h	15 km/h
Tyre T1	-1.6 (0.85)	-0.41 (0.77)	-0.24 (0.68)	-0.39 (0.99)
Tyre T2	-9.8 (0.55)	-0.21 (0.10)	0.53 (0.68)	-0.21 (0.20)
Tyre T3	-2.4 (0.95)	-0.35 (0.53)	0.81 (0.85)	0.76 (0.72)
Tyre F1	-15.5 (0.88)	-1.59 (0.74)	-1.09 (0.53)	-0.86 (0.24)

frequency than stationary ones. Figure 24 shows the stiffness variation of tyre T1 with changing vibration frequency at various driving speeds. The increase is less than 6% per octave when the tyre was rolling at a speed of 10 km/h (2.8 m/s). For the stationary tyre, stiffness increased by about 10% per octave. These stiffness changes are too small to have a significant effect on the vibration of tractors.

#### 4.3.6 Driving torque

The characteristics of the tyres T1, T2 and T3 were measured as they were driven at speeds of 1, 8, 10 and 15 km/h transmitting driving torques of up to 4.7 kNm. None of the tyres showed any significant change in stiffness due to this driving torque. On a two wheel drive tractor this torque would correspond to a driving thrust of 13.5 kN and a power requirement of approximately 40 kW at 10 km/h. This thrust is typical of that required to pull a three body plough in light soil. Therefore the results may not be valid for very high draught forces, however this is not a serious limitation since ride vibration problems occur mostly at high rolling speeds and low draught forces.

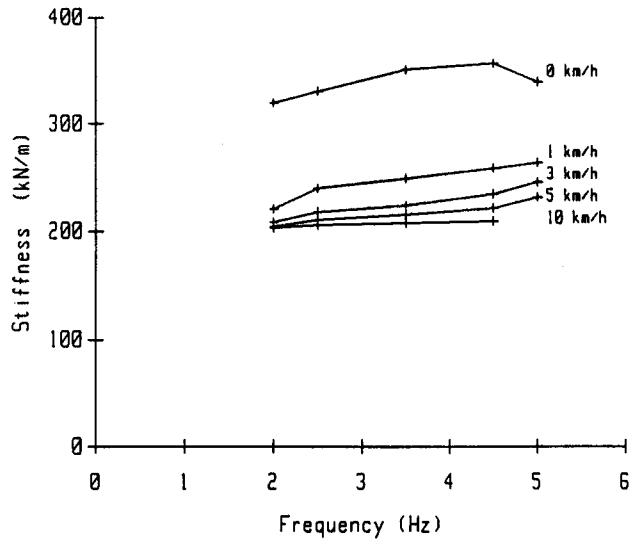


**Figure 24** The stiffness variation of tyre T1 with changing vibration frequency at various driving speeds

#### 4.3.7 Surface

The stiffness of tyre T5 was measured as it rolled over a range of typical agricultural surfaces. Over most surfaces the tyre behaved as if it was slightly softer than when on a flat concrete surface. A description of the surfaces and the effect on the stiffness is given in Table V. Probably the most remarkable result in this table is the drop in stiffness which occurs on the artificial rough track. This track is used in British, International and EEC standards to create typical tractor vibration. It is constructed of wooden slats 80 mm wide, with each slat separated from the next by a gap of 80 mm. It is on this track that many of the tests used to validate tractor vibration simulations have been made.

Tyres on this surface probably behave differently because of differences in the way the tyre deforms. The tread bars of the tyres are several centimetres high, so bending of the tread band introduces shear stress in the tread bars if they are unable to move over the surface on which they are resting. Such bending across the tyre occurs both as the tread band flattens to conform to the surface on which it is resting and in also response to flexing of the side walls during vibration. If this stress can to some extent be relieved then the tyre stiffness could be expected to be lower. Wooden slats, polished by the passage of tyres, are likely to allow the tyre tread bars to slide over them much more easily than a concrete surface. Even if no sliding takes place the stress will be less since only half of the tread surface is in contact with the track. This hypothesis could be tested by measuring the stiffness of a tyre while rolling on a slippery surface such as ice or metal lubricated with detergent.

#### 4.4 Factors dependent on the choice of tyre

##### 4.4.1 Tyre size

Table III gives the carcass stiffness and inflation pressure dependencies for all the tyres under consideration. This has been derived from linear regression on the experimental results and on data published by Kising. Figure 25 shows this data for rolling tyres in a graphical form.

**Table V** Effect of different ground surfaces on apparent tyre stiffness

Surface	Change in stiffness
Dry Farm Track	0%
Hard Parkland Grass	-3%
Pasture Grass	-3%
Dry Cultivated Land	-5%
Dry Seedbed	-5%
Stubble Field	-7%
Artificial Rough Track	-10%

The inflation pressure dependence of the rolling tyres varies only by a factor of two from the smallest to the largest tyre measured. Two tyres have carcass stiffnesses significantly different from the others. These are tyre F1, a ribbed front wheel tyre, and tyre AS3, a tyre from which the tread has been removed. The total variation of the carcass stiffnesses of all the other tyres is less than a factor of two. This figure shows two distinct groupings. The front traction tyres (AS1, 4, 6, 7, 8) which have a low inflation pressure dependence and the remainder of the traction tyres which have a higher inflation pressure dependence. Two exceptions to this are the front ribbed tyre F1 and the row crop tyre AS9, which has an inflation pressure dependence between that of the front and rear tyres.

##### 4.4.2 Tyre construction

There is insufficient data available in Table III on which to draw conclusions about the effect of tyre construction method on stiffness. However Tyres AS8 and AS7 are of the same size and have radial and cross ply constructions respectively. The stiffnesses of these two tyres suggest that there is little difference between the stiffness of radial and cross-ply tyres.



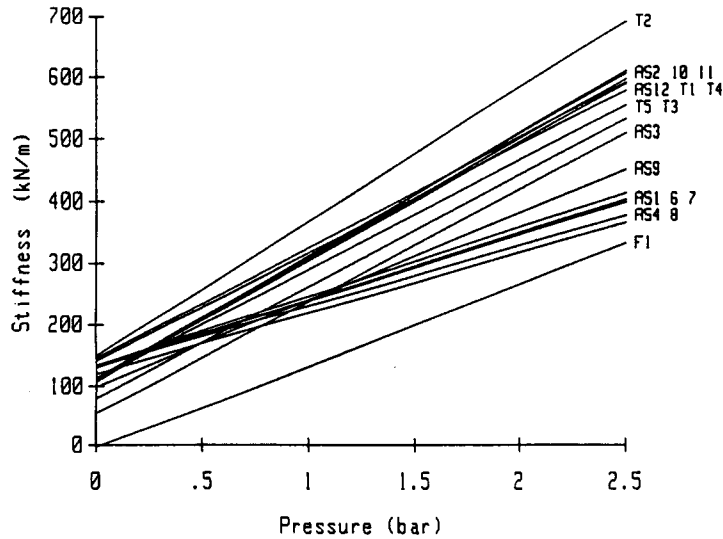


**Figure 25** The relationship between stiffness and inflation pressure for all the tractor tyres

#### 4.4.3 Ply rating

Once again not enough data is available to draw firm conclusions, however the available data suggests that there is little variation in stiffness with ply rating. Table III shows that the stiffnesses of tyres T1 and T4 are very similar. Tyre T1 is a 6-ply tyre and T4 an 8-ply. In all other respects they are very similar tyres.

#### 4.4.4 Age, wear and rubber composition

Independent assessment of these three variables cannot be properly made with the available data since they do not vary independently. Figure 26 shows that these factors taken together increase the carcass stiffness of both rolling and stationary tyres. The carcass stiffness of stationary tyres is more dependent on tyre age than that of rolling tyres. A linear regression calculated on the rolling tyre data suggests that for these tyres the carcass stiffness increases by 5.6 kN/m per year.

The inflation pressure dependence of the four newer tyres (T1, T4, T3, T5) with ages between 1 and 11 years varies by only 3%. It neither increases nor decreases consistently with tyre age. This suggests that the inflation pressure dependence is independent of tyre age. The inflation pressure dependence of the oldest tyre (T2) is 20% greater than the inflation pressure dependencies of the other four tyres. This result is unlikely to be due to measurement error since the coefficient of determination of this dependence is in excess of 99%, however in the absence of other information it must be considered a peculiarity of that tyre.

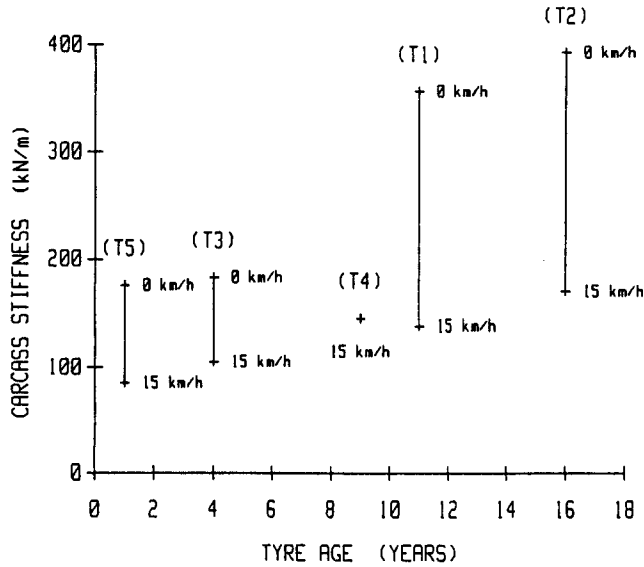


**Figure 26** Variation of tyre carcass stiffness with tyre age for rolling and stationary tyres

#### 4.4.5 Lug length

Three new tyres (AS2, AS12 and AS3) with different lug lengths were tested by Kising. The results are summarised in Table III. The tyre with low profile lugs (AS12) behaved almost exactly the same as the normal tyre (AS2), however the buffed tyre (AS3) was significantly different. The inflation pressure dependence of the stiffness remained unchanged, but the tyre carcass stiffness was reduced to half that of the tyre which had not had its tread removed.

#### 4.5 Discussion of results

Table VI summarises the results and Figure 27 shows the variation in the stiffness which might be expected under normal operating conditions. All the likely variations in tyre stiffness sum to a value as great as the total tyre stiffness itself. This variation is dominated by the inflation pressure, the tyre size and the tyre age and wear.

##### 4.5.1 Variation of tyre stiffness with rolling speed and frequency

Additional careful measurements at a range of rolling speeds have been made of the mean axle height and the tyre stiffness. The mean height of the axle above the ground was measured using an ultrasonic displacement transducer while the tyre stiffness and damping were being measured in the normal way. This measurements showed that as the rolling speed increased and the stiffness decreased, the mean axle height increased

**Table VI** Summary of results, showing the rate of change of tyre stiffness with the variation of various conditions

	Change in Measured Range	Change in Stiffness (kN/m)
Pressure	.7- 2 bar	+190 /bar
Rolling speed	0- 15 km/h	-150 (total)
Rolling speed	10- 15 km/h	-8 (total)
Load	16- 22.5 kN	(none)
Amplitude	7- 30 mm	± 1 /mm
Torque	0- 4.7 kNm	(none)
Frequency	2- 5 Hz	+5 /Hz
Tyre Size	18- 44 inch	200 (total)
Construction	radial, X ply	(none)
Ply rating	6- 8 ply	(none)
Age / Wear	new- very worn	+100 (total)
Lug Length	new- buffed	-60 (total)
Surface	(see table V)	40 (total)

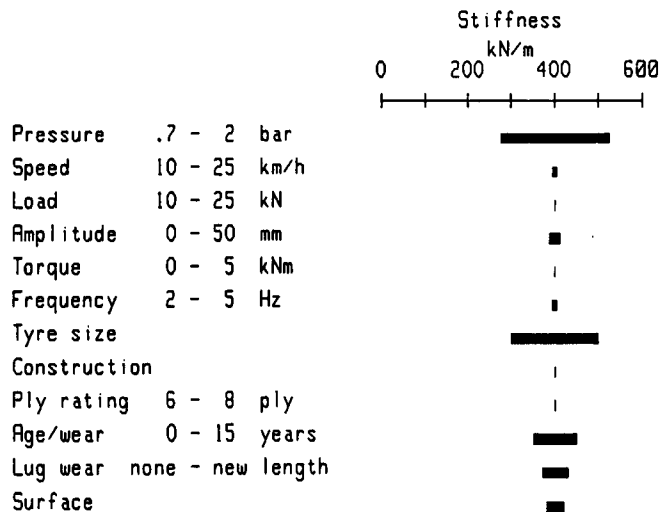


**Figure 27** Variation in tyre stiffness under normal operating conditions

(Figure 29). These changes would be contradictory if the tyre really behaved as a simple linear spring. While a simple model such as this may be useful for modelling the behaviour of a tyre under some limited conditions, it clearly is not a simple spring and so this model cannot be expected explain behaviour beyond the conditions for which it is appropriate. The tyre stiffness which affects the ride vibration of a vehicle is the force - deflection relationship about the mean deflection, rather than over the whole range of possible deflection.

Consideration of the deformation of a toroid indicates that when a tyre is deformed the tyre walls about the contact patch are both bent and stressed in shear. It is unlikely that the bending of the tyre walls contributes significantly to the remarkable stiffness of the

tyre carcass. It is more likely that this strength is derived from the shearing of the walls due to the tyres toroidal shape. It is well known that rubber creeps under stress (Clarke 1981). This means that a load applied to rubber gives rise to an immediate deformation, but that the deformation continues to increase slightly so that equilibrium conditions are not reached for several hours. Measurements can be made of the axle height of a tractor tyre which illustrate this. If the height of the axle of a tractor wheel is measured immediately it stops, and at frequent intervals thereafter it will be seen that the height of the axle decreases by several millimetres in the first few seconds and a further 5 mm during the following few hours (Figure 28).

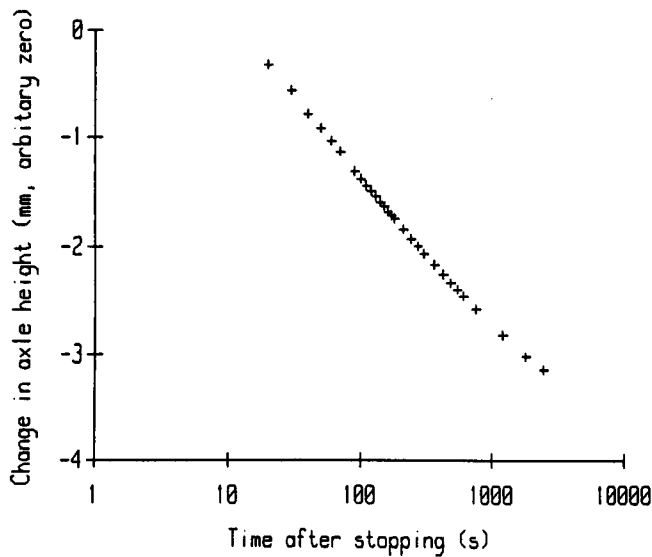


**Figure 28** Change in axle height with time of a loaded 13.6R38 tyre and wheel after stopping

When the tyre is rolling any given piece of rubber enters the contact patch region and is deformed for a short period and then relaxes for a much longer period. At low speeds the tyre is deformed for long enough to allow a significant amount of creep to occur in the rubber. At high rolling speeds little creep occurs. This difference results in the axle being a little higher at high rolling speeds than at very low speeds.

It has been shown that the variation of stiffness with speed is due to changes in the tyre carcass stiffness. Figure 20 indicates that there is a 25% decrease in carcass stiffness between the speeds of 0 and 1 km/h. This large change must be related to the time for which tyre rubber remains in the contact patch zone since no other factors change significantly with this small change in speed. Reasons for this dependence could be the rubber creep or temporary softening of the rubber due to repeated flexing. It seems

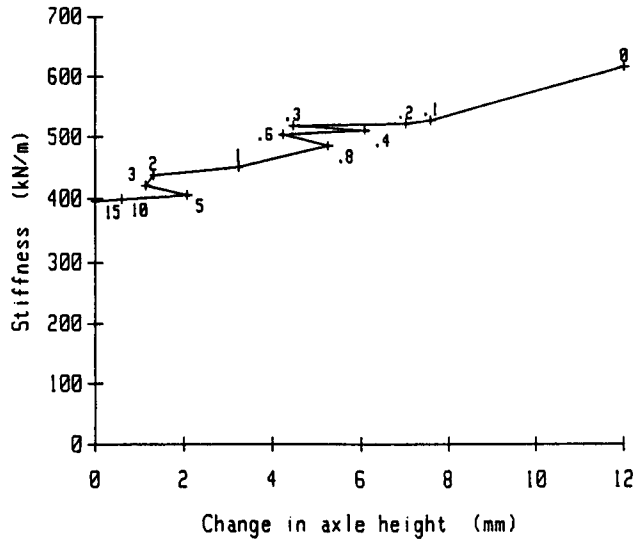


**Figure 29** Relationship between tyre creep and stiffness of tyre T1 measured at the marked driving speeds from 0 to 15 km/h

most likely that the tyre carcass stiffness changes as the deformed tyre rubber creeps since this will result in a change in stress distribution within the tyre carcass between the tyre rubber and the reinforcing cords. No reports of temporary softening of rubber due to repeated deformation on a time scale such as this have been found in the literature.

At low rolling speeds the rubber remains in the contact patch area long enough for it to pass through several cycles of deformation due to the vibration of the axle. At high rolling speeds the rubber is not in the contact patch area long enough to be deformed through even one full cycle of axle vibration. The dominant frequency of deformation of the tyre rubber therefore depends on the tyre rolling speed. At high rolling speeds it is related to the tyre rotation rate, while at low rolling speeds it is related to the axle vibration frequency. Since the dynamic stiffness of rubber increases with forcing frequency (Davey and Payne 1965) the tyre carcass can be expected to behave similarly.

If the stiffness is dependent on vibration frequency then it should be much more so at low rolling speeds than at high ones by the reasoning in the previous paragraph. This effect is shown in Figure 24. It also suggests that there should be some relationship between the change in stiffness with frequency at low speeds and the change in stiffness with rolling speed at high speeds. Figure 24 shows that at 1 km/h the tyre stiffness increased at a rate of about 10 kN/m per Hz (2.5% per Hz). Thus at high rolling speeds the stiffness would be expected to increase at a rate determined by the

increase in stiffness with vibration frequency and the rolling circumference. For the 13.6R38 tyres measured which have a rolling circumference of 4.66 m this indicates a very small increase in stiffness of 0.6 kN/m per km/h (0.15% per km/h).

#### 4.5.2 Age and wear

There are several reasons why tyre characteristics can be expected to change with age. Old tyres are often made from different rubber compounds to newer tyres so changes might be detected which reflect tyre development rather than actual degradation of older tyres. Synthetic rubber, of which agricultural tyres are usually made is known to harden on aging and through exposure to oxygen and ultraviolet light (Clarke 1981). Tyre walls also fatigue through repeated flexing, which may reduce the rubber stiffness (Davey and Payne 1965), and the tyre tread becomes lower through wear. The results presented are too few give anything but the most basic insight into the effect of these processes.

This work indicates that severe tyre lug and side wall wear decreases the carcass stiffness and that carcass stiffness increases with tyre age. The inflation pressure dependence of the stiffness is largely unaffected by age and wear. This suggests that a tyre which is worn very quickly might have a slightly lower stiffness in its worn state than in its new state, but a tyre which has been worn at a more normal rate is likely to be stiffer than when it was new. There is insufficient information to quantify or support this observation further. However this is consistent with the findings of Stayner and Boldero (1973) who found that the stiffness of a partially worn tyre did not necessarily fall between those of a new and a severely worn tyre.

#### 4.5.3 Tyre size

Because of its linear relationship with inflation pressure, the tyre stiffness can be represented by the relationship

$$K_t = K_c + P \Delta K_p$$

where  $K_t$  is the tyre stiffness in kN/m,  $K_c$  is the carcass stiffness in kN/m,  $P$  is the inflation pressure in bar and  $\Delta K_p$  the inflation pressure dependence in kN/m.bar.

Stiffness is the rate of change of the restoring force with deflection. A short experiment was made to observe the change in inflation pressure during tyre deformation. The tyre was inflated to a pressure of 1.38 bar while it supported no load. A vertical load was applied to the axle increasing gradually to 22.5 kN. During this process the inflation

pressure increased by only 0.05 bar (3.5%). This increase in the inflation pressure clearly provides only a small part of the change in restoring force. Most of the change in restoring force and hence the tyre stiffness, must therefore originate in changes in the effective ground contact area of the tyre. The inflation pressure can be considered to be almost constant.

The force ( $F$ ) developed by deforming this tyre through a distance  $x$  metres is given by:

$$F = x K_c + P x \Delta K_p$$

The force in the first part of this equation is due only to tyre carcass. The second part is the force developed by inflation pressure  $P$ . This is also the product of the pressure with the effective area ( $a$ ) over which it acts,

$$\text{so} \quad P x \Delta K_p = P a$$

$$\text{and hence} \quad a = x \Delta K_p$$

The rate of change of tyre stiffness with inflation pressure ( $\Delta K_p$ ) is determined by the rate of change of effective ground contact area.

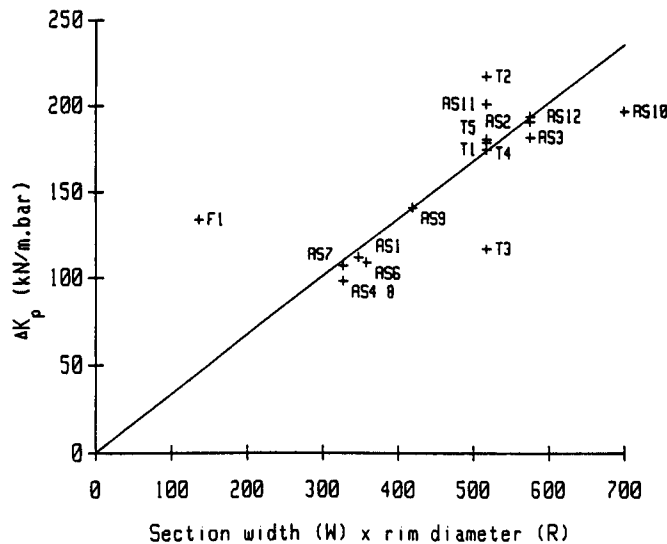


**Figure 30** Relationship between the product of tyre section width and rim diameter ( $W R$ ) and observed rate of increase of stiffness with inflation pressure ( $\Delta K_p$ )

Assume that for the limited range of normal tyre deflection, the width of the contact area remains constant and is proportional to the tyre section width  $W$ . Further, assume that the effective contact patch length is proportional to the tyre deflection and the tyre size as given by the rim diameter  $R$ , then

$$a \propto W R x$$

$$\text{so} \quad \Delta K_p \propto W R$$

Figure 30 shows the relationship between the value of  $\Delta K_p$  and the product  $W R$  for all the tyres given in Table III ( $W$  and  $R$  in units of inches are as specified by the tyre manufacturer). A linear regression for all the data on the plot except for the tyre F1 has a zero intercept of 0.297 kN/m per bar, a gradient of 0.34 kN/m<sup>3</sup> per bar and a coefficient of determination,  $r^2$  of 0.82. The linearity of this relationship suggests that the assumptions about the way the contact area varies are substantially valid. The increase in stiffness with pressure can be calculated as

$$\Delta K_p = 0.34 W R$$

Figure 31 shows the relationship between carcass stiffness and rim diameter. A linear regression has been calculated for all the data available except for that from tyres AS3, T1, T2, T4, and F1. These tyres have been excluded because they are either old, or have a different tread. The linear regression has a zero intercept of 172 kN/m, a

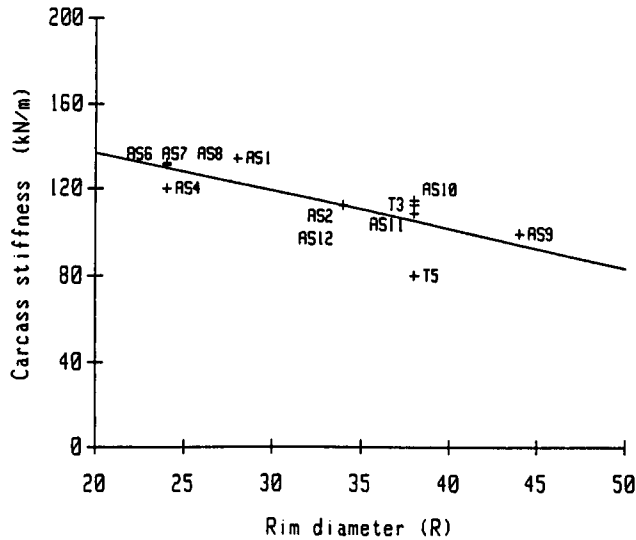


**Figure 31** Relationship between tyre carcass stiffness and rim diameter

gradient of -1.77 and a coefficient of determination,  $r^2$  of 0.70. This relationship is linear enough to enable the carcass stiffness of a new tyre to be estimated. The stiffness of a new tyre can therefore be estimated as:

$$K_t = 172 - 1.77 R + 0.34 W R P.$$



It has been shown earlier that the carcass stiffness of the tyres measured increases at a rate of 5.6 kN/m per year. This increase can also be introduced into the estimate of tyre stiffness,

$$K_t = 172 - 1.77 R + 5.6 A + 0.34 W R P,$$

where  $A$  is the tyre age in years.

When this relationship is applied to all the tyres given in Table II except for the undriven ribbed tyre F1, at all the inflation pressures measured (56 combinations), the stiffness is predicted with a mean error of only 3% and a standard deviation of 10%. Therefore 65% of the stiffness predictions are within  $\pm 10\%$  of the measured stiffness. The predicted values of stiffness are given in Figure 32. A wider range of tyres should be used to assess the general applicability of this empirical relationship, particularly with regard to old tyres of different sizes.

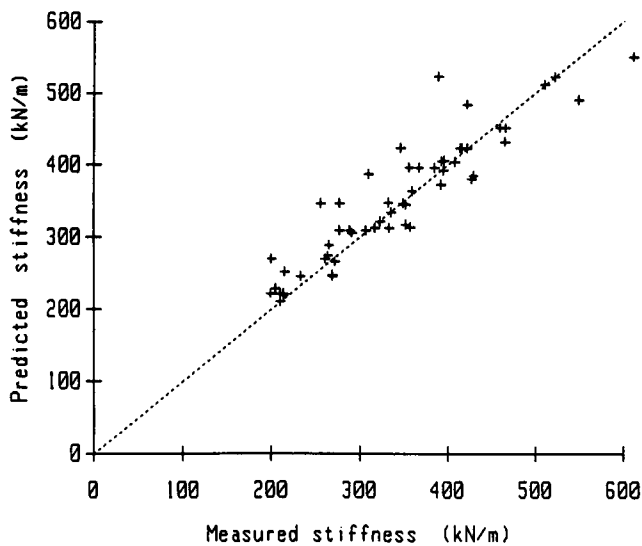


**Figure 32** Relationship between predicted and measured tyre stiffnesses

Currently the most common way of estimating the rolling tyre stiffness is to measure the stationary tyre stiffness. The results available show that with this method the rolling tyre stiffness is predicted with a mean error of 17% and a standard deviation of 24%. Therefore there is only a 25% probability of predicting the rolling tyre stiffness to within  $\pm 10\%$  by this method.

Based on the information currently available it therefore appears that this relationship is a more reliable source of information about the stiffness of rolling tyres than measurements made on non-rolling tyres.

#### 4.5.4 Undriven front tyre stiffness

Results are available for only one undriven front tractor tyre (Table III). The tread pattern on this type of tyre is different from that on traction tyres. Instead of a chevron tread pattern, it has three thick ribs running around the tyre, one on the centre line and one each side. This difference in tread may cause the tyre to deform differently to a traction tyre.

The dependence of the front tyre stiffness on rolling speed is very similar to that of the other larger tyres. Its dependence on amplitude is greater than that of the larger tyres. The rate of increase of stiffness with inflation pressure is larger than that which would be expected from a traction tyre of the that size. The carcass stiffness of this tyre is much smaller than any of the traction tyres, becoming very close to zero when the tyre is rolling.

#### 4.6 Conclusions

A tractor tyre typically has a stiffness of 400 kN/m. Under various normal operating conditions this could vary from less than 200 kN/m to more than 500 kN/m. The factors which have a large effect on the stiffness are the inflation pressure, the rolling speed, the tyre size and tyre age or state of wear. The type of surface which the tyre is rolling on also has some influence on the stiffness. Normal variations in tyre load, vibration amplitude, driving torque, ply rating and frequency have little effect on stiffness.

The stiffness of a stationary tyre does not have a simple relationship with that of a rolling tyre. Stationary tyre stiffness is more dependent on other factors such as amplitude and frequency than rolling tyre stiffness. The stiffness of a rolling tyre is usually lower than that of a stationary tyre. Stiffness decreases significantly with speed at low rolling speeds, but at speeds above 10 km/h is effectively constant.

The stiffness of a traction type tyre can be estimated from its size, inflation pressure and age using the following relationship:

$$K_t = 172 - 1.77 R + 5.6 A + 0.34 W R P$$

where  $K_t$  is the stiffness (kN/m),  $W$  and  $R$  are the tyre section width and rim diameter as given in the tyre size specification (in inches),  $A$  is the tyre age (years) and  $P$  is the inflation pressure (bar).

The nature of the surface over which the tyre rolls can reduce the stiffness. The wooden slatted surface of the rough track used to create tractor vibration for various international standards reduces the effective stiffness by 10%.

## 5 Variations in the damping characteristics of agricultural tyres

### 5.1 Introduction

The ride vibration of an unsuspended agricultural tractor is severely under damped. Its damping ratio in the vertical direction is typically less than 10%, so the vibration is dominated by a large response to the excitation at just a few well defined frequencies. The damping which originates from the tyres is much lower than that which is usually derived from the suspension system of a suspended vehicle. Therefore when the vibration of a suspended vehicle is being investigated, the effect of tyre damping is frequently neglected. As a result, little information about damping in tyres is available. Since the force generated by the tyre damping during vibration is small compared with that generated by the tyre stiffness it is rather difficult to measure accurately. However for unsuspended vehicles this damping is vital for controlling the vibration so it cannot be neglected.

The damping coefficient of several tyres have been measured under a range of operating conditions. The aim of these measurements was to establish values which could be used for vehicle vibration simulation. The way the damping changed with tyre characteristics and environmental factors was examined. This report draws mainly on experimental results produced by the author. Analysis of a few measurements published by Kising (1988) is included to provide more complete information.

### 5.2 Identity of the tyres tested

The tyres tested in this investigation were tyres T1 to T5 and tyre F1. Some results derived from measurements on tyres AS2 and AS3 are also used. These tyres are described in section 4.2 and in Table II.

### 5.3 Environmental factors which affect tyre damping

#### 5.3.1 Inflation pressure

Damping increases with inflation pressure. The damping coefficient of tyre T2 is plotted against inflation pressure in Figure 33. Linear regression lines have been calculated between the damping coefficient and the inflation pressure for tyres T1 to T5 and the

tractor front tyre F1. The results are given in Table VII. The relationship between damping and pressure is not as linear or as easily defined as that between stiffness and pressure. This is reflected in the lower coefficients of determination. At a rolling speed of 15 km/h the damping increased with inflation pressure at a rate which varied in the tyres measured from 0.36 to 0.53 kNs/m per bar (typically between 15 and 30% increase per bar). The zero pressure intercept of these regression lines which could be considered to be the tyre carcass damping varies between 0.3 and 1.3 kNs/m for the traction tyres.

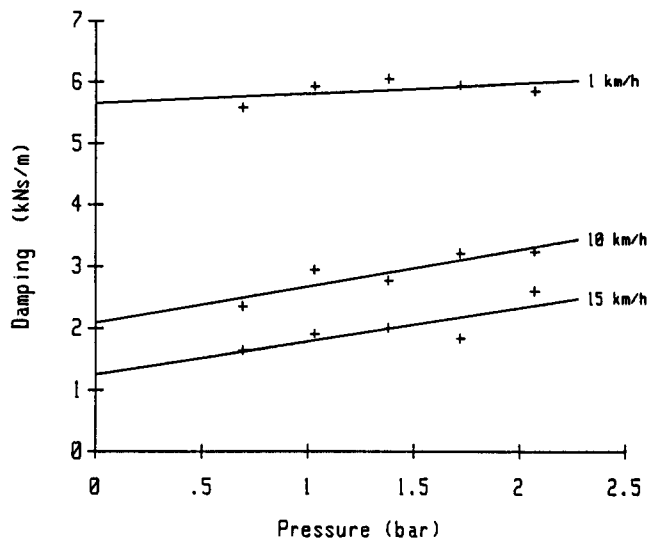


**Figure 33** Variation of damping of tyre T2 with inflation pressure

### 5.3.2 Rolling speed

The tyre damping changes with rolling speed throughout the whole speed range measured. The changes in damping with rolling speed of the traction tyres measured are given in Figure 34.

At very low rolling speeds the damping increased with increasing speed until a speed of about 0.6 km/h was reached. The amount it rose varied from no observable increase to as much as 10% increase. With further increases in rolling speed it decreased so that at a rolling speed of about 2 km/h the damping was reduced to its non-rolling level. Further increases in speed resulted in further decreases in the damping. At rolling speeds of between 10 and 15 km/h the rate of decrease was between 0.06 and 0.1 kNs/m per km/h, the actual value varying from tyre to tyre. Damping continued to decrease with further increases in speed. Kising has observed decreases in damping up to rolling speeds of 50 km/h. At rolling speeds of 10 km/h and above, the inflation

**Table VII** Variation of tyre carcass damping ( $C_c$ ) and the inflation pressure component ( $\Delta C_p$ ) with rolling speed.  $r^2$  is the coefficient of determination

	speed	$C_c$	$\Delta C_p$	$r^2$
Tyre T1	10 km/h	1.63	0.44	0.98
	15 km/h	1.31	0.39	0.90
	20 km/h	0.91	0.44	0.94
Tyre T2	10 km/h	2.09	0.59	0.79
	15 km/h	1.26	0.53	0.64
Tyre T3	10 km/h	0.67	0.31	0.99
	15 km/h	0.67	0.36	0.97
Tyre T4	10 km/h	1.00	0.43	0.94
	15 km/h	0.75	0.40	0.92
Tyre T5	10 km/h	0.49	0.35	0.92
	15 km/h	0.32	0.37	0.94
Tyre F1	0 km/h	1.34	0.39	0.74
	10 km/h	0.30	0.32	0.96
	15 km/h	-0.15	0.38	0.94

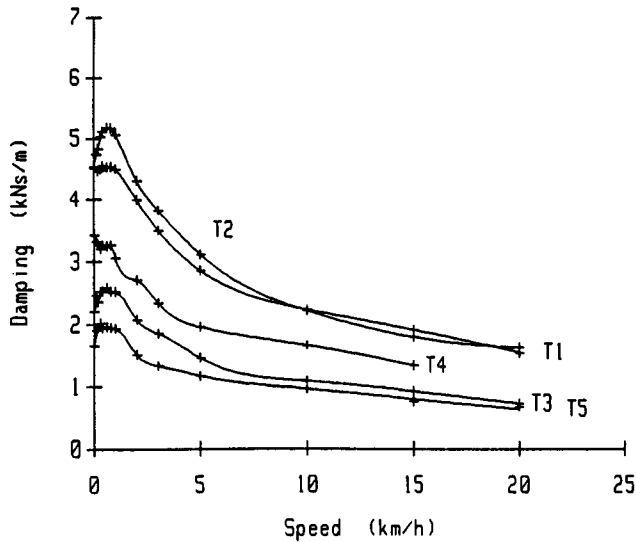


**Figure 34** Variation in damping coefficient with rolling speed at 1.38 bar for tyres T1 - T5

pressure dependence of the damping became almost constant and further changes in the damping with increasing rolling speed can be attributed to changes in the carcass damping of the tyre.

### 5.3.3 Tyre load and deflection

Loads of 16, 18.2 and 22.5 kN were imposed on the tyre. This caused an increase in the damping of between 0.05 and 0.2 kNs/m per kN of increased tyre load or up to 10% increase per kN. The variation for tyre T3 is shown in Figure 35. When the inflation pressure of the tyre was adjusted in order to maintain a constant tyre deflection, the tyre damping was found to increase by an amount which was consistent with the combined effects of the increase in damping due to the load and to the increase in damping due to the inflation pressure for that tyre.

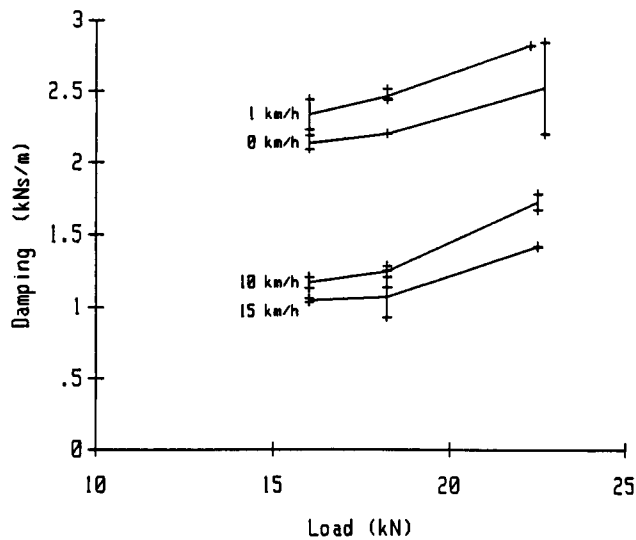


**Figure 35** Variation in damping of tyre T3 with load at 1.38 bar inflation pressure

### 5.3.4 Amplitude of vibration

Tyres T1, T2, T3 and F1 were excited with sinusoidal vibration with range of peak to peak amplitudes between 4 and 30 mm. At rolling speeds of 10 and 15 km/h the damping of tyres T1, T3 and F1 increased slightly with increasing amplitude while that of the very old tyre T2 decreased. The damping of all three tyres decreased with increasing amplitude at very low rolling speeds and when the tyres were stationary. Linear regressions have been calculated between the amplitude of oscillation and the damping. The rates of change of damping and the coefficients of determination are given in Table VIII. The change in damping with amplitude for tyre F1 is shown in Figure 36

### 5.3.5 Frequency of vibration

Damping was found to decrease with increasing vibration frequency. This effect was very much greater on stationary tyres than on rolling tyres. The measurements made

**Table VIII** Measured variation in damping with increasing amplitude of vibration in kNs/m per mm. Coefficients of determination ( $r^2$ ) are given in parentheses

	0 km/h	1 km/h	10 km/h	15 km/h
Tyre T1	-0.010 (.79)	-0.007 (.08)	.017 (.75)	.024 (.98)
Tyre T2	-0.142 (.60)	-0.049 (.25)	-0.042 (.95)	-0.030 (.96)
Tyre T3	-0.034 (.98)	-0.025 (.82)	.002 (.25)	.008 (.43)
Tyre F1	-0.105 (.97)	-0.036 (.94)	.018 (.42)	.012 (.24)

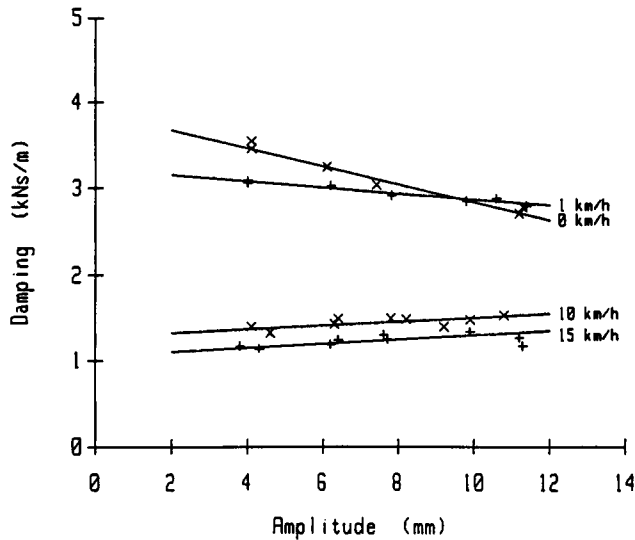


**Figure 36** Variation of damping with amplitude for ribbed front wheel tyre F1

covered frequencies between 2 and 5 Hz. This frequency range encompasses most of the ground induced ride vibration encountered on agricultural tractors. Figure 37 shows the measured variation of tyre T1 with frequency at various rolling speeds.

The damping coefficient of the tyres rolling at 10 km/h was found to decrease by about 20% per octave increase in vibration frequency, while the damping of stationary tyres decreased by more than 50% per octave.

### 5.3.6 Driving torque

The characteristics of the tyres T2 and T3 were measured as they were driven at speeds of 1, 8, 10 and 15 km/h transmitting driving torques of up to 2.8 kNm. The damping of tyre T1 was measured at these speeds up to a driving torque of 4.7 kNm. At speeds of 8 km/h and greater the damping coefficient of the tyres decreased by between 0.06 and 0.15 kNs/m with each 1 kNm of driving torque applied. This amounts to a relative change in damping of up to about 8% per kNm of torque (Figure 38). At a driving speed of 1 km/h the change in tyre damping varies for different tyres between no change and



an increase of 0.04 kNs/m per kNm of applied torque. These changes are small and as such are very unlikely to be have a significant effect on tractor vibration.

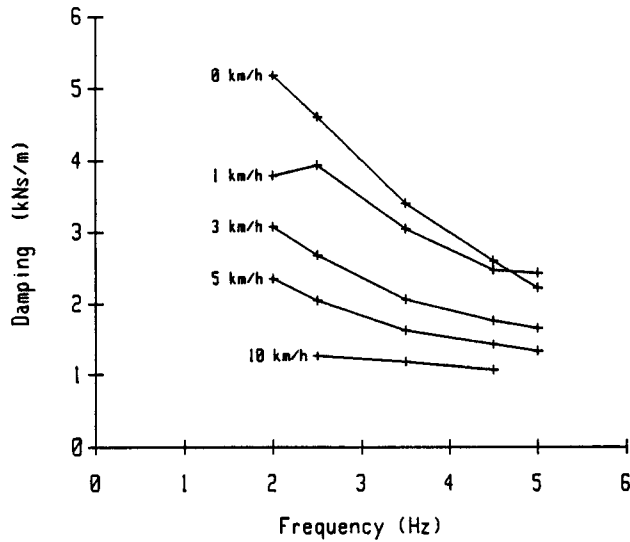


**Figure 37** Variation of damping coefficient of tyre T1 with vibration frequency at various rolling speeds

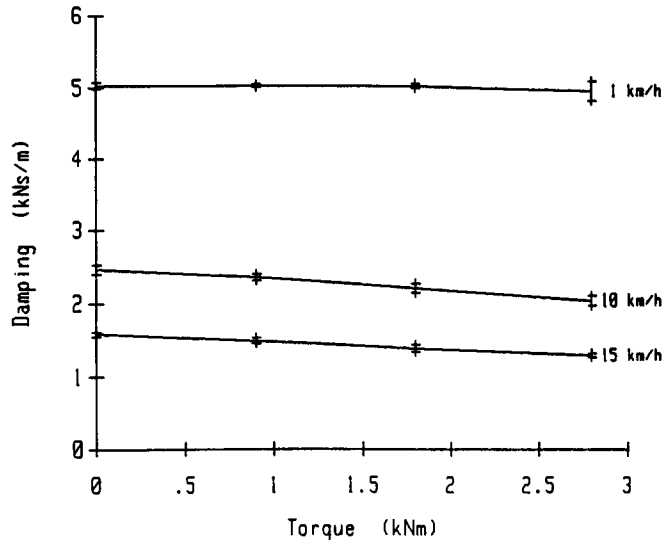


**Figure 38** Change in damping coefficient with driving torque for tyre T2

### 5.3.7 Surface

The damping coefficients of tyres T4 and T5 were measured as they rolled over a range of typical agricultural surfaces. Measurements were made at speeds of 5 and 10 km/h. Over grass and stubble the damping consistently was 20% greater than that measured on flat concrete. Measurements on the artificial rough track (described in section 4.3.7,

page 53) gave variable results showing no consistent change in damping. The variability of this measurement was probably due to the limited length of track available for measurement. Over soft surfaces very large increases in the damping of the tyre were measured. This was probably due to the energy dissipated by permanently deforming the ground surface. A summary of the results is given in Table IX

**Table IX** Changes in tyre damping on various surfaces.

Surface	Change in damping
Dry Farm Track	0%
Hard Parkland Grass	+20%
Pasture Grass	+20%
Dry Cultivated Land	+190%
Dry Seedbed	+80%
Stubble Field	+20%
Artificial Rough Track	-

#### 5.4 Factors dependent on the choice of tyre

##### 5.4.1 Age and wear

The differences in damping between the tyres shown in Figure 34 follow a pattern relating to the tyre wear or age. The new tyre T5 had the lowest damping. The two partly worn tyres (tyre T4, 6 ply and tyre T1, 8 ply) both had a higher damping coefficient than the new tyre across the whole range of driving speeds. Figure 39 shows the carcass damping and inflation pressure dependence of the damping for these tyres. This information has been drawn from Table VII. Although both carcass damping and the inflation pressure dependence increase with tyre age, most of the increase in damping is due to the increase in carcass damping. Wear and age can double the damping coefficient of a tyre. They have a much greater effect on a stationary tyre than on a rolling tyre.

##### 5.4.2 Ply rating

There is insufficient evidence from which to draw firm conclusions, however the variations in carcass damping shown in Figure 39 suggest that the tyres aged 9 and 16 years have a carcass damping below that which might be expected from the trend set by the other three tyres. These two tyres are of a 6-ply construction while the other tyres are of an 8-ply. From this figure a tentative conclusion can be drawn that the 6-ply tyres have a carcass damping which is about 0.3 kNs/m lower than that of a

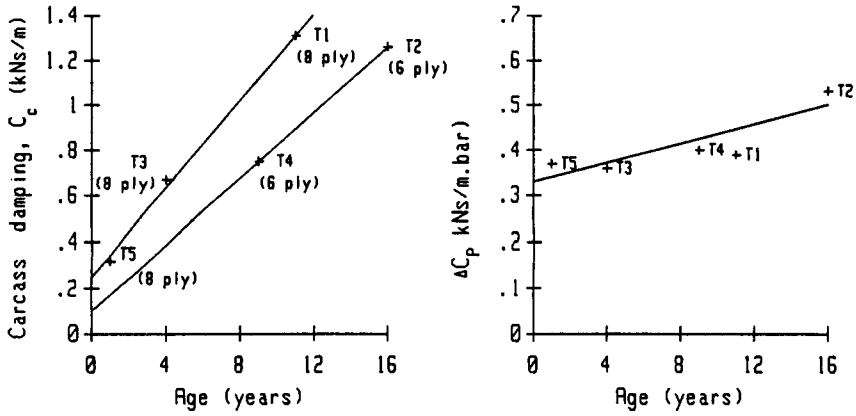


**Figure 39** Variation of carcass damping and inflation pressure dependence with tyre age

comparable 8-ply tyre

### 5.4.3 Lug length

Information is available from Kising (1988) which indicates that at rolling speeds below 30 km/h the lugs are responsible for about 30% of the damping of a new tyre (Figure 40). The effect of the lugs appears to become smaller as the rolling speed rises further.

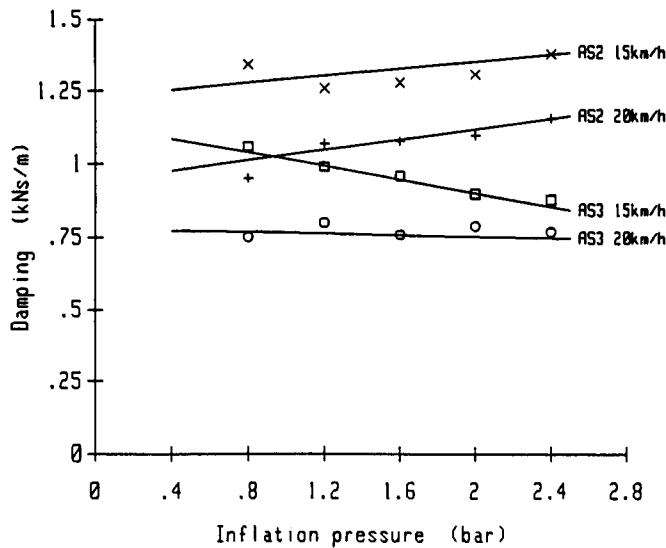


**Figure 40** The effect of tyre lugs on damping at 15 and 20 km/h. Tyre AS2 has lugs, on tyre AS3 they have been removed

## 5.5 Discussion

Table X summarises the results. Figure 41 shows the variation in the tyre characteristics which might be expected under normal operating conditions. This shows that tyre damping is significantly affected by the rolling speed, the inflation pressure, the tyre age and the surface over which the tyre is rolling. It is also measurably effected by all the other variables considered.

**Table X** Summary of damping results, showing the rate of change of damping with various factors.

	Change in measured range	Change in damping (kNs/m)
Pressure	.7- 2 bar	+0.4 /bar
Rolling speed	0- 15 km/h	-2 (total)
Rolling speed	10- 15 km/h	-0.3 (total)
Load	16- 22.5 kN	+0.1 /kN
Amplitude	7- 30 mm	0.01 /mm
Torque	0- 4.7 kNm	-0.1 /kNm
Frequency	2- 5 Hz	-0.3 /Hz
Ply rating	6- 8 ply	+0.15 /ply
Age / Wear	new- very worn	+2 (total)
Lug Length	new- buffed	0.5 (total)
Surface	(see table IX)	2 (total)

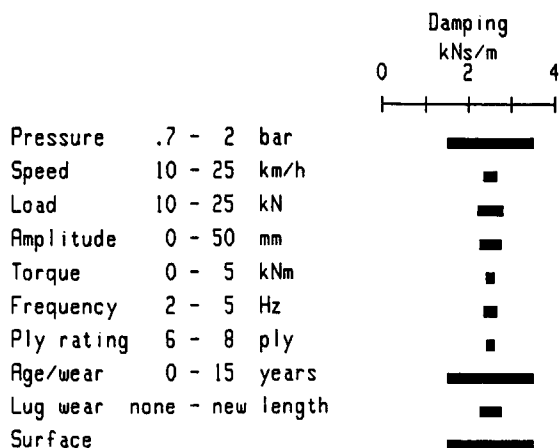


**Figure 41** Variations in tyre damping under normal variations in operating conditions

In general, tyre damping is more affected by changes in conditions than is the tyre stiffness. The variation of damping coefficient with these conditions is also less linear and varies more from tyre to tyre.

### 5.5.1 Agreement with previous work

The results presented are in disagreement with those from some other authors in the effect of inflation pressure on damping coefficient. Göhlich, Schütz and Jungerberg (1984) concluded that the damping coefficient of radial tyres was almost invariant with inflation pressure, whereas the results presented here and those of Göhlich and Sharon (1975) indicate an increase. When measurements made by Kising and Göhlich (1988) and by Kising (1988) are presented in terms of damping coefficients they show both increases and decreases with inflation pressure. Inflation pressure is the only variable identified in this series of experiments which has a greater effect on tyre stiffness than on the tyre damping coefficient. The discrepancy between accounts of the effect of inflation pressure on damping coefficient is probably due to changes in caused by the increasing tyre stiffness. The tyre measurement method used by Kising and Göhlich was to allow the tyre supporting a mass to vibrate freely. The damping was then estimated from the height or the spectral width of the natural frequency peak. The frequency at which the measurements were made was therefore determined by the stiffness of the tyre. The results presented in this paper indicate that the damping is dependent vibration frequency especially at the lower rolling speeds. Therefore the increase of natural frequency caused by inflation pressure could be expected to cause the damping coefficient to decrease. This is one possible cause of discrepancy. However this effect is not large enough to explain the whole of the discrepancy.

### 5.5.2 Rolling speed, frequency and amplitude dependence

The relationship between damping and rolling speed is more complex than that for tyre stiffness. It appears that two factors with opposing effects are involved. This causes it first to increase and then to decrease with increasing speed. It was argued in the previous chapter that the change of stiffness with rolling speed was due to changes in the length of time for which tyre rubber remained in the contact patch zone. It is reasonable to expect the if the stiffness is affected in this way then the tyre damping will be similarly affected. However variations in tyre damping with rolling speed differ from the variations in stiffness in that changes in tyre damping do not cease beyond a rolling speed of about 10 km/h. This, together with the complex nature of the damping variation with speed (both increasing and decreasing) suggest that another factor is also affecting the damping of the tyres.

It has been suggested that tyre damping can be modeled making use of dry, or Coulomb, friction within the rubber (Pacejka 1981). The tyre is described as comprising a number of rotating spokes, length  $r_0$  at fixed angles. Those in contact with the ground are deformed by their passage through the tyre contact patch in order to conform to the (flat) ground surface, and are also deformed by the variation in the axle height. This situation can be described algebraically.

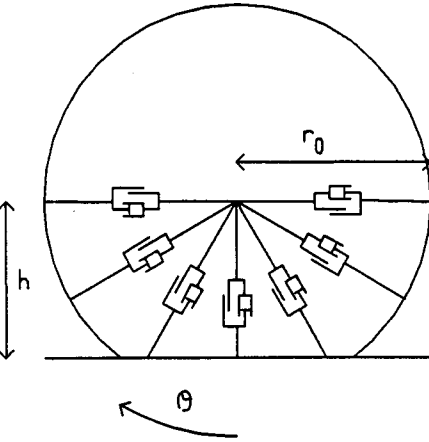


Figure 42 Rotating spoke tyre model

The deformed length,  $r$ , of a spoke which is in the contact patch zone is given by

$$r = \frac{h}{\cos(\theta t)}$$

where the  $h$  is the height of the axle above the ground.  $\dot{\theta}$  is the angular speed of rotation of the wheel and  $\theta = \dot{\theta} t$  is the angle which the spoke makes with the vertical.

The rate of change of length of the spoke,  $\dot{r}$ , can be obtain either from inspection of the system or from differentiation as

$$\dot{r} = \frac{\dot{h}}{\cos(\theta t)} - \frac{h\dot{\theta} \tan(\theta t)}{\cos^2(\theta t)} = \frac{\dot{h}}{\cos\theta} - \frac{h\dot{\theta} \tan\theta}{\cos^2\theta}$$

The frictional force experienced by the axle in the vertical direction,  $F$ , while the tyre rotates is obtained by integrating over all the spokes in the contact patch. This is assumed to be the cord of intersection between the circular tyre and the flat ground surface.

$$F = \int_{-\cos^{-1}(h/r_0)}^{\cos^{-1}(h/r_0)} f \cos(\theta) d\theta$$

where the force,  $f$ , is that developed by the damping elements in each spoke of the model. If this is purely due to Coulomb damping, then it is given by

$$f = c_1 \frac{\dot{r}}{|r|}$$

where  $c_1$  is the friction force. The frictional force can be evaluated for a range of tyre rotation speeds ( $\dot{\theta}$ ) and rates of change of axle height ( $\dot{h}$ ). Friction introduces a non-linearity into the system so this calculation is most easily done numerically. A simple computer routine can be written for this purpose by calculating the force produced by ten or twenty spokes and summing it.

Some results from such a routine are given in Figure 43. For this calculation values for a 13.6R38 tyre were used. The un-deformed tyre radius,  $r_0$ , is assumed to be 0.795 m and the axle height,  $h$ , is assumed to be 92% of this. This is typical for this tyre when it is properly inflated. Angular velocities of the spokes were chosen to represent circumferential speeds of up to 20 km/h. The rate of change of axle height used is representative of sinusoidal vibration at 4 Hz with an amplitude of  $\pm 8$  mm. The coefficient of friction  $c_1$  was set to a nominal value of 1 N per radian of tyre (ie the friction in all the spokes of the tyre adds up to  $2\pi$  Newtons). Figure 43 shows that over the normal range of operating speeds, this arrangement gives rise to damping forces which are approximately proportional to the rate of change of axle height and which decrease with increasing rolling speed.

In order to facilitate comparison with the measured results the equivalent viscous damping coefficient has been calculated. This was calculated by summing the energy dissipated over a sinusoidal cycle of axle height and recognising that the energy dissipated by a viscous damper under these circumstances is  $A^2 c \omega \pi$  where the amplitude of the axle motion is  $A$  and the angular frequency is  $\omega$ . The equivalent values of the coefficient of viscous damping are given in Figure 44. Comparison of the variation of these values with rolling speed with measured results given in Figure 34 indicates that this model has too much rolling speed dependence. Adding some viscous damping to spokes in the model reduces this rolling speed dependence. A ratio between these two coefficients which gives a reasonable approximation to the measured variation in damping with rolling speed is where the viscous damping coefficient (Ns/m) is four times that of the dry friction (N). Figure 45 gives the variation of damping with rolling speed using this ratio of coulomb and viscous damping. The coefficient of viscous damping is set at 1 Nm/s per radian and the Coulomb friction at 0.25 N per radian. Inspection indicates that the tyres in Figure 34 have damping levels between 1000 and 2000 times the levels produced by this model pointing to friction and viscous damping coefficients of between 0.25 - 0.5 kN per radian and 1 - 2 kNs/m per radian

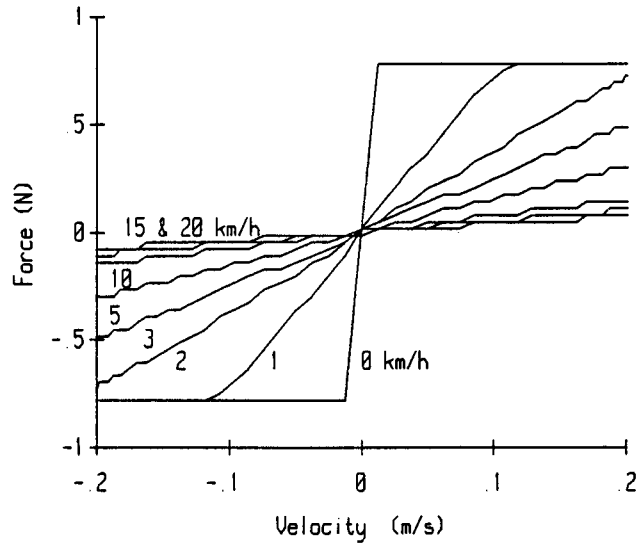


**Figure 43** Relationship between damping force and rate of change of axle height for various forward rolling speeds. Calculations made using Coulomb friction at a value of 1 N per radian

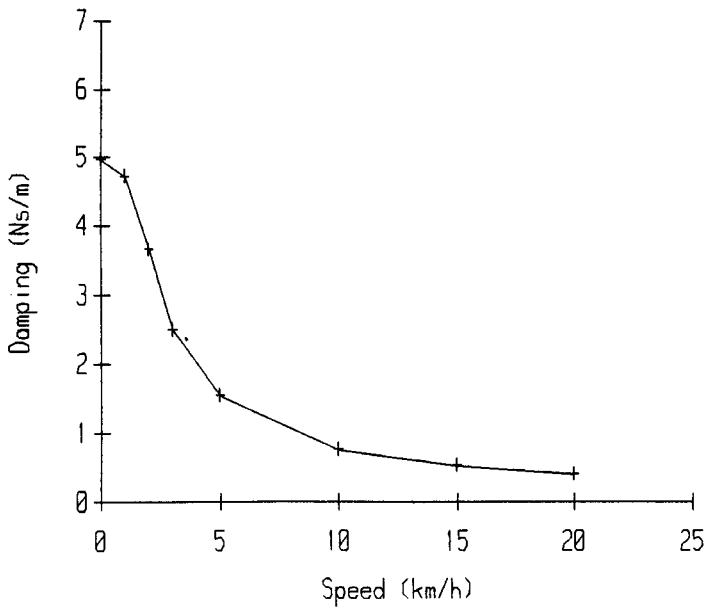


**Figure 44** Apparent values of viscous damping for the tyre modeled in Figure 43

respectively.

The effect of different excitation frequencies on the apparent damping of the tyre has been examined using this model. Results are shown in Figure 46. Comparison of these results with measured results given in Figure 37 shows broad agreement between the two sets of results. Comparison of Figure 47 with Figure 36 and Figure 48 with Figure 35 shows that this model is also able to describe the variation of damping



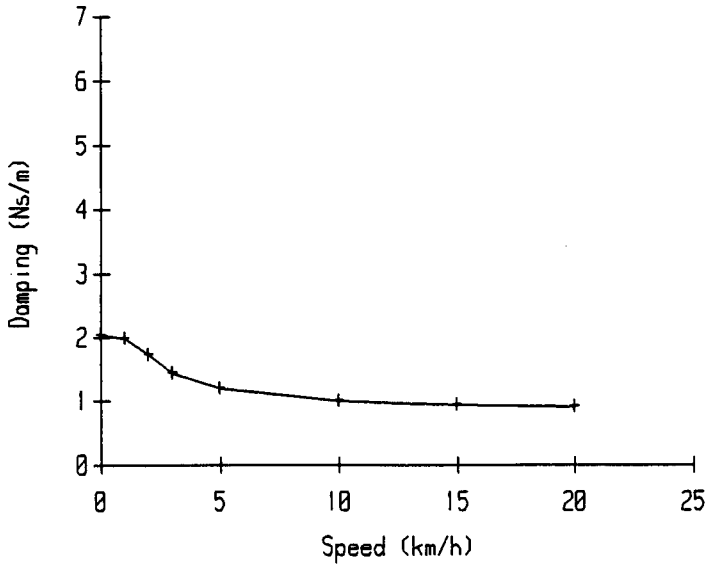


**Figure 45** Variation of apparent viscous damping coefficient with rolling speed using combination of viscous and coulomb damping in model

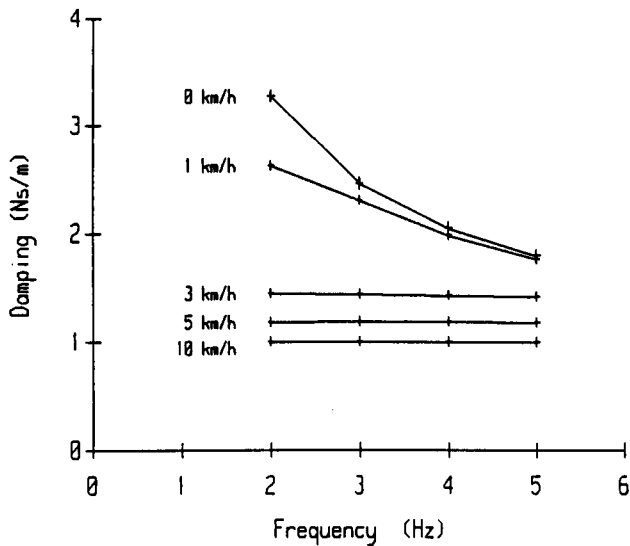


**Figure 46** Modeled variation of tyre damping with forcing frequency

coefficient with amplitude and rolling speed and produces increases in damping with deflection similar to those measured.

This model could be further extended to describe the variation of damping with inflation pressure by specifying a pressure dependence in the friction and damping coefficients, this is however of little interest since it would provide little new information about the tyre behaviour.

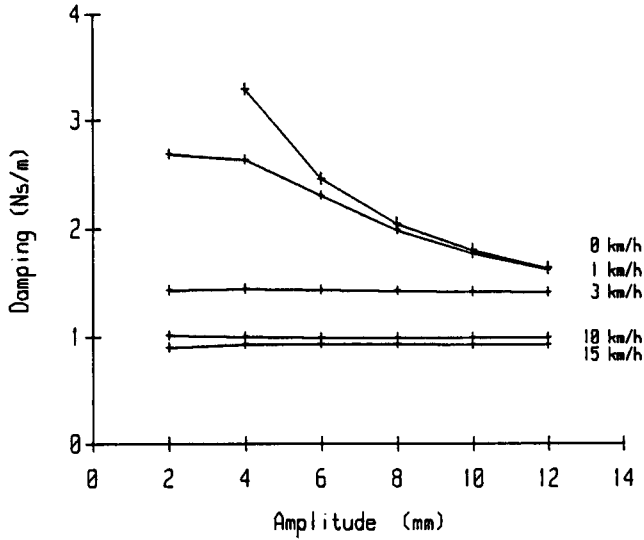


**Figure 47** Variation of modeled damping coefficient with amplitude of vibration

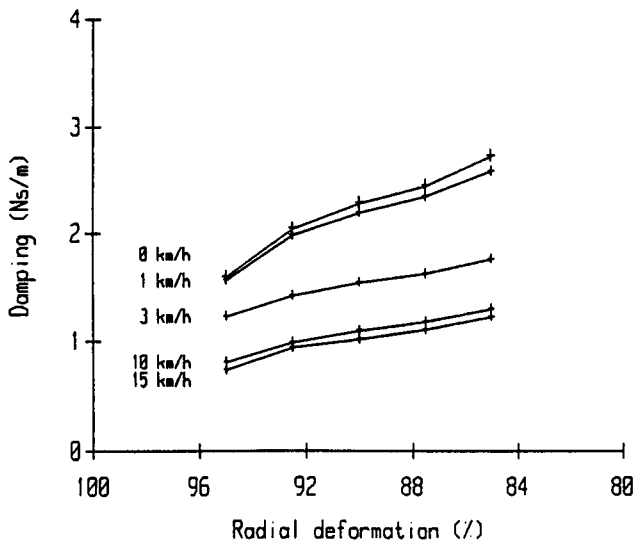


**Figure 48** Variation of modeled tyre damping coefficient with tyre deformation

Use of the model requires the Coulomb and viscous damping coefficients of a tyre to be determined. With this information the variation of damping with rolling speed, forcing frequency, amplitude and tyre deformation can be modeled. It might be possible to determine these parameters by measuring tyre damping at two rolling speeds or excitation frequencies and fitting the model to these data. Measurement of the load-deflection hysteresis of the stationary tyre might also provide one of these points.

### 5.5.3 Effect of tyre wear

The results presented indicate that older, more worn tyres are likely to have a higher damping coefficient than newer tyres. However results which were extracted from Kising (1988) indicated that at speeds below 30 km/h, the damping coefficient of a new tyre is about 30% greater than that of an otherwise identical new tyre from which the tyre lugs have been removed (Figure 40). This suggests that while increasing age of the tyre carcass and perhaps fatigue of the tyre walls increases the damping coefficient, the effect is reduced by the diminishing size of the tyre lugs. In practise the effect of tyre wear on damping is therefore likely to vary depending on the how the tyre has been used.

Stayner and Boldero (1973) measured the dynamic characteristics of a range of stationary tyres. They observed that the damping of new tyres was in general greater than that of severely worn tyres, but that the damping of partially worn tyres did not necessarily fall between these two values. The different effects on damping of tyre wear and tyre lug length provide a possible explanation for these observations.

### 5.5.4 Damping of undriven front tyre

The damping of tyre F1 behaves in a broadly similar way to that of the traction tyres (Figure 49). The variation of damping with rolling speed is similar to that of the other tyres measured except that the rise in the damping with speed reached a maximum at a lower speed. The 7.5-18 front tyre reaches a maximum damping coefficient at  $0.4 \pm .05$  km/h whereas the 13.6R38 tyres reached a maximum at  $0.6 \pm .1$  km/h. The rolling circumference of tyre F1 is 2.63 m as compared 4.66 m for tyres T1 - T5, so the damping coefficients of both the traction tyres and the front ribbed tyres reach a maximum at a speed of  $0.04 \pm .005$  revolutions per second. Table VII indicates that the carcass damping for this tyre is much lower than that of the traction tyres. The rate of increase in damping with pressure and the variation of damping with amplitude are similar to those observed for the traction tyres.

### 5.5.5 Estimating tyre damping

The results presented show that tyre damping varies significantly with many factors and that in some cases the relationships are dependent on each other. Although the way in which the damping of the different tyres varies with these factors is usually similar there is a wide range in the scale of the reaction between the tyres. No information is available regarding the damping coefficient of tyres of a representative range of different sizes. Because of the limitations of this measurement program and because of the variability of tyre damping it is not possible to provide any suggestions whereby the

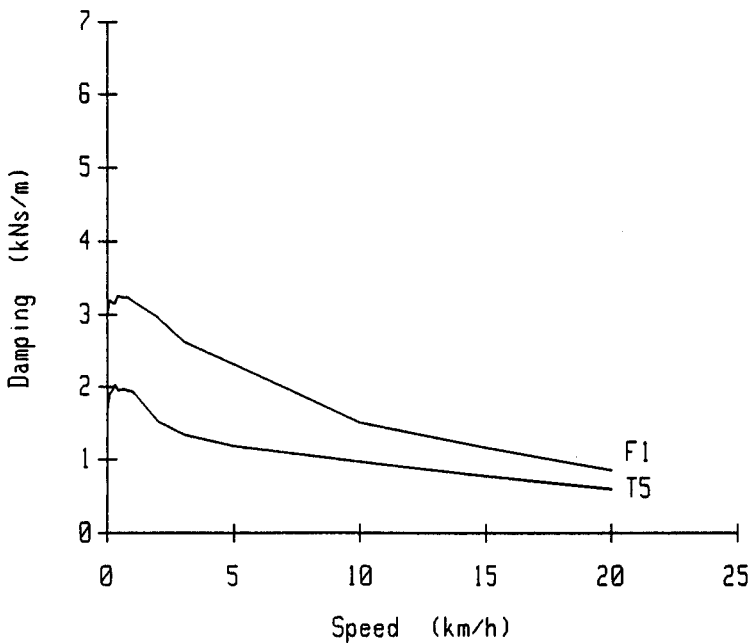


**Figure 49** Variation in damping with rolling speed of tyre F1 and traction tyre T5

damping of tyres can be estimated without measurements being made. In order to obtain accurate damping coefficients it is necessary to measure the tyre under conditions as close to those required as is possible. If values of the damping coefficient at several rolling speeds are known then the effect of varying tyre deformation, forcing frequency, rolling speed or vibration amplitude could be estimated using the rotating spoke model described. The rates of change of damping given in Table X should be used only very cautiously.

## 5.6 Conclusions

A typical value for the damping coefficient of a tyre appears to be between 0.8 and 3 kNs/m. It is most dependent on tyre age, the surface on which the tyre is rolling and on tyre inflation pressure. Rolling speed, tyre load, vibration amplitude, vibration frequency, driving torque, ply rating, and tyre lug length also affect the tyre damping. The variation in the damping coefficient of a tyre with vibration amplitude, forcing frequency, rolling speed and deformation can be explained in terms of a rotating spoke model, where the force developed by each spoke derives from viscous damping and dry friction. There is an unresolved discrepancy between the results presented here and those presented elsewhere regarding the effect of tyre inflation pressure on damping coefficient.

## 6 Application of improved tyre description to a simple dynamic system

### 6.1 Introduction

The value of an improved tyre description is best assessed by how it improves the accuracy of vibration predictions for a whole vehicle. However, on a whole vehicle, the longitudinal suspension characteristics of the tyres also influence the vertical vibration. Reliable measurements of these tyre characteristics have not yet been made. In order to assess the effect of an improved description of the radial characteristics of tyres, comparison of vibration measurements and predictions have been made on a simple system which only effectively has vertical freedom. Since the carriage is constrained in this way, the vibration is not affected by the longitudinal suspension characteristics of the tyre. The results indicate the accuracy of simulation which can be achieved using a simple linear tyre model. A comparison of the simulation accuracy with that which could have been expected prior to this research is made. For this purpose the characteristics of stationary tyres have been used. Such measurements could have been made following the method of Stayner and Boldero (1973). Predictions of the vibration of a whole tractor are compared with measurements in the next chapter.

### 6.2 Measurement of vibration

For these measurements a trailer supported by a single wheel was required. The trailer had to be supported in an upright position but to be free to vibrate in the vertical direction. It had to be capable of being towed or driven over a rough surface at a constant speed. These requirements were completely met by the carriage of the dynamic tyre test vehicle which was previously used to measure the tyre characteristics. However when it was used in this experiment, the ram driving the inertial mass was not powered, so the rear carriage behaved as a single mass supported entirely by the tyre. The centre of mass of the carriage was almost directly above the wheel centre so there was little pitching or rolling motion. The acceleration of the centre of the axle was recorded for comparison with results obtained from computer simulation.

The same piece of equipment was used to produce the tyre data and to validate it, however the two measurements were quite independent of each other. The tyre stiffness and damping measurement depended only on the magnitude and phase relationship

between the acceleration at the axle and the force at the axle. It can be described as a first order system, independent of the motion of the carriage and any other forces. The vibration measurements used to validate the simulation depended on the dynamics of the whole carriage. It is described by second order equations which include the tyre characteristics, the carriage mass and all other external forces such as friction in the supporting links. Because of these fundamental differences, it is exceedingly unlikely that a systematic error should occur in the tyre characteristic measurement the effect of which is cancelled out by the same error during the measurement of the vibration.

The wheel was rolled over one wheel track of a standard 100 m rough track, built according to International Standard ISO/TR5007 (1979). The surface of this track is made up from wooden slats 80 mm wide separated by gaps of 80 mm. Accurate speed and position measurements were made by monitoring the passage of these slats past an ultrasonic displacement transducer mounted close to the wheel axle. Another important feature of the track is that the tractor towing the test wheel could drive with its wheels on level concrete, straddling the rough profile, while the test wheel rolled over the profile. This ensured that the motion of the wheel carriage was due only to the input from the test wheel.

Measurements were made at six speeds from 5 to 17½ km/h and with two combinations of tyre load and inflation pressure. These are given in Table XI. Two measurements of the vibration under each set of conditions were made. Variation in the rms acceleration measured during the pairs of runs did not exceed 5% or 0.08 m/s<sup>2</sup>.

**Table XI** Summary of experimental conditions

Tyre:	13.6 R 38 (tyre T4)		
Track:	artificial rough track		
Load/Pressure combinations	light:	1860 kg	1.38 bar
	heavy:	2230 kg	1.03 bar
Rolling speeds:	5, 7.5, 10, 12.5, 15, 17.5 km/hr		

### 6.3 Model of dynamic system

The system was modelled as shown in Figure 50. A linear spring and viscous damper representing the tyre characteristics act between the carriage mass and ground profile. The carriage is represented as a simple mass. A second source of damping,  $C_p$ ,

representing the resistance to carriage motion due to the linkage between the tractor and the carriage is also included. The model is entirely linear and so makes no provision for the tyre leaving the track surface or for dry friction in the linkage arms.

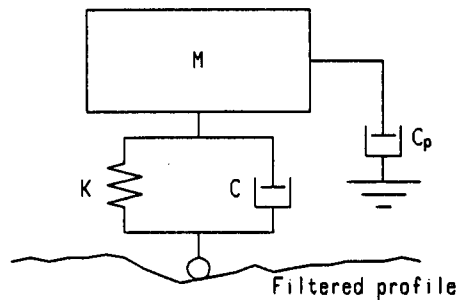


**Figure 50** Schematic model of the vibrating wheel carriage

The computer program used for this simulation works in the time domain. It calculates tyre forces and the resultant axle acceleration from the tyre and carriage data supplied. It then calculates the carriage velocity and displacement from the acceleration using Runge-Kutta-Nyström integration. An integration step length of around 1 ms is used to ensure accurate, stable integration. A cubic spline is used to interpolate between the defined ground profile points in order to achieve this step length. The results of this simulation were transferred to a different computer and then subjected to exactly the same analysis as the measured vibration.

The tyre stiffness and damping values used for the simulation were measured immediately before rolling the carriage over the rough track to measure the carriage vibration. The measured stiffness was reduced by 10% to account for the apparent variation in stiffness due to the nature of the track surface as given in Table V on page 54. The damping coefficient was not reduced (Table IX, page 72).

The parasitic damping due to the linkage connecting the carriage to the tractor was estimated to be 1 kNs/m. This estimate was obtained by measuring the rate of decay of free oscillation when the rear carriage and tyre were supported on steel coil springs as described in section 3.4 on page 43.

Two different estimates of the track profile were used.

- a) Surveyed profile estimate: Each point was measured by hand to within  $\pm 3$  mm using the concrete base as a reference level as described by Lines (1983). The

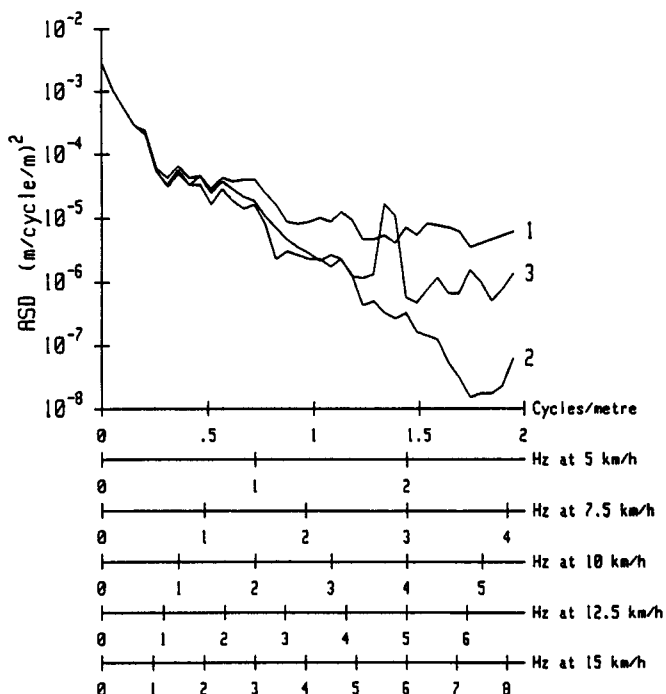


**Figure 51** Power spectral estimates of the profile of the rough surface used to excite the wheel carriage. (1) Surveyed estimate, before tyre enveloping filter. (2) Surveyed estimate with tyre enveloping filter. (3) Recorded estimate

profile was then filtered to account for the tyre enveloping function using the simple tapered moving average filter described by Nguyen and Lines (1988).

- b) Recorded profile estimate: The profile was measured by rolling the wheel over the track at a very low speed (0.8 km/hr) and using an ultrasonic displacement transducer to measure the locus of the axle above the concrete base. This signal was recorded and digitised.

The power spectra of these profile estimates are compared in Figure 51. Up to a spatial frequency of 1.2 cycles per metre, the two spectra are similar, though not identical. Above this frequency they diverge significantly. The spectrum of the recorded profile estimate shows a very strong peak at 1.4 cycles per meter which is unlikely to be a true representation of the track profile since it is not present in the other measurement of track profile. It is more likely to be due to variation of the tractor speed during measurement caused by the engine governor. This causes the tractor to pitch and so vary the height of the sensor. At a frequency of about 1.4 cycles per meter both of the measured track spectra (curves 1 and 3) in Figure 51 become almost horizontal. This probably indicates that the measuring system has reached the limit of its accuracy.



The improvement in modelling accuracy made possible using rolling tyre characteristics is evaluated by comparing the accuracy of the simulation results with the accuracy of the results produced when the model made use of tyre stiffness and damping coefficients obtained from stationary tyres bouncing on a flat surface. Such tyre data was available prior to this research from experiments such as those by Stayner and Boldero (1973). The stationary tyre data actually used for this comparison was obtained from the tyre under examination which was measured on the dynamic tyre test vehicle using the same method as was used to obtain the rolling tyre data. The tyre characteristics used for this simulation are given in Table XII.

**Table XII** Tyre characteristics used for simulation.

---

Nominal speed (km/h)	Actual speed (m/s)	Load (kg)	Damping (kNs/m)	Stiffness (kN/m)
17.5	4.927	1860	1.30	380
17.5	5.017	2300	0.99	315
15	4.242	1860	1.44	383
15	4.307	2300	1.24	317
12.5	3.354	1860	1.68	386
12.5	3.460	2300	1.37	320
10	2.728	1860	1.72	388
10	2.861	2300	1.60	324
7.5	2.072	1860	1.96	393
7.5	2.133	2300	1.44	331
5	1.374	1860	2.24	403
5	1.409	2300	1.66	334

For all speeds the parasitic damping used was 1.0 kNs/m and the quoted stiffness was reduced by 10% to account for the effect of surface.

Comparisons were made at all speeds using the following stationary tyre characteristics

	Load	Damping	Stiffness
Light	1860	3.42	545
Heavy	2300	3.80	450

---

#### 6.4 Analysis of results

The results of the simulation and the measurements have been compared to show

- a) the accuracy of vibration prediction which can be achieved using this simple model,

- b) the improvements in modelling accuracy which derive from the use of rolling tyre characteristics instead of data from stationary tyres and
- c) the effect of different track profile estimates.

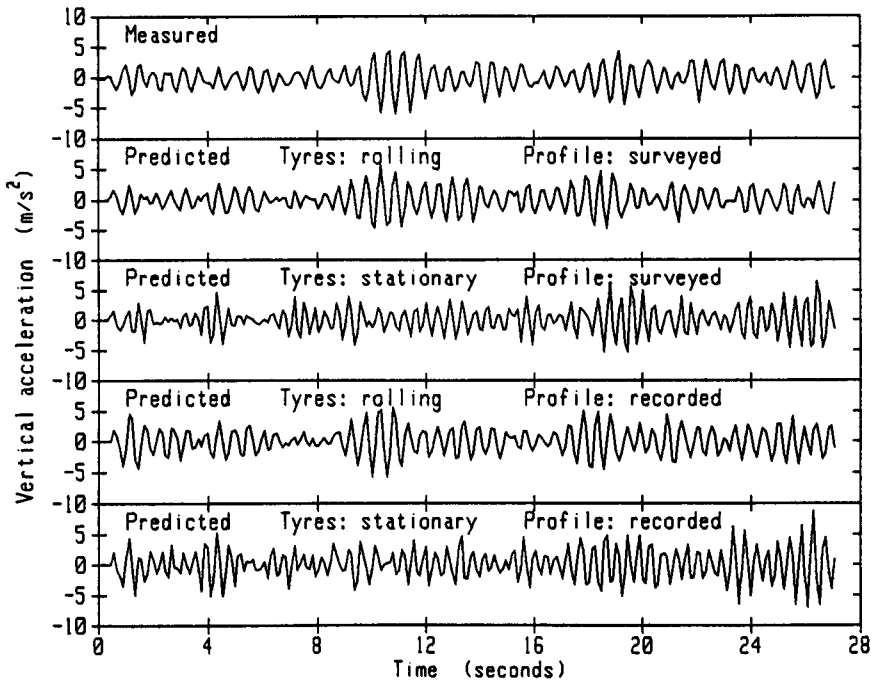


**Figure 52** Measured and modelled acceleration time histories. Heavy load condition at 12.5 km/h. An example of one of the best predictions.

Sample acceleration time histories are given in Figure 52 and Figure 53. They show both a good and a bad match between measurement and predicted results. The predicted vibration produced using both profile estimates are shown, and the results produced using the stationary tyre characteristics are shown for comparison. Figure 52 clearly shows much more accurate vibration prediction than Figure 53. The envelope shape of the acceleration time histories made using the rolling tyre characteristics is also much more similar to the measured one than is the envelope shape produced using stationary tyre characteristics. However in general it is difficult to make objective comparisons between long time histories just by observation. Point by point comparisons also have little value since a very small inaccuracy in the dominant frequency could quickly cause the measured and modelled signals to become out of phase, leading to apparent differences in the two signals out of all proportion to the importance of this error. Therefore comparisons have been made of the root mean square (rms) acceleration levels, the acceleration power spectra and the acceleration envelope.

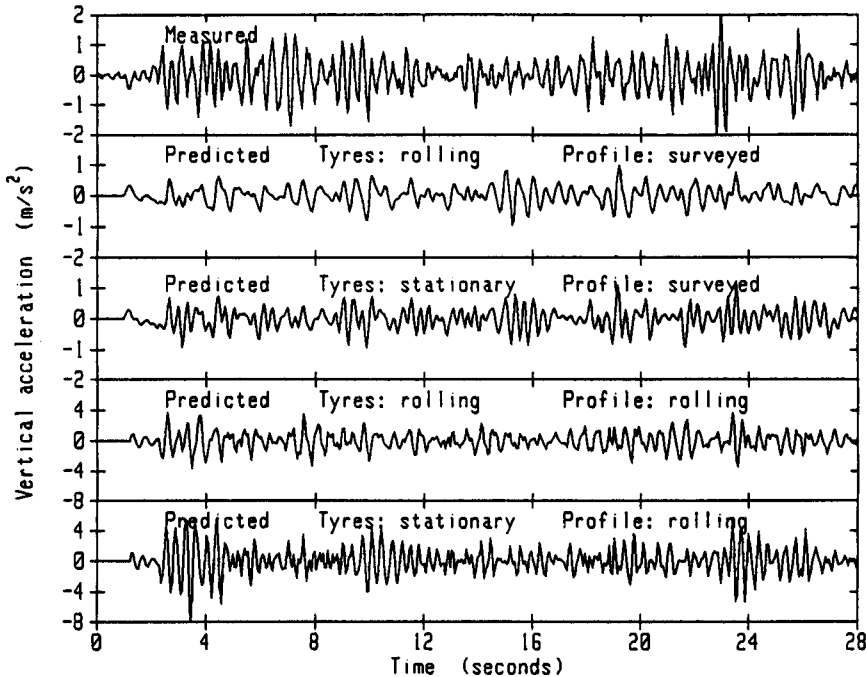


**Figure 53** Measured and modelled acceleration time histories. Light load condition at 5 km/h. An example of one of the worst matches

Overall observation of the results shows that at the lowest two driving speeds the vibration predictions are much less accurate than at the higher speeds. The errors at these speeds frequently do not follow the trend set by the higher speeds. Some possible reasons for this are discussed later, but since they appear to represent a special case, with different sources of error, they have been removed from the analysis of the results.

#### 6.4.1 Root mean square acceleration levels

The rms acceleration levels predicted using the surveyed estimate of the profile are shown in Figure 54. The ratio error in the predicted rms acceleration levels has been calculated as the ratio of the predicted level to the measured level. A perfect match would yield a ratio error of 1.0. The ratio errors produced using the surveyed estimate of the track profile are shown in Figure 55. The means and variances of these errors are given in Table XIII. In this table the results for the two load conditions have been combined and the results relating to the two lowest driving speeds have been neglected. By assuming that the errors are likely to be distributed normally about the mean it is possible use a normal distribution curve to estimate the probability of an rms level being predicted to within a given tolerance. Table XIII indicates that on the basis

of this information we might expect the rms levels to be predicted to within  $\pm 30\%$  for more than 97% of the measurements.

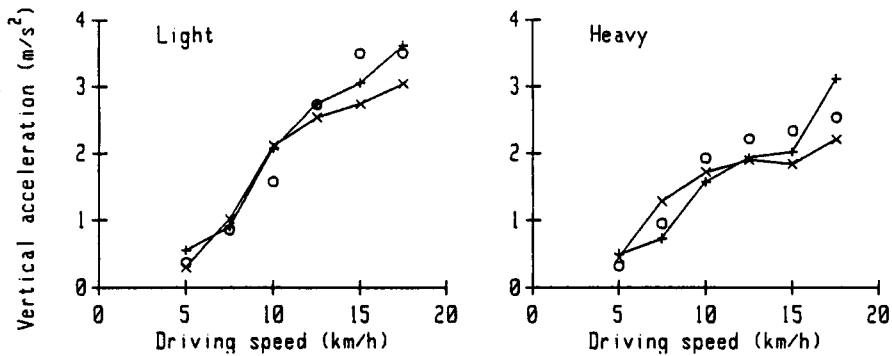


**Figure 54** Measured rms acceleration levels (+) compared with those predicted (x), and also the results of the simulation made using non-rolling tyre characteristics (o). The surveyed estimate of the track profile was used to obtain these data

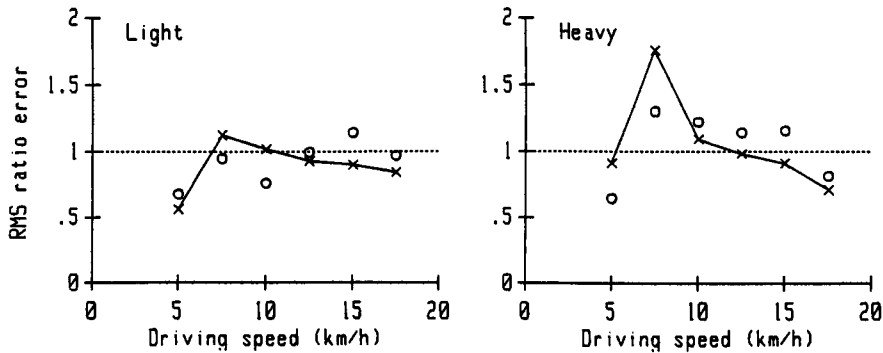


**Figure 55** Ratio errors in the prediction of rms acceleration levels. Predictions made using rolling tyre (x) and stationary tyre (o) characteristics

This result appears to represent only a small improvement over the results which were obtained using stationary tyre data. Although the rms predictions made using the rolling and the stationary tyre characteristics have similar overall accuracy, Figure 55 shows that those made using the rolling tyre characteristics follow a smoother trend, implying that the source of the error has a simple relationship with rolling speed or excitation level. In contrast the predictions made using the stationary tyre characteristics - particularly at the light load condition are much more random. This pattern of results also appears in other measures of simulation accuracy.

#### 6.4.2 Acceleration power spectra

The measured vibration power spectrum for any of the conditions has one dominant peak close to 2 Hz. The predicted vibration spectra based on the rolling tyre data have

**Table XIII** Comparison between the accuracy of the vibration predictions made using rolling and stationary tyre characteristics. Predictions made using the surveyed estimate of the surface profile

	Rolling	Stationary
<u>RMS acceleration</u>		
mean ratio error	0.92	1.03
standard deviation of ratio error	0.12	0.17
probability of less than $\pm 10\%$ error	0.51	0.44
probability of less than $\pm 30\%$ error	0.97	0.92
<u>Peak height</u>		
(quantity compared: square root of PSD peak height)		
mean ratio error	0.88	0.84
standard deviation of ratio error	0.13	0.25
probability of less than $\pm 10\%$ error	0.44	0.26
probability of less than $\pm 30\%$ error	0.93	0.68
<u>Peak frequency</u>		
mean ratio error	1.00	1.21
standard deviation of ratio error	0.01	0.07
probability of less than $\pm 10\%$ error	>0.9999	0.07
probability of less than $\pm 30\%$ error	>0.9999	0.91
<u>Peak width</u>		
(quantity compared: half power width/frequency)		
mean ratio error	1.02	1.15
standard deviation of ratio error	0.07	0.24
probability of less than $\pm 10\%$ error	0.84	0.28
probability of less than $\pm 30\%$ error	>0.9999	0.71
<u>Acceleration envelope shape</u>		
mean of normalised cross correlations	0.91	0.84
standard deviation of above	0.07	0.04
mean of normalised rms envelope error	0.36	0.63
standard deviation of above	0.07	0.08

power spectra very similar to the measured spectra. The only exception is the predictions made for the 5 km/h runs. The predictions made using stationary tyre characteristics compare much less well. Examples of predicted and measured spectra are given in Figure 56.

In addition to subjective assessments of the similarity of the power spectra, quantities related to the height, the peak or mode frequency and half power width of the main peaks of the spectra have been compared. The square root of the peak height has been used for comparison since this is related to the rms acceleration at that frequency. Errors in the peak height can be due to errors in the damping estimate of the system or in the excitation of the system. The ratio errors in predictions of the square root of the peak height have been calculated in the same way as for the rms error. Table XIII

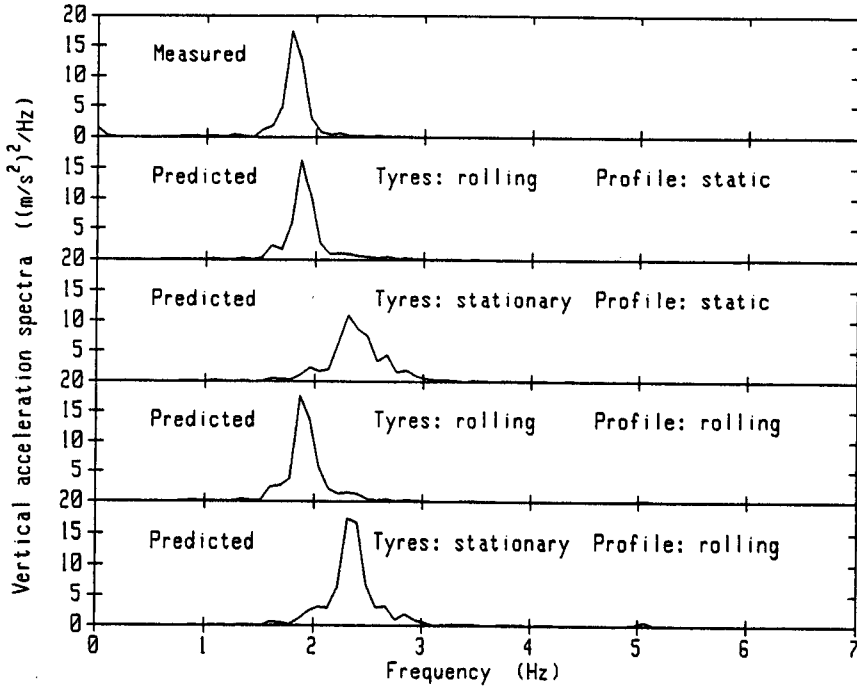


**Figure 56** The measured and predicted vibration power spectra at 12.5 km/h

shows that by making use of the rolling tyre characteristics, over 90% of the predictions of this quantity are calculated to within an accuracy of 30%. Less than 70% of the predictions would previously have achieved this accuracy.

The mode frequencies of the power spectra have been compared (Figure 57). This quantity is related directly to the stiffness of the system. Since the damping is low, neither the system damping nor the input excitation is likely to influence this quantity. Table XIII shows that the ratio error in the frequency prediction varies very little for different load conditions and speeds. The frequency prediction are consistently accurate to less than  $\pm 3\%$  when the predictions use rolling tyre characteristics and take into account the observed apparent softening of the tyre stiffness on this type of track surface. Prior to these measurements the predicted frequency would have been more than 20% too high.

The half power width of the spectra peaks divided by the frequencies have also been compared (Figure 58). This quantity is related closely related to the damping ratio of the system. Table XIII shows that the rolling tyre data enables almost 85% of the peak widths to be predicted to within  $\pm 10\%$ . Without this data less than 30% of the predictions would have been this accurate.

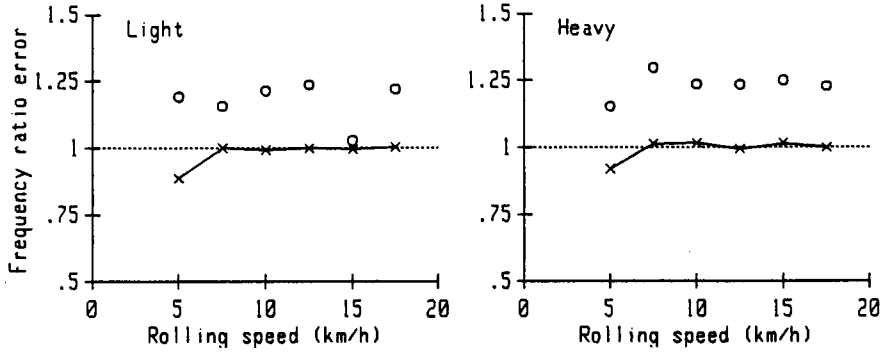


**Figure 57** Ratio errors in the prediction of natural mode frequency using rolling tyre (x) and stationary tyre (o) characteristics

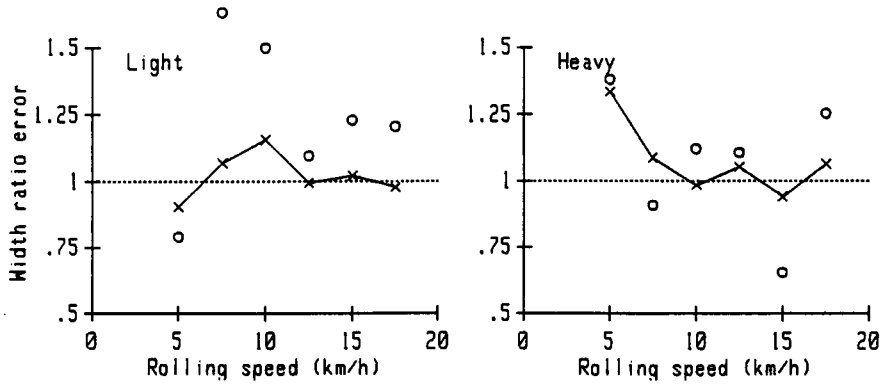


**Figure 58** Ratio error in the prediction of half power width of spectra peaks. Predictions made using rolling tyre (x) and stationary tyre (o) characteristics

6.4.3 Envelope shape

The envelope has been calculated for each of the simulated and measured acceleration time histories by complex demodulation. The similarity of the envelope shapes  $R$  can be evaluated, as the maximum value of the normalised cross correlation calculated between the predicted and measured vibration envelopes.

$$R = R_{xy}(\tau)_{\max} / [R_{xx}(\tau)_{\max} R_{yy}(\tau)_{\max}]^{1/2}$$

where  $R_{xy}(\tau)_{\max}$  is the maximum value of the correlation function between time history envelopes  $x$  and  $y$ . If the two time histories were identical then this value  $R$ , would be 1.0. If the two time histories were entirely independent then the value of the similarity  $R$  would be 0.0. These values of the similarity of the measured and predicted envelopes are given in Figure 59. Means and standard deviations are given in Table XIII.

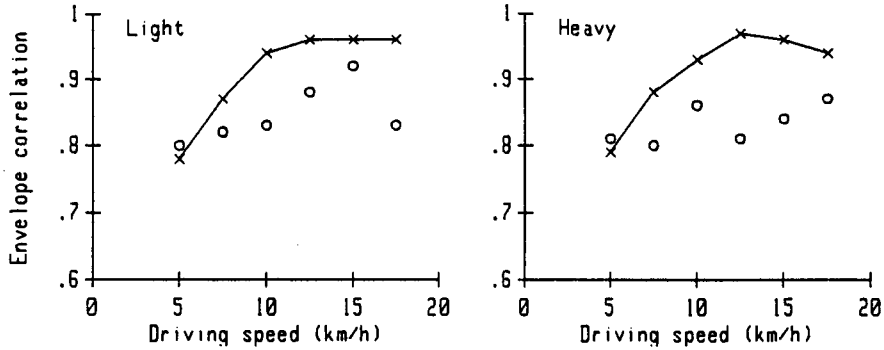


**Figure 59** Similarity of envelope shapes evaluated as the maximum value of the normalised cross-correlation between measured and predicted envelopes. Simulation results using rolling tyre (x) and stationary tyre (o) characteristics

The normalised envelope error has also been computed as the root mean square of the difference between the measured and simulated envelopes. This error is normalised by dividing it by the root mean square of the envelope of the measured acceleration. The process of calculating this error is shown schematically in Figure 60.

Values of the normalised envelope error are shown in Figure 61. Table XIII shows that by this measure the simulation results using the rolling tyre characteristics were almost twice as accurate as those produced using the stationary tyre characteristics.

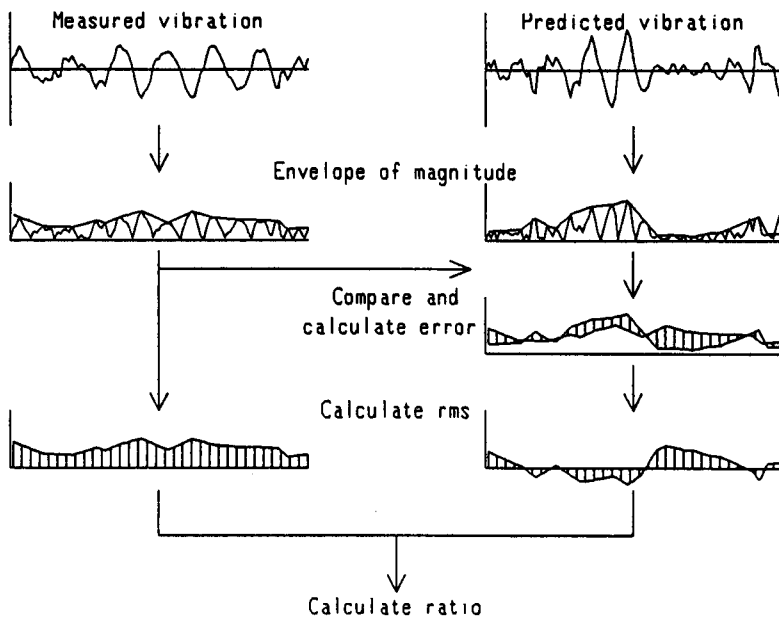


**Figure 60** Calculation of the root mean square of the envelope error



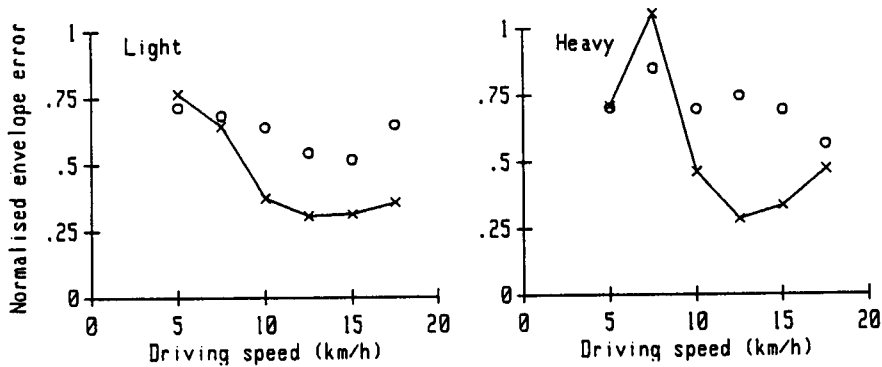


**Figure 61** Normalised root mean square acceleration envelope error. Predictions made using rolling tyre (x) and stationary tyre (o) characteristics

#### 6.4.4 Comparison of the use of different profile estimates

Results obtained using the recorded profile estimate are summarised in Table XIV. Again the results at 5 and 7.5 km/h have been excluded from the analysis. The difference between the other simulation results is small. The simulation made using the recorded profile estimate is usually a little more accurate and the difference between the results using rolling and stationary tyre characteristics a little larger.

#### 6.5 Discussion of results

For this experiment a one degree of freedom system was used which reduced the number of unknown factors. The rolling speed, the tyre position, and the tyre characteristics were well defined. But even under these conditions significant errors did occur. The errors were largest at low rolling speeds.

##### 6.5.1 Errors in vibration predictions at 5 and 7.5 km/h

In the analysis of results which has been presented, simulation results relating to rolling speeds of 5 and 7.5 km/h have been neglected. The errors which some of these results show are significantly larger than the errors at the higher speeds and clearly not part of a trend across the whole speed range. The reasons for these errors are inaccuracy in the input profile spectrum and the response of the vehicle to profile components of a small wavelength.

Measurements presented in Figure 10 showed that in the test track the coherence between track input and vehicle response depended on vehicle rolling speed. At a rolling speed of 6 km/h the coherence at frequencies above 2 Hz was less than 0.3. It is therefore to be expected that predictions of vibration at low rolling speeds will be very inaccurate.

The measured natural frequency of the wheel carriage at 5 km/h was 1.9 Hz (heavy load) and 2.3 Hz (light load). These correspond to spatial frequencies of 1.34 and 1.66 cycles/m. At a spatial frequency of 1.35 cycles/m there is what appears to be a spurious spike in the recorded profile estimate (Figure 51). At this frequency the power in the spectrum is about 13 times greater than that at the surrounding frequencies. The rms excitation at this frequency is therefore about 3.6 times greater than would be expected. The frequency of this spike is very close to the natural frequency of the wheel carriage under the heavy load condition at 5 km/h. If it is spurious then the predicted vibration under this condition will be much larger than the measured vibration. Figure 62 shows this to be the case.

**Table XIV** Comparison between the accuracy of the vibration predictions made using rolling and stationary tyre characteristics. Predictions made using the recorded estimate of the surface profile

	Rolling	Stationary
<u>RMS acceleration</u>		
mean ratio error	1.04	1.13
standard deviation of ratio error	0.14	0.20
probability of less than $\pm 10\%$ error	0.52	0.31
probability of less than $\pm 30\%$ error	0.97	0.78
<u>Peak height</u>		
(quantity compared: square root of PSD peak height)		
mean ratio error	1.01	0.91
standard deviation of ratio error	0.19	0.26
probability of less than $\pm 10\%$ error	0.40	0.28
probability of less than $\pm 30\%$ error	0.89	0.72
<u>Peak frequency</u>		
mean ratio error	1.01	1.21
standard deviation of ratio error	0.01	0.07
probability of less than $\pm 10\%$ error	>0.9999	0.05
probability of less than $\pm 30\%$ error	>0.9999	0.89
<u>Peak width</u>		
(quantity compared: half power width/frequency)		
mean ratio error	0.96	1.09
standard deviation of ratio error	0.12	0.38
probability of less than $\pm 10\%$ error	0.55	0.20
probability of less than $\pm 30\%$ error	0.98	0.56
<u>Acceleration envelope shape</u>		
mean of normalised cross-correlations	0.93	0.86
standard deviation of above	0.04	0.03
mean of normalised rms envelope error	0.38	0.68
standard deviation of above	0.10	0.09

Above this frequency the discrepancy between the two estimates of the profile becomes large. It is therefore clear that significant errors in the vibration prediction will occur due to errors in the input spectra of at least one set of vibration predictions due to errors in the profile estimate at these frequencies. However Figure 51 shows that at about this point both the spectra become almost level suggesting that the noise floor of the systems used to measure the profiles has been reached. This is reasonable since the levels correspond to an rms of 2 mm for the surveyed spectrum and 1 mm for the recorded spectrum.

For the reasons outlined above the vibration input to the simulations made at a rolling speed of 5 km/h was considered unlikely to be accurate and so the results have not been used in the analysis.

At a spatial frequency of 0.8 cycles/m there is another discrepancy between spectra of the recorded and the surveyed profile estimates (Figure 51). At this frequency the power in the surveyed estimate is almost twice that of the recorded estimate. The natural frequency of the wheel carriage under the heavy load condition at a rolling speed of 7.5 km/h is 1.7 Hz which corresponds with this spatial frequency. The vibration prediction made using the rolling tyre characteristics correctly predicts this frequency (Figure 57) and so this error can be seen in the prediction of vibration rms (Figure 55). Vibration predictions made at this speed under the light load condition or using the characteristics of stationary tyres do have the natural frequency at this frequency and consequently do not suffer from this error (Figure 55 and Figure 62).

However since one of the vibration predictions at 7.5 km/h is necessarily wrong, good comparisons could not be made, so all the measurements made at this speed have also been omitted from the analysis of results.

#### 6.5.2 Errors occurring across the whole speed range

The acceleration rms is usually the most important single result to be obtained from a simulation. Although the average prediction of rms levels is not greatly improved by the use of rolling tyre characteristics, Figure 55 shows that such use produces results which more closely follow the trend of the measured results. The implication of this is that an advance has been made in the prediction of rms acceleration levels but that there is still a speed or amplitude related error to be addressed.

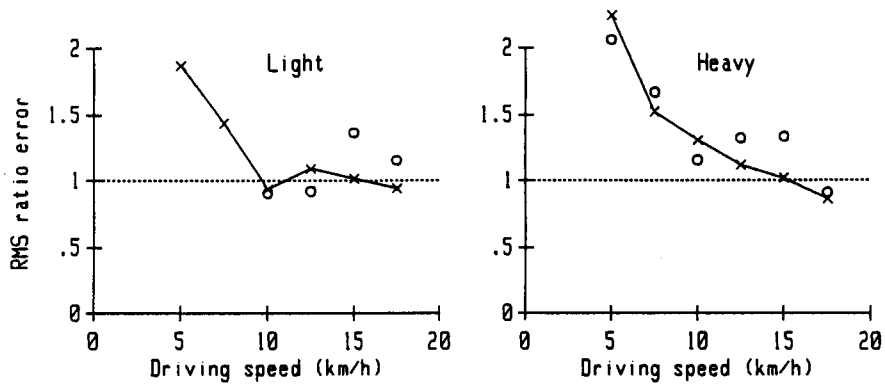


**Figure 62** Ratio errors in the prediction of acceleration rms. Predictions made using Rolling profile estimate with rolling tyre (x) and stationary tyre (o) characteristics

One possible source of error in the prediction of rms levels is inaccuracy of the tyre damping coefficient. Half power peak width is a measure of the tyre damping, and does not include the effect of the linkage damping. Table XIII shows that the half power peak width of the vibration is predicted with significantly greater accuracy than the rms acceleration levels when rolling tyre characteristics are used. When stationary tyre characteristics are used the reverse is true. This suggests that errors in the damping coefficient of the tyre are not the most significant source of error in the rms predictions. Most of the error in the peak width probably derives from roughness of the spectra due to short sampling periods.

Another possible source of this error is in the profile estimates used. The two methods used to obtain the profile estimates were very different in their approach. The only factor which the profile measurements have in common is the assumption that the tyre enveloping function which can be measured under almost steady state conditions is a suitable approximation to the situation under investigation. Since a comparison of the results (Figure 55 and Figure 62) shows a similar trend, the errors using these two profile estimates it is unlikely that this is the source of the problem.

The remaining possibility is that this error is due to friction in the linkage between the tractor and the wheel carriage. It was assumed to be a source of viscous damping in addition to that of the tyre. However if this resistance to motion were to have the characteristics of dry friction (coulomb damping), then its effect on the overall damping of the system would become smaller as the vibration became larger. This would lead to the predictions of the rms acceleration levels being too small at higher speeds and too great at low speeds, as is the case.

A third possible reason for the discrepancy between measure and predicted vibration is in accuracy in the measurement of the vibration. Repeat measurements indicated that variations in the acceleration rms between runs did not deviate by more than 5% (mean deviation 3%). The greater part of this deviation is likely to have been due to differences in the rolling speed. Although the rolling speed was measured accurately and this speed introduced into the simulation, variations in the speed between runs were inevitable since the speed was set using a normal tractor tachometer which could not be read with great precision. Variations in the rms acceleration between runs is too small to account more than a small part of the observed discrepancy between measured and modeled results.

### 6.5.3 Tyre irregularity

Kising (1988) has identified variations in tyre radius as a cause of simulation error. The influence of this factor would have been most noticeable when integer multiples of the tyre rotation frequency coincide with the natural frequency of the system. The rolling circumference of the tyre used is 4.66 m. Examination of the acceleration power spectra gives no indication that there are additional sources of vibration at frequencies corresponding to the first or second harmonics of the tyre revolution frequency. This indicates that for the tyre and speeds used non-uniformity of the tyre is not a significant problem. However at higher speeds, when the first harmonic of the tyre rotation frequency coincides with the natural frequency of the system this might still be a significant factor.

### 6.5.4 Natural frequencies

Probably the most remarkable feature of the results presented is the accuracy with which the mode frequency of oscillation of the carriage is predicted. The predictions of frequency at all except the lowest rolling speed are within 3% of the measured frequency. This confirms that the stiffness of the rolling tyre has been modeled accurately and that it does not change appreciably with changes in vibration amplitude.

### 6.5.5 Prediction of time history

The measures of the similarity between the predicted and measured acceleration envelope shapes show a significant improvement over those calculated using stationary tyre characteristics. Acceleration envelope shape is very dependant on the profile used in the simulation. Under most circumstances it is not the actual time history which should be predicted well but rather statistical data relating to this time history. This information is usually available from the acceleration PSDs. So although time history

prediction is a can be a useful check on prediction accuracy, it is in itself not usually very important.

## 6.6 Conclusions

A single degree of freedom system comprising a tyre rolling over a rough profile while supporting a mass has been modelled. Measured rolling tyre characteristics were used. For comparison, stationary tyre characteristics were also used. These were measured on the tyre being used, but were of the type available prior to this research. The results of the simulation are compared with measured acceleration time histories.

All the measures of simulation accuracy which have been applied show improvement using this data when compared with the data which were available previously. Most noticeable is the prediction of mode frequency, where errors can be consistently less than 3%. The rms acceleration levels can reliably be predicted to better than 30% and in half of the cases examined, to better than 10%. The width and heights of the peak in the spectrum can also be reliably predicted within 30%. Without the use of data derived from rolling tyres this level of accuracy is not attainable. The error in the predicted acceleration envelope is almost half that which occurs when using the stationary tyre data of the sort which was available prior to this research.

At speeds below 10 km/h the vibration prediction is least accurate. This appears to be due to errors in the estimates of the profiles at high spatial frequencies. At these frequencies the variations in level are small and appear to be approaching the limits of accuracy of the measurement systems used.

At higher speeds the main shortcoming of the simulation is a small systematic error in the prediction of rms levels. Predicted rms levels do not rise as rapidly with speed as the measured levels. This error does not seem to be due to errors in the profile specification, the tyre stiffness or the tyre damping. The most likely cause of this is the assumption that the restraining linkage behaves as a viscous damper. This is of course not a problem which arises on a tractor.

## 7 Application of improved tyre description to an agricultural tractor

### 7.1 Introduction

In the previous chapter measured tyre characteristics were used to model the vibration of a simple one wheel trailer. It was shown that the use of more accurate tyre characteristics significantly improved the accuracy of prediction of the frequencies of the natural modes of vibration and the rms acceleration levels. In order to assess the effect that an improved description of the vertical tyre characteristics is likely to have under more normal circumstances they have been tested using a whole tractor. In the past a model which seemed to predict the vibration of one tractor accurately proved to be extremely inaccurate for other tractors (Stayner, Collins and Lines 1984). Mindful of this, an attempt has been made to broaden the testing of this model by using several combinations of load, tyre inflation pressure and track surface. The modelling has been done both without longitudinal tyre stiffness and damping, and using estimates of the tyre stiffness and damping.

### 7.2 Measurement of vibration

Measurements of vibration were made of a Massey Ferguson MF698T tractor. This is a standard mid-range two wheel drive tractor in common use in Britain. Some details of the tractor are given in Table XV. The vibration of the tractor in pitch and vertical directions was measured using accelerometers mounted between the driver's seat and the cab floor. These were recorded on magnetic tape for analysis later. The use of the cab floor was considered suitable since the natural frequency of a cab on its sound isolating mounts is several octaves above the dominant frequencies of vibration of the tractor. Additional weights were placed on both the front weight carrier and on the rear wheels to change the weight and pitch moment of inertia of the tractor. Tyre inflation pressures were also varied. The tractor was driven at speeds between 10 and 17.5 km/h over the artificial standard rough track (SBT) used in the previous experiment (section 6.2 on page 83) and also over an unmetalled farm track known locally as the Hussey Highway (HH). On the artificial rough track the measurements were limited to the length of the track which is 100 m or to thirty seconds of measurement time. On the farm track measurement started at the same point on the track and lasted for thirty seconds regardless of tractor speed.

**Table XV** The Massey Ferguson MF698T

wheel base	2.436 m	
	<i>front</i>	<i>rear</i>
tyre size	7.50-18	13.6R38
ply rating	8-ply	8-ply
track width	1.41 m	1.64 m
<i>tyre pressures</i>		
load condition 1 (heavy)	3.45 bar	1.31 bar
load condition 2 (heavy)	3.45 bar	2.07 bar
load condition 3 (heavy)	2.76 bar	1.03 bar
load condition 4 (light)	3.45 bar	1.31 bar
	<i>heavy</i>	<i>light</i>
total mass	5120 Kg	3617 Kg
load on front axle	18520 N	12750 N
load on rear axle	31710 N	22730 N
centre of gravity height	0.838 m	0.903 m
distance from rear axle	0.896 m	0.873 m
pitch moment of inertia	6210 Kg m <sup>2</sup>	4414 Kg m <sup>2</sup>

### 7.3 Model of dynamic system

The program used to model this tractor was produced by Collins (1990). It was developed for the purpose of modelling the motion and loads on tractor and implement combinations in transport. The model is based on ADAMS software (Automatic Dynamic Analysis of Mechanisms) but also uses a large number of user written subroutines. For the purpose of this simulation it was reduced to a seven degree of freedom model of a tractor with no implements attached. The tractor is described as a rigid body, attached to a front axle which has independent roll freedom. The tyres were each modelled as three Voigt-Kelvin units, one contacting the ground in the vertical direction, one in the lateral direction and one in the longitudinal direction. The tyres were free to loose contact with the ground, in which case all the tyre forces returned to zero.

The ground profile input used for the artificial rough track was the static measurement profile described in section 6.3 on page 84, however for this both left and right wheel tracks of the surface were used. The profile was filtered using the same enveloping filter as in the previous experiment.

The profile of the farm track has been measured at 50 mm interval on both wheel tracks using standard surveying methods. However this measurement was made several years before this experiment. In the intervening period the track has been periodically



repaired. However it is largely the passage of tractors over the track that created the track roughness when it was measured. This has changed very little, so the same factors have operated on the track since it was levelled. It therefore is reasonable to expect that the spectrum of the track will be similar to that measured even though the actual roughness may be less and the time history of the profile different.

The vertical stiffness and damping of the tyres used on the tractor were not themselves measured. However tyres of similar size and construction had been measured and the characteristics of these were used. Because of the age of the tyres, tyre T3 was considered to be most similar measured tyre to those on the tractor, therefore its characteristics were used in the simulation. The measured stiffness of the tyre T3 at the relevant speeds was adjusted for the different inflation pressures used in the simulation by the measured rate of 177 kN/m per bar. The damping of tyre T3 was adjusted for inflation pressures by 0.36 kNs/m per bar and for different loads by 0.071 kNs/m per kN of load. The characteristics used for the front tyre were based on the measurements of tyre F1. The stiffness at the relevant speeds was increased by 134 kN/m per bar and the damping by 0.38 kNs/m per bar of inflation pressure. The stiffness of both front and rear tyres were reduced by 10% when they were on the artificial rough track. These adjustments were made in accordance with the results of the experiments on tyre T3 and F1 described in chapters 4 and 5. The tyre characteristics used are given in Table XVI.

The stiffness and damping of the tractor tyres in the longitudinal and lateral directions were initially set to zero. Later the longitudinal stiffness of the rear tyres was set to 450 kN/m. This value was extracted from the work by Stayner and Boldero (1973), being still the best available estimate of longitudinal tyre stiffness. The damping of the tyres was varied and increased substantially over the measurements published by Stayner and Boldero. This adjustment was justified by the observations of Stayner Collins and Lines (1984) and Lines (1986), that horizontal plane damping of rolling tyres is very much greater than the damping of non-rolling tyres. A Voigt-Kelvin model of the tyre in the longitudinal direction was used even though it is recognised that the a description of the tyre as a damper and spring in series is more suitable.

The lateral tyre characteristics were not changed in this way. They should have no effect on the vertical and pitch motion of the tractor. The equations of motion governing a body of this type given by Stayner, Collins and Lines (1984) show that for small angles of rotation the motion of the tractor in the vertical, longitudinal and pitch directions is

**Table XVI** Tyre characteristics used for simulation

Pressure (bar)		track	speed (km/h)	Stiffness (kN/m)		Damping (kNs/m)	
Rear	Front			Rear	Front	Rear	Front
<i>load condition 1 (heavy)</i>							
1.31	3.45	SBT	10	328	426	1.12	1.47
			12.5	324	426	0.96	1.34
			15	320	426	0.77	1.20
			17.5	317	426	0.67	1.00
			20	313	426	0.57	0.79
1.31	3.45	HH	10	364	473	1.12	1.47
			12.5	360	473	0.96	1.34
			15	356	473	0.77	1.20
			17.5	352	473	0.67	1.00
			20	348	473	0.57	0.79
<i>load condition 2 (heavy)</i>							
2.07	3.45	SBT	10	417	435	1.43	1.47
			12.5	431	435	1.25	1.34
			15	446	435	1.08	1.20
2.07	3.45	HH	12.5	499	483	1.25	1.33
			15	495	483	1.08	1.20
			17.5	491	483	0.98	1.00
<i>load condition 3 (heavy)</i>							
1.03	2.76	SBT	10	283	345	1.08	1.17
			12.5	279	345	0.90	1.04
			15	275	345	0.73	0.90
1.03	2.76	HH	12.5	310	383	0.90	1.03
			15	306	383	0.73	0.90
			17.5	302	383	0.53	0.70
<i>load condition 4 (light)</i>							
1.38	2.76	SBT	10	339	345	0.83	1.17
			12.5	336	345	0.65	1.04
			15	332	345	0.48	0.90
1.38	2.76	HH	12.5	373	383	0.65	1.03
			15	369	383	0.48	0.90
			17.5	365	383	0.38	0.70
<i>stationary tyre characteristics used</i>							
load condition 1				446	630	2.2	2.9
load condition 2				598	630	2.6	2.9
load condition 3				390	532	2.1	2.5
load condition 4				460	532	2.2	2.5

independent of the motion in the roll, lateral and yaw directions.

#### 7.4 Analysis of results

The results of the simulation and the recorded, digitized time histories were analysed in exactly the same way, using the same analysis programs. First vertical acceleration of the tractor was combined with the pitch to calculate the vertical and pitch

acceleration of the tractor at the tractor centre of gravity. The power spectra of the vertical and pitch acceleration time histories were then calculated using an analysis bandwidth of 0.1 Hz. From these spectra the vertical and pitch rms acceleration levels of the tractor body, between frequencies of 0.5 and 10 Hz were calculated. The frequencies of the dominant peaks in the spectra were also measured.

The errors in the prediction of rms acceleration levels and the mode frequencies were then calculated as the ratio of the predicted to the measured quantity. By assuming that the errors of the predictions are spread around the mean with a normal distribution, the probability of predicting the frequencies or rms acceleration levels correctly to within  $\pm 10\%$  or  $\pm 30\%$  has been calculated.

#### 7.4.1 Root mean square acceleration levels

The root mean square (rms) acceleration levels measured and predicted under the various conditions are shown in Figure 63. Analysis these data is given in Table XVII. It appears from these results that the rms levels are predicted as accurately by the simulation using stationary tyre characteristics as by that using rolling tyre characteristics. The probability of correctly predicting the rms acceleration when the tractor was on the unmetalled farm track has not been calculated since there is no reason to expect that the magnitude of the surface roughness of the track would be similar to that used in the simulation. The errors in the rms predictions are strongly influenced by those occurring at the highest two speeds, 17.5 and 20 km/h. If these two were to be neglected then the probability of predicting vertical rms levels to within  $\pm 10\%$  would increase to 0.58 for the simulation using rolling tyre characteristics and to 0.42 when stationary tyre characteristics were used. There is however no clear reason why these two results should be considered exceptional.

The effect of adding both longitudinal stiffness and longitudinal damping to the tyre characteristics is to reduce the rms acceleration levels in the vertical and the pitch directions (Table XVIII).

#### 7.4.2 Acceleration power spectra

Some sample vertical acceleration power spectra are given. Figure 64 shows one of the most accurate predictions and Figure 65 one of the least accurate. The frequencies of the two main spectra peaks have been identified. Since the power spectra were calculated from the rather short signals lengths available, they are rough due to a lack of data at some frequencies. Identifying the peaks of such power spectra involves some subjective judgment since the roughness of the PSD can cause other points to have a

**Table XVII** Comparison between the measured and predicted vibration of the tractor

	Rolling	Stationary	Rolling	Stationary
<u>RMS acceleration on SBT</u>				
	Vertical		Pitch	
mean ratio error	1.13	0.97	0.72	0.65
standard deviation of ratio error	0.25	0.18	0.13	0.13
probability of less than $\pm 10\%$ error	0.28	0.41	0.08	0.07
probability of less than $\pm 30\%$ error	0.68	0.89	0.58	0.35
<u>RMS acceleration on HH</u>				
mean ratio error	2.08	1.50	1.37	0.94
standard deviation of ratio error	0.33	0.25	0.23	0.18
<u>Peak frequencies on SBT</u>				
	First peak		Second peak	
mean ratio error	1.02	1.20	1.03	1.28
standard deviation of ratio error	0.09	0.12	0.08	0.10
probability of less than $\pm 10\%$ error	0.74	0.19	0.74	0.04
probability of less than $\pm 30\%$ error	0.999	0.80	0.999	0.56
<u>Peak frequencies on HH</u>				
mean ratio error	0.94	1.14	0.95	1.12
standard deviation of ratio error	0.09	0.16	0.12	0.12
probability of less than $\pm 10\%$ error	0.64	0.43	0.55	0.40
probability of less than $\pm 30\%$ error	0.998	0.84	0.98	0.93

**Table XVIII** Effect of longitudinal stiffness and damping on predicted vibration at 10 km/h on the artificial rough track with load condition 1

Longitudinal stiffness (kN/m)	Longitudinal damping (kNs/m)	Vertical rms (m/s <sup>2</sup> )	Pitch rms (rad/s <sup>2</sup> )	frequencies of peaks (Hz)		
0	0	1.91	1.50		2.21	3.27
455	0	1.68	1.66	1.65	2.63	3.65
455	1	1.42	1.34	1.65	2.58	3.66
455	3	1.25	1.15	1.68	2.57	3.67
455	5	1.15	1.06	1.70	2.48	
0	1	1.84	1.44		2.21	3.10
0	3	1.74	1.35		2.19	3.24
0	5	1.65	1.25		2.20	3.31
measured result		1.79	1.98		2.15	3.09

higher value than the one which may be selected as the most peak. In order to avoid distortion of the results through this, the spectra were examined and the mode frequencies identified without reference to the source of the data or to the other comparable spectra. The ratio errors in the frequency of the predicted modes are

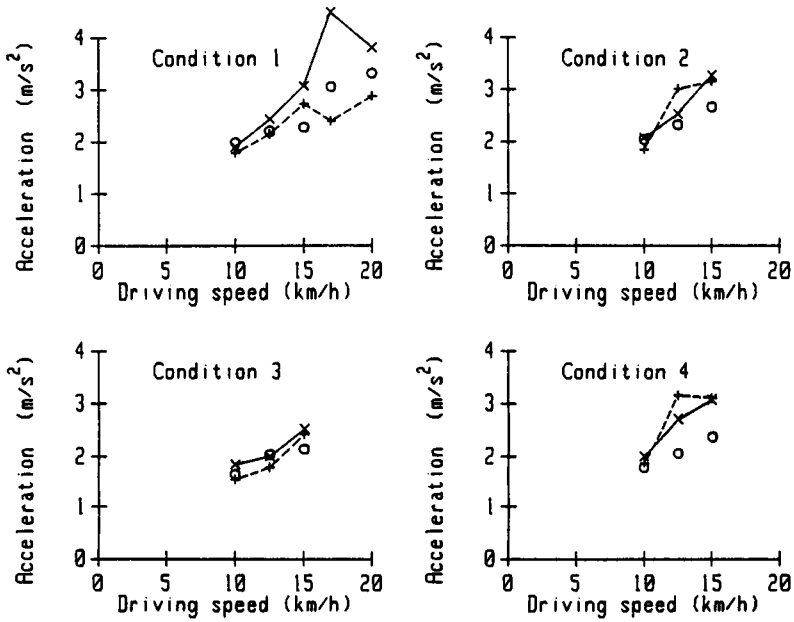


**Figure 63** Measured and predicted vertical rms acceleration for different conditions of load and tyre inflation pressure. Measured results (+), predictions using rolling tyre characteristics (x) and stationary tyre characteristics (o)

shown in Figure 66. Analysis of these results (Table XVII) shows that the mode frequencies are predicted very much more accurately when rolling tyre, rather than static tyre characteristics are used in the simulation.

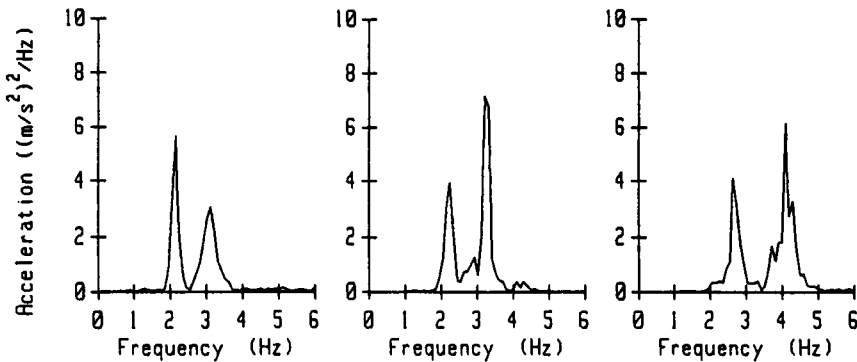


**Figure 64** Vertical acceleration spectra for tractor on the artificial rough track at 10 km/h with load condition 1. Measured (left), predicted (centre) and prediction made using stationary tyre characteristics (right)

When the rear tyres were given a longitudinal stiffness, a third vibration mode was produced, which can be seen in the additional peak in the spectrum (Table XVIII). The frequencies of the other natural modes were also increased. These effects of the longitudinal stiffness are not seen in the measurements.

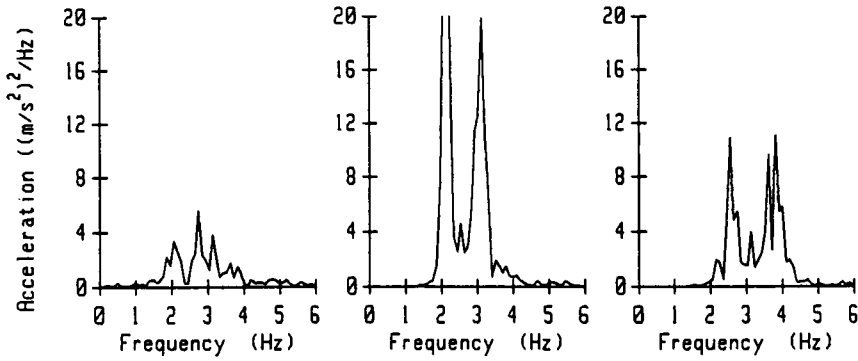


**Figure 65** Vertical acceleration spectra for tractor on the artificial rough track at 17.5 km/h with load condition 1. Measured (left), predicted (centre) and prediction made using stationary tyre characteristics (right)

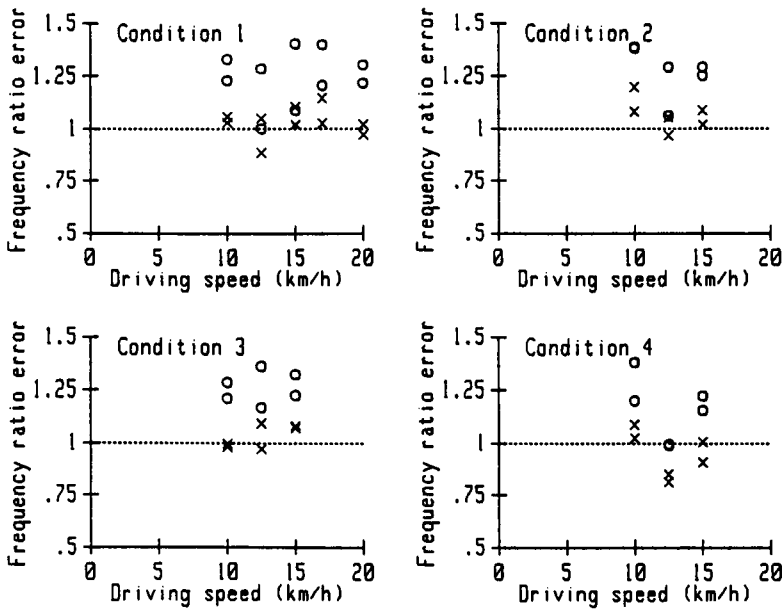


**Figure 66** Comparison of the ratio errors of the prediction of mode frequencies made using rolling tyre (x) and stationary tyre (o) characteristics

### 7.5 Discussion of results

An obvious deficiency of the initial model is the lack of any longitudinal tyre stiffness and damping on the rear wheels. In most previous simulation attempts the longitudinal characteristic of the driven tyres have been represented by a Voigt-Kelvin unit. However when this description of the tyre is introduced into the model a third natural mode appears in the vertical and pitch vibration spectra which cannot be observed in the measured vibration. The frequencies of the other two modes are also increased by this additional stiffness, so they are no longer predicted correctly. The best predictions were made using a damper without a spring to represent the longitudinal tyre characteristic.

It has been shown by Lines (1987) and by Crolla, Horton and Stayner (1990) that a Voigt-Kelvin unit is not an appropriate way to represent the longitudinal characteristics of tyres. A spring and damper in series appears to better represent the system. This is sometimes known as the Maxwell model. The behaviour of such a system merits a little consideration since its behaviour is not the same as that of a spring and damper in parallel. Consider a system which includes a spring set in series with a very light viscous damper. This system will derive no stiffness or damping from this unit. If the damper is very heavy, no damper motion will take place and all the vibration will occur in the spring. Again the system will derive no damping from this unit. The stiffness of the system will however have increased. At damping levels between these two extremes both damper and spring motion will take place, and both will contribute to the characteristics of the system. Decreasing the damping coefficient of the damper in such tyre model can therefore either increase or decrease the energy dissipated from the system depending on the damping and stiffness of the components. Decreasing the damping will also decrease the contribution of this element to the system stiffness.

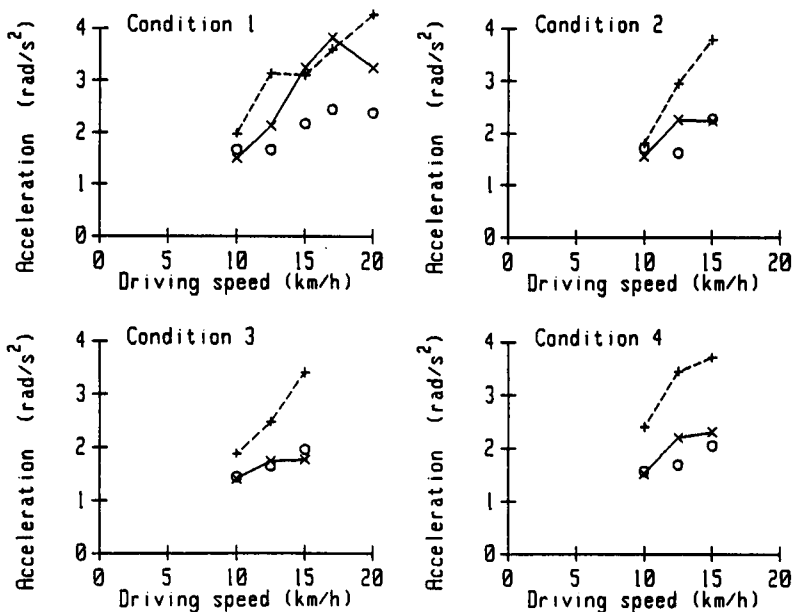


**Figure 67** Measured (+) and predicted (x) pitch vibration rms acceleration. Predictions made using stationary tyre characteristics are also shown (o)

From this reasoning it is clear that introducing such a description of the longitudinal characteristics of the tyre would not increase the frequencies of the other modes by as much as a Voigt-Kelvin model. If the damper was suitably light it would not introduce another visible peak in the spectra either. It would however be able to absorb some of the vibration energy of the vehicle. If the damping coefficient of this damper is light and

it reduced progressively with increasing rolling speed as it is expected to do, it would result in a greater increase of vibration with speed than has been predicted. This would be particularly marked in the longitudinal and pitch vibrations. Comparison of Figure 63 and Figure 67 shows that the measurements made are consistent with this proposal.

## 7.6 Conclusions

The tractor vibration simulation using the measured vertical tyre characteristics consistently predicts the frequencies of the natural modes of vibration with more accuracy than was possible using previously available data. The natural frequencies of vibration can be confidently predicted by this method to within  $\pm 30\%$ . Frequency predictions can be made to within  $\pm 10\%$  in about 60% of the cases examined.

The predictions of acceleration rms are not however improved by the use of the measured stiffnesses of rolling tyres. Rms acceleration levels in the vertical and pitch directions are predicted to within  $\pm 30\%$  of the measured values in about 60% of the cases examined. The predictions made using the characteristics of stationary tyres have a similar accuracy.

The addition of longitudinal tyre damping improves the accuracy of rms acceleration predictions. Reliable prediction of the levels of vibration are unlikely to be achieved until the longitudinal characteristics are measured. The simulation results are consistent with the proposal that a spring and damper in series is a more accurate description of the tyre in this direction than a spring and damper in parallel.



## 8 Prediction of the natural frequencies for a range of tractors

### 8.1 Introduction

It has been shown in chapter 7 that the natural frequencies of vibration of a four wheel tractor in the pitch and vertical directions can be predicted with confidence to within  $\pm 30\%$  and usually to within  $\pm 10\%$ . These predictions were made using the vertical stiffness of the tractor tyres and neglecting the longitudinal stiffness. Reduced to its simplest form the tractor model used for these predictions can be represented as a simple suspended beam as shown in Figure 68. It has also been shown in chapter 4 that the vertical stiffness of traction tyres can be estimated from the size, age and inflation pressure of the tyre. It should therefore be possible to estimate the frequencies of the natural modes of vibration of other tractors from a knowledge only of the tyre size, age and inflation pressure and from the tractor centre of gravity position, mass and moment of inertia.

### 8.2 Analysis using existing data

Measurements of the characteristics of seven different tractors have been made previously at Silsoe (Collins 1982). The tractors were selected to cover a wide range of types. They included two and four wheel drive tractors with equal and unequal size wheels, front and rear cab positions, suspended and unsuspended axles. The masses and moments of inertia of the tractors were measured. The vertical stiffness of the stationary tyres was measured using the method outlined by Stayner and Boldero (1973) and the tyre sizes and inflation pressures noted. The vibration spectra of these tractors as they drove over a rough track was also recorded.

Five of the seven tractors had no suspension except for that provided by the tyres so predictions of the natural frequencies of these tractors have been made. Details of these tractors are given in Table XIX.

The stiffnesses of the traction tyres have been estimated from the relationship given in section 4.5.3:

$$K = 172 - 1.77 R + 5.6 A + 0.34 W R P$$

where  $K$  is the stiffness in kN/m of a tyre of size  $W$ - $R$ , age  $A$  years inflated to  $P$  bar. All the tractors measured were relatively new so the tyres were assumed to be 1 year old.

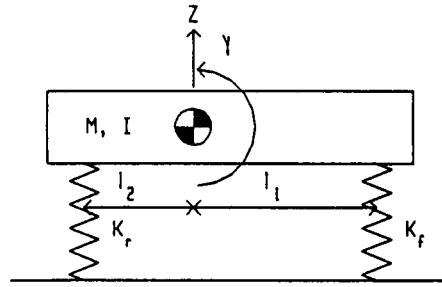


**Figure 68** Representation of tractor model with vertical ( $Z$ ) and pitch ( $\gamma$ ) freedom. Tractor mass  $M$ , pitch moment of inertia  $I$ , front stiffness  $K_f$ , rear stiffness  $K_r$

**Table XIX** Tractor data

Tractor	Mass (kg)	$I$ (kgm <sup>2</sup> )	$l_1$ (m)	$l_2$ (m)	Tyres: front rear	Size	Pressure (bar)
Leyland 272	3235	2669	1.33	0.71	Dunlop T8 Kleber Super 50	7.50-16 13.6-38	2.06 1.1
Massey Ferguson 590	3434	3946	1.48	0.81	Goodyear Goodyear	7.50-18 12-38	2.3 1.3
Deutz Intrac 2004A (4-wd)	3748	3666	1.16	1.04	Dunlop TG 32 Fulda	10.5-20 16.9/14R30	2.06 1.1
County 774 (4-wd)	4767	3862	0.81	1.01	Goodyear Goodyear	13.6R38* 13.6R38	0.83 1.2
David Brown 996 (4-wd)	3573	4315	1.06	1.04	Dunlop Goodyear	11.2/10-24 13.6/12-36	1.7 1.5

\* water ballasted

$I$  is the pitch moment of inertia,  $l_1$  and  $l_2$  are the horizontal distances between the centre of gravity and the front and rear axles respectively.

Siefkes (1989) has noted that the tyre stiffness of water ballasted tyres is increased by about 25% (section 1.7.10). The estimated stiffness of the front tyres of the County 774 tractor was accordingly increased by this amount.

A method for estimating the stiffness of the two front un-driven tyres is also required for this prediction. Table III shows that the carcass stiffness of the measured ribbed tyre ( $F_1$ ) is almost zero and that the inflation pressure dependence of the tyre is 134 kN/m per bar. If it assumed that the same form of relationship could be used to estimate the stiffness of undriven wheel tyres as was used for traction tyres then this relationship will be

$$K = \frac{134}{7.5 \times 18} W R P$$

or approximately  $K = W R P$

Using these two simple equations the tyre stiffnesses of the five tractors were estimated.

Motion of the tractor model shown in Figure 68 is governed by the following matrix equation of motion

$$\begin{pmatrix} K_f + K_r - M\omega^2 & K_f l_1 - K_r l_2 \\ K_f l_1 - K_r l_2 & K_f l_1^2 + K_r l_2^2 - I\omega^2 \end{pmatrix} \begin{pmatrix} z \\ \gamma \end{pmatrix} = 0$$

The eigen frequencies of this model can be extracted as the roots of the characteristic equation of the matrix

$$\omega^4 M I - \omega^2 I (K_f + K_r) - \omega^2 M (K_f l_1^2 + K_r l_2^2) + (K_f + K_r)(K_f l_1^2 + K_r l_2^2) - (K_f l_1 - K_r l_2)^2 = 0$$

Values for the front and rear stiffness of the model ( $K_f$  and  $K_r$ ) represent the combined stiffness of both left and right tyres of the tractor so they must have twice the value of the estimated tyre stiffness  $K$ . These values of  $K_f$  and  $K_r$  can be inserted into the above equation and the eigen frequencies extracted.

Vertical and pitch vibration for these tractors was examined and the natural frequencies of motion identified from the peaks in the power spectra. The power spectra were calculated from relatively short signal lengths so the identification of the peaks in the power spectra contained an element of subjective judgment in discriminating between the peaks caused by the dynamics of the system and those caused by poor sampling of the input spectra. Bias was avoided by making the identifications without reference to the predicted frequencies. The vertical and pitch vibration power spectra for the tractors at several driving speeds were examined. The two frequencies identified as the natural frequencies were those that were most clearly identifiable in all the vertical, pitch and longitudinal motion spectra.

The tyre stiffnesses and the predicted and measured natural frequencies of the tractors are given in Table XX. The predicted natural frequencies are also shown plotted against the measured natural frequencies in Figure 69

**Table XX** Tyre stiffnesses and the predicted and measured natural frequencies of vertical and pitch vibration

Tractor	Stiffness		Predicted		Measured	
	Rear (kN/m)	Front (kN/m)	Frequencies (Hz)	Frequencies (Hz)	Frequencies (Hz)	Frequencies (Hz)
<i>Tyre stiffnesses predicted from tyre size, age and inflation pressure</i>						
Leyland 272	306	247	2.76	3.50	2.4	3.4
Massey Ferguson 590	314	311	2.70	3.64	2.7	3.7
Deutz Intrac 2004A	316	273	2.82	3.14	3.0	3.4
County 774	323	323	2.49	2.78	2.5	3.3
David Brown 996	365	271	2.71	3.14	2.5	3.0
<i>Tyre stiffnesses determined from free vibration of stationary tyres</i>						
Leyland 272	340	332	2.92	4.05		
Massey Ferguson 590	360	377	2.89	4.01		
Deutz Intrac 2004A	465	571	3.57	4.35		
County 774	564	653	3.55	3.68		
David Brown 996	432	332	2.99	3.42		

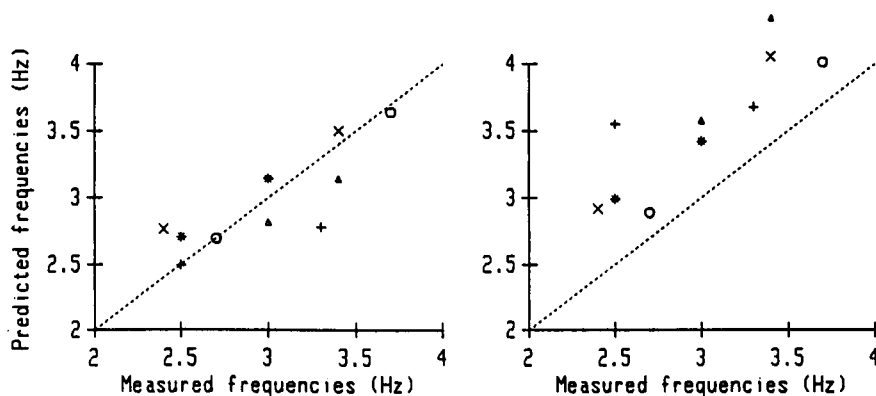


**Figure 69** Predicted and measured natural frequencies of vibration in the pitch and vertical directions. Predictions made using the estimated tyre stiffnesses (left) and using measured stationary tyre stiffnesses (right). Leyland 272 (x), Massey Ferguson 590 (o), Deutz Intrac 2004A ( $\Delta$ ), County 774 (+), David Brown 996 (\*)

The ratio errors of the frequency predictions have been calculated as the predicted frequency divided by the corresponding measured natural frequency. The mean ratio error of the frequencies predicted using the tyre stiffness estimates was 0.998 (ie the average error in frequency prediction was only 0.2%). This can be compared with a mean ratio error for the predictions made using the measured stationary tyre stiffnesses

of 1.19 (ie 19% error). The standard deviations of the ratio errors were 0.09 and 0.11 respectively. If the ratio errors are assumed to be normally distributed about a mean then the reliability of the predictions can be estimated from the mean and standard deviation of the errors by referring to a normal distribution table. This shows that when the tyre characteristics are estimated from the tyre size, 75% of the predictions of natural frequencies can be expected to be within  $\pm 10\%$  of the measured value. In excess of 99.9% of these predictions can be expected to be within  $\pm 30\%$ . However when the natural frequencies are predicted using the measured stationary stiffnesses of the tyres, only 19% of the predictions are likely to be within  $\pm 10\%$  of the measured frequencies and less than 85% within  $\pm 30\%$ .

### 8.3 Discussion

The two largest errors in frequency prediction arise with the County 774 (0.84) and the Leyland 272 (1.15). The vertical and pitch vibration spectra of the County 774 tractor, clearly shows three well defined modes. This is the only tractor to consistently show the third mode. This extra mode at approximately 1.5 Hz, derives from the longitudinal stiffness of the tyres. In the previous section it was shown that the introduction of a third mode of vibration increased the frequencies of the other natural modes. This simple two degree of freedom model is therefore unsuitable for this tractor.

In the case of the Leyland 272, the most obvious reason for the error is that the stiffness of the front tyres has been wrongly estimated. However examining the way in which the two natural mode frequencies change with tyre stiffness, indicates clearly that if it is errors in the tyre stiffness which causes this mode frequency to be predicted wrongly, then the error is in the rear tyre stiffness rather than the front. A rear tyre stiffness of 80% of the estimated stiffness would give much better frequency prediction (Figure 70).

### 8.4 Conclusions

This investigation has demonstrated that using very little information the natural pitch and vertical frequencies of vibration of a tractor can be reliably and easily predicted to within  $\pm 30\%$ . The value of these predictions is not limited to just one type of tractor design or to one drive system. It is recognised however that the range of overall tractor sizes covered by investigation was not great. This is substantially more accurate than predictions which can be made using data from non-rolling tyres and furthermore, these predictions require no special measurements to be made of the tyre.

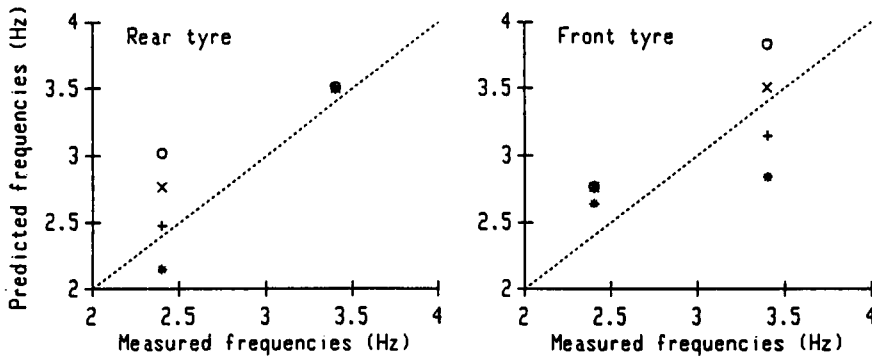


**Figure 70** Natural frequency predictions obtained by variation of the rear and front tyre stiffness by factors of 1.2 (o), 0.8 (+) and 0.6 (\*). The original prediction (x) is also shown

The results also clearly show that the stiffness of the rolling tractor tyres is more reliably obtained from the empirical equation given than from measurements of stationary tyre stiffness.

## 9 General Conclusions

Before this program of work was started little was known about the suspension characteristics of rolling tyres. However it was already clear that they were significantly different from the characteristics of stationary tyres. Since very little information was available, tractor vibration simulation continued to depend on the measured characteristics of stationary tyres.

In order to address this need a dynamic tyre test vehicle was designed and built to enable the suspension characteristics of a range of tyres to be measured in the radial, the lateral and the longitudinal directions over a range of agricultural surfaces. This thesis presents the results of measurements on tyres in the radial direction. These results are combined with further analysis of tyre radial characteristic measurements that have been published during the period of work by Kising (1988).

The stiffness of rolling tyres in the vertical direction is generally lower than the corresponding stiffness of a stationary tyre. It is also less sensitive to changes in other variables such as amplitude and frequency. Tyre stiffness has been found to vary significantly with inflation pressure, tyre size and tyre age. At low speeds it decreases with increasing rolling speed but at speeds over about 10 km/h little further decrease takes place.

Examination of the relationship between stiffness and inflation pressure enables a zero pressure carcass stiffness and a constant inflation pressure dependence to be identified. The inflation pressure dependence is almost independent of rolling speed and tyre age but it increases with tyre size. The carcass stiffness increases with tyre age and with tyre size and decreases with rolling speed up to a speed of about 10 km/h.

The stiffness of rolling tyres has been found to be independent of tyre load and driving torque within normal operating ranges. Variation of stiffness with amplitude of vibration and frequency were found to be small. The available data also suggest that tyre stiffness is not substantially affected by ply rating or by whether it is of a radial or cross-ply construction. Apparent tyre stiffness was found to decrease slightly when the tyre rolled over some agricultural surfaces. It was found to decrease by 10% when the tyre was

rolling on the slatted artificial rough surface specified in British and International standards as a rough surface for exciting tractor vibration.

An empirical relationship has been developed for predicting the stiffness of traction type tyres at rolling speeds of over 10 km/h.

$$K_t = 172 - 1.77 R + 5.6 A + 0.34 W R P$$

where  $K_t$  is the stiffness in kN/m of a tyre of age  $A$  (years) which has a section width  $W$  (inches), rim diameter  $R$  (inches) and is inflated to a pressure of  $P$  (bar). The section width and rim diameter are given in the specification of the tyre size by the manufacturer. This relation was found to be valid for a wide range of traction type tyres. From the data available it appears that this relationship predicts the stiffness of traction tyres with a mean error of 3% and a standard deviation of 10%. The relationship is not valid for the ribbed tyres designed for un-driven wheels.

The damping of the tyres has also been measured. In general the damping is found to be more sensitive to variations in conditions than the stiffness. It increases significantly with tyre age and with inflation pressure. Tyre damping decreases with rolling speed at speeds over about 1 km/h. Measurements show that it continues to decrease with speed up to a rolling speed of 50 km/h. Damping has been found to vary with tyre load, amplitude of vibration driving torque, frequency of vibration and ply rating. Over some soft surfaces the apparent damping was observed to increase to as much as twice its normal value. Much of this was probably caused by permanent deformation of the surface rather than by changes in the behaviour of the tyre. Variations in the damping coefficient of tyres with frequency, amplitude of vibration, rolling speed and load can be modeled by describing the tyre as a set of spokes connecting the hub and the ground, rotating at the wheel rotation speed. These spokes dissipate force by both Coulomb and viscous damping.

The value of this new information has been tested by using it to predict the vibration behaviour of a simple single wheel carriage and of a whole tractor. The single wheel carriage was used because it enabled the effect of the vertical tyre characteristics on simulation accuracy to be assessed without the added complication of the behaviour of tyres in the longitudinal direction. This is as yet largely unknown. Vibration predictions were made using both the measured rolling suspension characteristics of the tyres and the stationary characteristics. This enabled the improvement in simulation accuracy achieved by using the rolling tyre data to be measured.



The single wheel carriage was rolled over a known rough surface at various rolling speeds, loads and tyre inflation pressures. The vibration of the carriage was both measured and predicted using a time domain simulation. The acceleration time histories, vibration spectra and rms vibration levels were compared. All the measures of accuracy used indicated that the simulation using the rolling tyres was more accurate than the simulation using stationary tyre characteristics. The frequency of vibration was consistently predicted to within  $\pm 3\%$  whereas using the stationary tyre characteristics there was only 90% probability of predicting the frequency to within  $\pm 30\%$ . The half power width of the natural frequency peak, which is a measure of the system damping was also predicted much more accurately. These results indicate that both the effective stiffness and damping of the tyre were accurately modelled. Rms amplitudes of vibration were predicted to within  $\pm 30\%$  in 97% of the cases, however prediction to within  $\pm 10\%$  occurred in only 50% of the cases. The main reason for this inaccuracy is thought to be inaccuracy in the modelling of the links used to stabilise the single wheel carriage rather than in the modelling of the tyre behaviour. Errors in the specification of the profile caused predictions at speeds below 10 km/h to be less accurate than those made at higher rolling speeds.

The vibration of a tractor driving over known rough surfaces was also measured. Several driving speeds, load and tyre inflation pressure combinations were used. The natural frequencies of vibration in the vertical and pitch directions were reliably predicted to within  $\pm 30\%$  and to within  $\pm 10\%$  in about 65% of the cases. This accuracy was achieved in less than 20% of cases using the stationary tyre characteristics. The rms vibration levels were predicted to within  $\pm 30\%$  for about 60% of cases. There was little difference between the accuracy of vibration level predictions made using the stationary and rolling tyre characteristics. This is because the higher damping of the stationary tyres compensated for the poor modelling of the longitudinal suspension characteristics of the tyres.

The natural frequencies of motion in the vertical and pitch directions of a range of tractors have been predicted. These predictions were made using the empirical method for estimating tyre stiffness. In over 70% of these predictions the natural frequencies were correct to within  $\pm 10\%$ . They were consistently correct to within  $\pm 30\%$ . Predictions made using the same method but based on the measured stationary tyre characteristics were much less accurate.

This work has shown that the accuracy of vibration simulation of unsuspended vehicles can be significantly improved by the use of rolling tyre characteristics rather than those

measured on a stationary tyre. The stiffness of rolling tyres is more accurately estimated from a simple formula than by measurements of stationary characteristics. The natural frequencies of vibration of a tractor can usually be predicted with acceptable accuracy. Significant advances still have to be made in the prediction of rms levels of vibration. This will be achieved only when the longitudinal suspension characteristics of the traction tyres have been measured and modelled more accurately.

10 References

ADAMS (1987). ADAMS User manual, version 5.2. Mechanical Dynamics Inc. Ann Arbor, Michigan

Apetaur M. (1968). Berechnung der Kräfte und Moment in der Reifenlängsebene auf empirischer Basis (Calculations of the moment in the tyre longitudinal plane on an empirical basis). *Automobiltechnische Zeitschrift*, 12 pp. 417 - 420

Captain K.M., Boghani A.B. and Wormley D.N. (1979). Analytical tyre models for dynamic vehicle simulation. *Vehicle System Dynamics*, 8(1) pp. 1 - 32

Chiesa A. (1965). Vibration performance differences between tyres with cross biased plies and radial plies. *S.A.E.*, paper 990B

Chiesa A. and Rinonapoli L. (1967). Vehicle stability studied with a non-linear seven degree model. *S.A.E.*, paper 670476

Chiesa A. and Tangorra G. (1959). The dynamic stiffness of tyres. *Revue Generale de Caoutchoucs*, 36(10) pp. 1321 - 1329

Claar II P.W. (1982). Effect of agricultural tractor and trailer combinations on operator ride vibration. *A.S.A.E.*, paper 82-1551

Claar II P.W., Buchele W.F., Marley S.J. and Sheth P.N. (1980). Agricultural tractor suspension system for improved ride comfort. *S.A.E.*, paper 801020

Clark S.K. (ed) (1981). Mechanics of pneumatic tyres. U.S. Dept of Transportation, National Highway Traffic Safety Administration, Washington

Collins T.S. (1982). Tractor ride vibration: field measurements and evaluation. (Private Communication)

Collins T.S. (1991). Modelling a non-linear tractor and implement system using ADAMS. Paper to be presented at the 5th European conference on Terrain-Vehicle-Systems, Budapest, September 1991.

Crolla D.A. (1981). Off road vehicle dynamics. *Vehicle System Dynamics*, 10 pp. 253 - 266

Crolla D.A., Horton D.N.L. and Alstead C.J. (1987). A mathematical model of the effect of trailers on tractor ride Vibration. *Journal of Agricultural Engineering Research*, 36 pp. 57 - 73

Crolla D.A., Horton D.N.L. and Stayner R.M. (1990). Effect of tyre modelling on tractor ride vibration predictions. *Journal of Agricultural Engineering Research*, 47, pp. 55 - 77

Crolla D.A. and Maclaurin E.B. (1985). Theoretical and practical aspects of the ride vibration dynamics of off-road vehicles - part 1. *Journal of Terramechanics*, 22(1) pp. 17 - 25

Dale A.K. (1978). The theoretical prediction of tractor ride vibration. Proceedings of the Institution of Measurement and Control Conference. London

Davey A.B. and Payne A.R. (1965). Rubber in Engineering Practice. Maclaren and Sons Ltd, London

Dupuis H. and Christ W. (1966). Untersuchung der Möglichkeit von Gesundheitsschädigungen im bericht der Wirbelsäule bei Schlepperfahrern (Investigation of the possibility of vertebral column damage to tractor drivers). Research report, Max Planck-institut für landarbeit und landtechnik, Bad Kreutznach

Dupuis H. and Christ W. (1972). Untersuchung der Möglichkeit von Gesundheitsschädigungen im bericht der Wirbelsäule bei Schlepperfahrern. -Zweite Folgeuntersuchung (Investigation of the possibility of vertebral column damage to tractor drivers. -Second follow up study). Research report, Max Planck-institut für landarbeit und landtechnik, Bad Kreutznach Heft A 72/2

Dupuis H. and Zerlett G. (1986). The effects of whole body vibration. Springer-Verlag Berlin Heidelberg

EEC. (1978). Council directive on the approximation of the laws of member states relating to the drivers seat on wheeled agricultural or forestry tractors. 78/786/EEC. Amended 1983 and 1988

Gehman S.D. (1957). Dynamic properties of elastomers, *Rubber chemistry and technology*. 30 pp. 1202 - 1250

Gibbon J.M. (1970). Tractor operators survey. Departmental Note No 45/1952 National Institute of Agricultural Engineering, Silsoe (unpublished)

Göhlich H., Schütz F. and Jungerberg H. (1984). Untersuchen zum vertikalen Schwingsverhalten von Ackerschleppern (Investigation of the vibration behaviour of agricultural tractors). *Grundlagen der Landtechnik*, 34(1), pp. 13 - 18

Göhlich H. and Sharon I. (1975). The dynamic behaviour of tractor tyres and their influence on tractor vibration. A.S.A.E., paper 75-1012

Hahn W.D. (1973). Über das Feder-Dämpfer Verhalten von Luftreifen (On the spring and damper characteristics of pneumatic tyres). *Automobil Industrie*, 4 pp. 29 - 40

Harral B.B. and Cove C.A. (1982). Development of an optical displacement transducer for the measurement of soil surface profiles. *Journal of Agricultural Engineering Research*, 27, pp. 421 - 429.

Harrison A.P. (1984). Ride vibration measurements of a Zetor 8111 tractor. (private communication)

t'Hart J. (1977). Suspended drivers cab for off road vehicles. Report No V 173e-E3, Technische Hogeschool, Delft

Hilton D.J. and Moran P. (1975). Experiments in reducing tractor ride vibration with a cab suspension. *Journal of Agricultural Engineering Research*, 20(4) p 433

Hlawitschka E. (1971). Federungs- und Dämpfungsverhalten von Reifen auf gekrümmten Aufstandsflächen (Stiffness and damping of tyres on a curved surface). *Deutsche Agrartechnik*, 21(2) pp. 72 - 75

Hooker R.G. (1980). A model for the radial dynamic behaviour of pneumatic tyres. *International Journal of Vehicle Design*, 1(4) pp. 361 - 372

ISO. (1974). A Guide to the evaluation of whole body vibration. International Standard IS2631

ISO. (1979). Agricultural wheeled tractors -operators seat measurement of transmitted vibration. International Standard ISO/TR5007

Jungerberg H. (1984). Ein Beitrag zur experimentellen und numerischen Simulation von Traktorschwingungen (Experimental and numerical simulation of tractor vibration). Fortschrittberichte der VDI Zeitschriften, Verein Deutscher Ingenieure, Reihe 14, Nr 26

Kauss W. and Weigelt H. (1980). Die gefederte Traktorkabine - verbesserter Schwingungsschutz und Fahrkomfort (The suspended tractor cab - improved vibration characteristics and driving comfort). *Landtechnik* 8/9 p 396

Kising A. (1988). Dynamische Eigenschaften von Traktor-Reifen (Dynamic properties of tractor tyres). *Fortschritt-Bericht VDI*, Reihe 14 Nr.40

Kising A. and Göhlich H. (1988 a). Dynamic characteristics of large tyres. Paper No 88.357 Presented to AG ENG 88, Agricultural engineering conference, Paris, March 2 - 5

Kising A. and Göhlich H. (1988 b). Ackerschlepper-Reifendynamik, Teil 1: Fahrbahn- und Prüfstandsergebnisse (Agricultural tractor tyre dynamics, part 1: roadway and test stand results). *Grundlagen der Landtechnik* 38(3) pp.78 - 87

Kising A. and Göhlich H. (1988 c). Ackerschlepper-Reifendynamik, Teil 2 :Dynamische Federungs- und Dämpfungswerte (Agricultural tractor tyre dynamics, part 2: dynamic spring rate and damping values). *Grundlagen der Landtechnik* 38(4) pp. 101 - 106

Kutzbach H.D. and Schrogl H. (1987). Dynamic behaviour of rolling tractor tyres. Proceedings 9th International ISTVS Conference, Barcelona

Laib L. (1979). On the dynamic behaviour of agricultural tyres. *Journal of Terramechanics*, 16(2) pp. 77 - 85

Lines J.A. (1983). Profile of NIAE smooth bumpy track. Divisional Note DN 1193, National Institute of Agricultural Engineering, Silsoe (unpublished)

Lines J.A. (1985). The ride vibration transfer functions of tractors. Divisional Note DN 1238, National Institute of Agricultural Engineering, Silsoe

Lines J.A. (1987). Ride vibration of agricultural tractors: transfer functions between the ground and tractor body. *Journal of Agricultural Engineering Research*, 37 pp. 81 - 91

Lines J.A. (1991). Rolling tyre characteristics and their effect on prediction of unsuspended vehicle ride. Proceedings of the 5th European Conference on Terrain Vehicle Systems, Budapest, Hungary. 4-6th September 1991

Lines J.A. and Murphy K. (1991). The stiffness of agricultural tyres. *Journal of Terramechanics*, 28(1)

Lines J.A. and Murphy K. (1991). The radial damping coefficient of agricultural tyres. *Journal of Terramechanics*, 28(2)

Lines J.A. and Peachey R.O. (1991). Predicting the ride vibration of a simple unsuspended vehicle. *Journal of Terramechanics*

Lines J.A., Peachey R.O. and Collins T.S. (1991). Predicting the ride vibration of an unsuspended tractor using the dynamic characteristics of rolling tyres. *Journal of Terramechanics*

Lines J.A. and Stayner R.M. (1989). Improved operator performance from reduced vibration, Proceedings of the Institute of Acoustics, 11(5) pp. 135 - 142

Lines J.A., Whyte R.T. and Stayner R.M. (1989). Agricultural vehicle suspensions - suspensions for tractor cabs. Report Presented to the third International Symposium of the International section of the ISSA for research on prevention of Occupational Risks, Vienna, 19 - 21 April

Lines J.A. and Young N.A. (1989). A machine for measuring the suspension characteristics of agricultural tyres. *Journal of Terramechanics*, 26(3/4) pp. 201 - 210

Lippmann S.A. and Nanny J.D. (1967). A quantitative analysis of the enveloping forces of passenger tyres. *S.A.E.*, paper 670174

Lippmann S.A., Piccin W.A. and Baker T.P. (1966). Enveloping characteristics of truck tyres - A laboratory study. *S.A.E.*, paper 650184

Matthews J. (1973). The measurement of tractor ride comfort. *S.A.E.*, paper 730795

Matthews J. (1964). Ride comfort for tractor operators, part 1:review of existing information -part 1. *Journal of Agricultural Engineering Research*, **9**(1)

Matthews J. (1977). The ergonomics of tractors. *ARC Research review*, **3**(3) pp. 59 - 65

Matthews J. and Talamo J.D.C. (1965). Ride comfort for tractor operators. *Journal of Agricultural Engineering Research*, **10**(2) pp. 93 - 108

Nguyen N.V. and Lines J.A. (1988). The enveloping characteristics of an agricultural tyre. Divisional Note DN/1461, AFRC Institute of Engineering Research, Silsoe

Nix J. (1987). *Farm Management Pocket book*. Eighteenth Edition. Wye College, University of London

Overton F.A., Mills B. and Ashley, C. (1970). The vertical response characteristics of the non-rolling tyre. Institute of Mechanical Engineers, Automobile Division, **184** part 2A (2)

Pacejka H.B. (1981). In-plane and out-of-plane dynamics of pneumatic tyres. *Vehicle System Dynamics* **10**, pp. 221 - 251

Painter D.L. (1981). A simple deflection model for agricultural tyres. *Journal of Agricultural Engineering Research*, **26**(1) pp. 9 - 20

Peachey R.O., Lines J.A. and Stayner R.M. (1989). Agricultural vehicle suspensions - tractor front axle suspension. Report for the proceedings of the 3rd International Symposium of the International Section of the ISSA for Research on Prevention of Occupational Risks, Vienna, 19 - 21 April



Plackett C.W. (1983). Hard surface contact area measurement for agricultural tyres. Divisional Note DN 1200, National Institute of Agricultural Engineering, Silsoe

Rasmussen R.E. and Cortese, A.D. (1968). Dynamic spring rate performance of rolling tyres. S.A.E., paper 680408

Rosegger R. and Rosegger S. (1960). The health effects of Tractor driving. *Journal of Agricultural Engineering Research*, 5(3)

Schöltz D.C. (1966). A three-point linkage dynamometer for restrained linkages. *Journal of Agricultural Engineering Research*, 11, pp. 33 - 47

Shukla L.N. (1967). The effects of ballast on the springiness of tractor tyres. *Canadian Agricultural Engineering*, 9 pp. 93 - 95

Siefkes T. (1989). Dynamische Kennwerte von AS-Reifen im Prüfstands-versuch und im Freiland (Characteristics of agricultural tyres -laboratory and field test results). VDI/MEG Kolloquium Landtechnik, Heft 7 Reifen Landwirtschaftlicher Fahrzeuge, München 27 - 28th April

Stayner R.M. (1988). Suspensions for agricultural vehicles. Paper presented to the international conference on Advanced Suspension systems. Institute of Mechanical Engineers, London 24 - 25 October

Stayner R.M. and Bean A.G.M. (1975). Tractor ride investigations: A survey of vibrations experienced by drivers during field work. NIAE Departmental Note DN/E/578/1445 (unpublished), Silsoe

Stayner R.M. and Boldero A.G. (1973). The dynamic stiffness of tractor tyres, measurements in the horizontal plane. Dept. Note DN/TC/386/1445, National Institute of Agricultural Engineering, Silsoe (unpubl.)

Stayner R.M., Collins T.S. and Lines J.A. (1984). Tractor ride vibration simulation as an aid to design. *Journal of Agricultural Engineering Research*, 29 pp. 345-355

Stayner R.M., Hilton D.J. and Moran P. (1975). Protecting the tractor driver from low frequency ride vibration. Paper presented to the Institution of Mechanical Engineers, paper 200/75

Ulrich A. (1983). Untersuchungen zur Fahrdynamik von Traktoren mit und ohne Anbaugeräte (investigation of the ride dynamics of tractors with and without mounted implements). Forschungsbericht Agrartechnik des Arbeitskreises Forschung und Lehre der Max-Eyth-Gesellschaft Nr.82 Berlin: MEG

Whyte R.T. and Lines J.A. (1987). Subjective assessment and objective measurement of the ride vibration of a suspended cab tractor. Paper presented to meeting of the informal group on the Human Response to Vibration, Shrivenham, 21 - 22 September

Wolken L.P. (1972). Dynamic response of a prime mover to random inputs. A.S.A.E., paper 72-613

Yong R.N., Boonsinsuk P. and Fattah E.A. (1980). Tyre load capacity and energy loss with respect to varying soil support stiffness. *Journal of Terramechanics*, 17(3) pp. 131 - 147